

Specialization: Transport Engineering and Logistics

Report number: 2016.TEL8016

Title: **Development of a Method for
Assessment of the Remaining
Fatigue Life of Steel Structures of
Existing STS Cranes**

Author: J.A. van Jole

Title (in Dutch) Ontwikkeling van een methode voor het beoordelen van vermoeiing in de stalen structuren van bestaande portaalkadekranen

Assignment: Master thesis

Confidential: no

Initiator (university): Prof.dr.ir. G. Lodewijks

Initiator (company): Ing. W. van Cappellen (Cargotec Netherlands, Rotterdam)

Supervisor: Ir. W. van den Bos

Date: September 2, 2016

This report consists of 168 pages and 4 appendices. It may only be reproduced literally and as a whole. For commercial purposes only with written authorization of Delft University of Technology. Requests for consult are only taken into consideration under the condition that the applicant denies all legal rights on liabilities concerning the contents of the advice.

Student:	J.A. van Jole	Assignment type:	Master Thesis
Supervisor (TU Delft):	Ir. W. van den Bos	Creditpoints (EC):	35
Supervisor (Cargotec):	Ing. W. van Cappellen	Specialization:	TEL
		Report number:	2016.TEL.8016
		Confidential:	No

Subject: Development of a Method for Assessment of the Remaining Fatigue life of Steel Structures of Existing STS Cranes

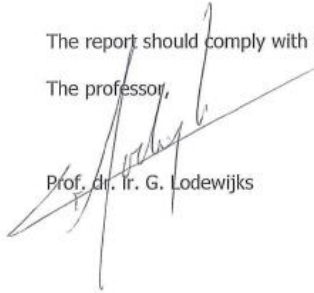
STS cranes (Ship-to-Shore cranes) are designed for a finite fatigue life, but it is often preferred by the terminal operators to keep the crane in operation once the fatigue life has expired. The reason that the cranes remain in operation is because the steel structure is generally in good condition when the design fatigue life expires. However, the risk of fatigue failure increases when the crane is operated after it reached its expected service life. Therefore the remaining fatigue life of the crane needs to be assessed in order to enable operation of the crane after it reaches its design fatigue life without compromising safety.

Methods to assess the remaining fatigue life in industries like offshore and aviation are standardized, but for cranes such methods do not exist. Therefore an assessment method for the steel structure of the crane needs to be put forward. This method should include the structural parts of existing cranes. Parts like cables, drive systems and wheels will not be included.

The goal of this research is to create a method to assess the remaining fatigue life of existing STS cranes. The assessment method should be able to calculate the remaining lifetime of the crane and determine whether inspection of the crane is necessary (and if so, how long the intervals should be). After inspections are completed, the method should determine whether repair works need to be performed to ensure the structural integrity of the crane.

The report should comply with the guidelines of the section. Details can be found on the website.

The professor,



Prof. dr. Ir. G. Lodewijks

Development of a Method for Assessment of the Remaining Fatigue Life of Steel Structures of existing STS Cranes

**Establishing Lifetime Prediction, Inspection Intervals and
After-Inspection Procedures**

MASTER OF SCIENCE THESIS

For the degree of Master of Science in Mechanical Engineering at Delft
University of Technology

J.A. van Jole

2 September 2016

Faculty of Mechanical, Maritime and Materials Engineering (3mE) · Delft University of
Technology



The work in this thesis was supported by Cargotec. Their cooperation is hereby gratefully acknowledged.



Copyright ©
All rights reserved.

Preface

This thesis presents my graduation research which is performed to complete my master of science in Mechanical Engineering at the section of Transportation Engineering at the Delft University of Technology. Together with my supervisors at the university and at Kalmar I was able to set up a project on fatigue cracks in steel structures of existing STS cranes. This project was conducted for a period of six months at the crane services department at Kalmar Rotterdam.

I would like to thank several people for enabling me to do this project. First I want to thank professor Gabriel Lodewijks and ir. Wouter van den Bos from the Delft University of Technology for their guidance during this project. I also want to thank Willem van Capellen from Kalmar for providing me with the opportunity to work on this project as well as supervising me.

I also want to thank Dirk Spanjer from Airbus defence and space for our discussion on the execution of crack growth models and Yarko Yurechko and Oleg Ishchuck for their support regarding the SDC Verifier software.

In addition I would like to thank my parents and girlfriend for their support during the course of my study, without them I would not be where I am today.

Johan van Jole,
2 September 2016

Abstract

STS cranes (Ship-to-Shore cranes) are designed for a finite fatigue life, but it is often preferred by the terminal operators to keep the crane in operation once the design fatigue life has expired. When the crane is operated after it reached its expected service life, the risk of fatigue failure increases. Therefore the structural lifetime of the crane needs to be assessed in order to enable operation of the crane after it reaches its design fatigue life without compromising safety.

Methods to assess the remaining fatigue life in industries like offshore and aviation are standardized, but for cranes such methods do not exist. Therefore an assessment method for the structure of the crane needs to be put forward. The assessment method should be able to calculate the remaining lifetime of the crane and determine whether inspection of the crane is necessary (and if so, how long the intervals should be). After inspections are completed, the method should determine whether repair works need to be performed to ensure the structural integrity of the crane.

The main research question of this thesis is formulated as follows:

What is the most appropriate method to assess the remaining fatigue life of steel structures of existing STS cranes?

To determine which type of fatigue assessment methods can be applied to STS cranes, a review of assessment methods for STS cranes, bridges, aircraft and offshore structures is performed. The method that is selected when the crane is operated within its design fatigue life is the calculation procedure for fatigue used in the design stage, because this means that the remaining fatigue life can be determined using information that is already available. When the crane is operated outside its design limits, a crack growth model is used to calculate the remaining fatigue life.

The steel structure of a general STS crane consists of four main components; bolted connections, pinned connections, welded connections and base material. It is determined that the majority of fatigue failures in steel structures occurs at welds, fatigue cracks in the base material contribute slightly and the amount of fatigue failures of bolted and pinned connections is negligible. The fatigue assessment model therefore only considers cracks in the base material and in welds. The components at the connections at the forestay and backstay, the connections between the crane boom and the portal beams as well as the connections at the legs are even more susceptible to fatigue failure because these areas are subjected to relatively large fluctuating loads.

In order to determine the remaining fatigue life of the crane, the crack size which will cause failure needs to be known. This critical crack size depends on the geometry of the detail under consideration, the used material and the stress at that detail. This means that the critical crack size is not constant across the steel structure of a general STS crane. When the critical crack size is known, the crack growth rate needs to be calculated in order to determine the time between crack initiation and failure.

The structure needs to be checked for cracks before a member is expected to fail. Therefore the value for the remaining fatigue life is used to schedule inspections as well. The inspection interval depends on the crack size which can be determined with sufficient reliability, which in turn depends on the type of inspection method that is deployed.

In case cracks are found during inspections, repair methods are available to extend the remaining fatigue life of the crane. The methods that can be used to repair cracks in steel structures of STS cranes are the gouge-and-weld method, mounting doubler plates, drilling crack arrest holes and modifying the structure. The selection of the repair method is based on the remaining fatigue life of the structure, the location of the crack and potential earlier fatigue crack repair works.

The most appropriate method to assess the remaining fatigue life of the crane therefore consists of an inspection schedule, where the inspection intervals are determined based on the remaining fatigue life. When the crane is operated within its design limits, the inspection intervals are based on the safety factors for fatigue as defined in the EN 13001 design standard for cranes. When the crane is operated after its design fatigue life is expired, the remaining fatigue life is calculated using a crack growth model.

The inspection methods that are used to inspect the crane are determined based on the value for the critical crack size and the crack size which can be accurately determined by the inspection methods. When the remaining fatigue life is insufficient, repair works are scheduled to repair the crack and thus extend the fatigue life of the crane. The repair methods are selected based on the type of crack (cracks at the surface or internal cracks) and its location. This method is repeated until it is not economically feasible to further extend the fatigue life of the crane.

Abstract in Dutch (Samenvatting)

Kadekranen worden ontworpen voor een vooraf vastgestelde vermoeiingslevensduur, maar het komt vaak voor dat de kranen langer in bedrijf worden gehouden omdat ze na het verstrijken van de berekende vermoeiingslevensduur over het algemeen in goede staat verkeren. Wanneer de kranen in bedrijf worden gehouden nadat de berekende vermoeiingslevensduur is bereikt, neemt het risico op vermoeiingsfalen toe. Dit betekent dat de levensduur van de stalen structuur moet worden beoordeeld nadat de vermoeiingslevensduur is bereikt om de kraan in bedrijf te kunnen houden zonder concessies te doen met betrekking tot de veiligheid.

In een aantal bedrijfstakken (bijvoorbeeld offshore en vliegtuigbouw) zijn methoden om de resterende levensduur te bepalen gestandaardiseerd, dit is echter niet het geval voor kadekranen. Daarom moet er een beoordelingsmethode voor vermoeiing van de stalen structuur van kranen worden opgesteld. Deze beoordelingsmethode moet in staat zijn om de resterende levensduur van de kraan te bepalen en om vast te stellen of inspecties nodig zijn (en indien dit nodig is, hoe lang het interval tussen de inspecties zou moeten zijn). Na het uitvoeren van inspecties moet de beoordelingsmethode kunnen bepalen of er reparatiewerkzaamheden nodig zijn om de restlevensduur van de kraan te vergroten.

De onderzoeksvraag in dit onderzoek luidt als volgt:

Wat is de meest geschikte methode om de restlevensduur van de stalen structuur van bestaande kadekranen te bepalen?

Om te bepalen welk type beoordelingsmethoden kunnen worden toegepast op kadekranen is er een overzicht van de bestaande methoden voor kadekranen, bruggen, vliegtuigen en offshore structuren gemaakt. De gekozen methode die wordt gebruikt binnen de ontwerplevensduur van de kraan is gebaseerd op de methoden die worden gebruikt tijdens het ontwerp van de kraan, omdat dit betekent dat de resterende levensduur bepaald kan worden met behulp van beschikbare gegevens. Wanneer de kraan wordt gebruikt buiten zijn ontwerplevensduur zal een scheurgroei-model worden gebruikt om de resterende levensduur te berekenen.

De stalen structuur van een kadekraan bestaat uit vier basiscomponenten; boutverbindingen, pen-gat verbindingen, gelaste verbindingen en plaatmateriaal. Vermoeingsfalen in stalen structuren komt voornamelijk voor bij gelaste verbindingen, een klein gedeelte van de vermoeingsscheuren kan worden gevonden in het plaatmateriaal en scheuren in boutverbindingen en pen-gat verbindingen zijn te verwaarlozen. Daarom neemt het vermoeings beoordelingsmodel alleen de scheuren in lassen en plaatmateriaal in overweging. De componenten bij de verbindingen van de hangstangen, de verbindingen tussen de katrijbaan en de portaalbalken en de verbindingen rondom de poten zijn in hogere mate belast op vermoeing door de relatief grote spanningsverschillen.

Om de restlevensduur van een kraan te bepalen moet de scheurgrootte waarbij falen optreedt worden bepaald. Deze kritieke scheurgrootte hangt af van de geometrie van het detail onder beschouwing, de materiaaleigenschappen en de spanning in het detail. Dit betekent dat de kritieke scheurgrootte niet constant is over de stalen structuur van de kraan. Wanneer de kritieke scheurgrootte bekend is moet de scheurgroeisnelheid worden bepaald om het interval tussen het ontstaan van de scheur en vermoeingsfalen te bepalen.

De structuur moet op scheuren worden geïnspecteerd voordat een onderdeel faalt. Daarom wordt de waarde voor de resterende levensduur van de kraan gebruikt voor het plannen van de inspecties. Het inspectie interval hangt af van de scheurgrootte die gedetecteerd kan worden met een voldoende betrouwbaarheid. Dit hangt af van de gekozen inspectiemethode die wordt gebruikt om de inspectie uit te voeren.

Wanneer er scheuren worden gevonden tijdens de inspecties zijn er reparatiemethoden beschikbaar om de resterende levensduur te verlengen. De beschikbare methoden zijn het opengutsen en dichtlassen van de scheur, het monteren van overzetplaten, boren van scheurstopgaten en het veranderen van de structuur. De reparatiemethode die wordt geselecteerd hangt af van de resterende levensduur van de structuur, de locatie van de scheur en of er al eerder reparatiewerkzaamheden zijn uitgevoerd.

De meest geschikte methode om vermoeing in de stalen structuur van kadekranen te bepalen bestaat daarom uit een inspectieregime, waarbij de inspectie intervallen worden bepaald aan de hand van de resterende levensduur van de kraan. Wanneer de kraan wordt gebruikt binnen de ontwerp levensduur zijn de inspectie intervallen gebaseerd op de veiligheidsfactoren voor vermoeing zoals vermeld in de EN 13001 ontwerp norm voor kranen. Wanneer de kraan buiten de ontwerp levensduur wordt gebruikt wordt de resterende levensduur bepaald door middel van een scheurgroeimodel.

De inspectie methoden die gebruikt worden bij het uitvoeren van de inspecties worden bepaald aan de hand van de kritieke scheurgrootte en de scheurgrootte die met voldoende betrouwbaarheid kan worden gedetecteerd. Wanneer de resterende levensduur niet voldoet worden reparaties uitgevoerd om de scheur dicht te maken. De reparatiemethoden worden geselecteerd op basis van het type scheur (oppervlaktescheur of interne scheur) and de locatie van de scheur. De vermoeings beoordelingsmethode wordt herhaald tot het niet meer economisch voordelig is om de resterende levensduur te verlengen.

List of Acronyms

ADTT	Average Daily Truck Traffic
AGV	Automated Guided Vehicle
DNV	Det Norske Veritas
FAA	Federal Aviation Authority
FEA	Finite Element Analysis
FEM	Finite Element Method
FPSO	Floating Production, Storage and Offloading
HAZ	Heat Affected Zone
HCF	High Cycle Fatigue
ISO	International Organisation for Standardization
LCF	Low Cycle Fatigue
LEFM	Linear Elastic Fracture Mechanics
LRFD	Load and Resistance Factor Design
LOV	Limit of Validity
NDT	Non-Destructive Testing
POD	Probability of Detection
PWHT	Post Weld Heat Treatment
SCF	Stress Concentration Factor
SIF	Stress Intensity Factor
STS	Ship-to-Shore

SWL	Safe Working Load
TOS	Terminal Operating System
WFD	Widespread Fatigue Damage
XFEM	Extended Finite Element Method

List of Symbols

α	Scaling parameter
γ	Surface energy
ϵ	Strain
λ	Scaling parameter
ν	Poisson ratio
σ	Stress
$\Delta\sigma$	Stress range
σ_{fail}	Stress at which the material will fail
σ_{yield}	Yield stress
a	Crack length
a_{crit}	Critical crack size
C	Crack growth constant
E	Young's modulus
G_c	Griffiths critical energy release rate
K_c	Critical stress intensity factor for plane stress
K_{Ic}	Fracture toughness (critical stress intensity factor for plane stress)
K_{th}	Threshold stress intensity factor
m	Crack growth exponent
N_i	Initial number of cycles
N_f	Number of cycles at failure
R_p	Plastic zone radius
t	Thickness of the material
Y	Geometry factor

Table of Contents

Preface	i
Abstract	iii
Abstract in Dutch (Samenvatting)	v
List of Acronyms	vii
List of Symbols	ix
1 Introduction	1
1-1 Background	1
1-2 Fatigue in Structures of STS Cranes	2
1-3 Research Goal	3
1-4 Scope	4
1-5 Structure of the Report	5
2 Standards on Fatigue Life Assessment	7
2-1 Standards on Inspection of Cranes	7
2-2 Standards on Inspection Of Bridges	8
2-2-1 Fatigue Life Assessment by Classification	8
2-2-2 Fatigue Life Assessment According to the Eurocodes	8
2-2-3 Fatigue Life Assessment Based on Crack Growth	10
2-2-4 Fatigue Life Assessment by LEFM	10
2-2-5 Fatigue Life Assessment Based on Data Analysis	10
2-3 Standards on Inspection of Offshore Structures	11
2-3-1 Fatigue Life Assessment by LRFD	11

2-3-2	Fatigue Life Assessment Using SCF's	12
2-3-3	Fatigue Life Assessment Correcting for Measurement Error	12
2-3-4	Fatigue Life Assessment Accounting for Corrosion	13
2-4	Standards on Inspection of Aircraft	14
2-4-1	Damage Tolerant Design Philosophy	14
2-4-2	Widespread Fatigue Damage Concept	15
2-4-3	Fatigue Life Assessment by Probabilistic Fatigue Reliability Calculations	16
2-5	Fatigue Damage Monitoring Methods	16
2-5-1	Evaluating Crack Growth by Marking	16
2-5-2	Evaluating Fatigue Damage by Load Measurements	17
2-5-3	Evaluating Fatigue Damage Using Strain Gauges	19
2-6	Overview	20
3	Identification of Fatigue Critical Details	23
3-1	General Fatigue Analysis of STS Gantry Cranes	23
3-2	Fatigue Failure Modes of Fundamental Parts of Steel Structures	26
3-2-1	Fatigue Failure Modes of the Base Material	26
3-2-2	Fatigue Failure Modes of Welded Connections	27
3-2-3	Fatigue Failure Modes of Bolted Connections	28
3-2-4	Fatigue Failure Modes of Pinned Connections	28
3-3	Conclusion	29
4	Crack Growth Calculations	31
4-1	Calculation of the Critical Crack Size	31
4-1-1	Theory Behind the Critical Crack Size	31
4-1-2	Griffith Equation for the Critical Crack Size	33
4-1-3	Stress Intensity Factor	33
4-1-4	Stress Calculations in Plates	34
4-2	Linear Crack Growth Calculations	36
4-2-1	Fatigue Failure Modes	36
4-2-2	Calculation of the Stress Intensity Factor	37
4-2-3	Crack Growth Rate Calculation Procedure	39
4-3	Non-Linear Crack Growth Calculations	41
4-3-1	Low Cycle Fatigue	41
4-3-2	Structural Deformations	42

5	Implementation of Calculation Model	43
5-1	Verification of the Calculation Model	43
5-1-1	Verification of Fracture Mechanics Model	43
5-1-2	Plastic Radius Calculation	44
5-1-3	Calculation of the Geometry Correction Factor	45
5-2	Sensitivity of the Model	48
5-2-1	Influence of Yield Strength	49
5-2-2	Influence of Fracture Toughness	50
5-2-3	Influence of Crack Growth Parameters	51
5-2-4	Influence of Maximum Stress	53
5-2-5	Influence of Stress Range	54
5-2-6	Influence of Geometry Factor	55
5-2-7	Influence of Initial Crack Size	56
5-2-8	Summary of the Sensitivity Analysis	57
6	Measurement of Crack Sizes	59
6-1	Crack Detection and Measurement Methods	59
6-2	Influence of Crack Detection Method on Inspection Regime	63
7	Repair Methods for Cracks in Steel Structures	67
7-1	Load Path Redundancy and Reducing the SWL	67
7-2	Gouge-and-Weld Method	68
7-3	Drilling Crack Arrest Holes	71
7-4	Doubler Plates	72
7-5	Overview of Crack Repair Methods	73
8	Fatigue Life Assessment Method	75
8-1	Structure of the Assessment Method	75
8-2	Evaluation of SN-curves	79
8-3	Determining the Inspection Procedure	80
8-3-1	Selection of Inspection Method	81
8-3-2	Global Inspection of the Structure	81
8-3-3	Detect and Measure Fatigue Cracks	82
8-4	Calculation of the Remaining Fatigue Life Using Fracture Mechanics	83
8-5	Selection of Repair Method	83
8-5-1	Gouge-and-Weld Method	85
8-5-2	Mounting Doubler Plates	85
8-5-3	Drilling Crack Arrest Holes	86
8-5-4	Redesign of Detail	87

9 FEM Example of Fatigue Life Calculation Method	89
9-1 Set-up of Example FEM Model	89
9-2 Visualisation of SN-curve Method	94
9-2-1 Characteristic Values Used in the Analysis	94
9-2-2 Results of Implemented Fatigue Check	96
9-3 Visualisation of Fracture Mechanics Method	102
9-3-1 Implementation of Fracture Mechanics Model in SDC Verifier	102
9-3-2 Results of Fracture Mechanics Calculations	103
10 Conclusion	107
10-1 Conclusion	107
10-2 Recommendations for Further Research	109
A Research Paper	111
B Flowcharts Fatigue Assessment Model	115
C Fatigue Assessment Calculation Model	123
D Calculation of Geometry Factors	125
D-1 Geometry Factors For Cracks in Plates	125
D-2 Geometry Factors For Cracks in Cylinders	129
D-3 Geometry Factors For Cracks at Holes	130
D-4 Geometry Factors For Cracks at Welds	130
Bibliography	137

List of Figures

1-1	Example of a STS gantry crane (source: www.flickr.com).	2
1-2	Aftermath of the accident in Bremen, where a crane collapsed due to fatigue failure of the forestay (source: www.fleetmon.com).	3
2-1	Example of S-N curves which describe the allowable stress range as a function of the amount of load cycles for different connection classes (source: www.twi-global.com).	9
2-2	Example of the LRFD method, where the load effect and fatigue resistance curves are shown. (source: www.pwri.go.jp)	11
2-3	Illustration of the probabilistic method to determine the remaining fatigue life of offshore structures. The initial defect distribution is converted to a time to failure distribution (green line), which is sampled at a given value of the probability of failure to obtain the remaining fatigue life. The crack size distribution found at the inspection performed at t_1 deviates from the calculated distribution (blue line), therefore the remaining fatigue life is updated (source: [1])	13
2-4	Aftermath of the accident of flight 243, which was caused by a fatigue failure originating from multiple locations (source: www.nytimes.com)	15
2-5	Marking of bolted connections to determine whether the bolts have turned during operation (source: www.appliedbolting.com)	17
2-6	Illustration of loading spectra for container and grab cranes (source: [2]).	19
3-1	Indication for the location of and the the backstay (left) and the forestay (right) at STS gantry cranes.	24
3-2	A weld applied from the outside of the connection, as pictured from the inside of the structure (image provided by Cargotec).	24
3-3	Result of the model used to illustrate the fatigue sensitive areas of the structure of a general STS gantry crane (image provided by SDC verifier).	25
3-4	Location of the root and toe of a butt weld (source: www.weldersuniverse.com).	27
3-5	Terminology used in bolted connections (source: www.martinrobey.com).	28
3-6	Depiction of an assembled pinned connection (source: www.synergiscadblogger.com).	29

4-1	Schematic plot of the surface and strain energy as a function of crack size (source: http://www.mse.mtu.edu/).	32
4-2	Schematic representation of the plastic zone around the crack tip (source: www.impact-solutions.co.uk).	34
4-3	Plot of the fracture toughness as a function of plate thickness (source: http://www.afgrow.net).	35
4-4	Illustration of the three failure modes for fatigue (source: http://www.slideshare.net).	37
4-5	Crack growth rate plotted against the SIF, the crack growth rate is in red and the Paris law is represented by the dotted line (source: www.totalmateria.com).	39
4-6	Example of large deformations as a result of a fatigue crack. LEFM models are not valid in this case (image provided by Cargotec).	42
5-1	Example of the geometry factor calculation model. In this case the geometry factor for a center crack in a plate subjected to bending or tensile loads is calculated.	47
6-1	Schematic representation of crack detection by magnetic particle inspection (source: www.industrialndt.com).	60
6-2	Schematic representation of the color penetration test (source: www.asnt.org).	61
6-3	Schematic representation of the radiographic inspection method (source: www.iprt.iastate.edu).	61
6-4	Schematic representation of the ultrasonic inspection method (source: www.elumeco.com).	62
6-5	Visualisation of the formation of eddy currents (source: www.nde-ed.org).	62
6-6	Example of POD curves for visual inspection for varying degrees of accessibility of the structure.	63
7-1	Schematic representation of the load path redundancy concept (source: www.stressebook.com).	68
7-2	Schematic representation of the gouging process (source: www.alloyavenue.com).	69
7-3	Schematic representation of the grinding processes (source: www.fgg.uni-lj.si).	70
7-4	Two crack arrest holes are used to stop a center crack which is initiated at a welded detail (source: www.alwayscivil.blogspot.com).	71
7-5	Example of a repair using a doubler plate which is fastened by bolts (source: www.dsiac.org).	72
8-1	Flowchart of the fatigue assessment model for steel structures of existing STS gantry cranes.	76
8-2	Examples of SN-curves for steel and aluminium (source: www.efunda.com).	79
8-3	Flowchart of the process of determining the inspection procedure for steel structures of existing STS gantry cranes.	80
8-4	The brace which failed as a result of a fatigue crack originating from the hydrophone support, which is still attached to the wreckage (source: www.olechris.page.tl).	82
8-5	Flowchart of the process of determining the repair method for cracks in steel structures of existing STS gantry cranes.	84
8-6	Illustration of the preferred location of crack-arrest holes (source: [3]).	87
9-1	Example of an existing lemniscate crane (source: www.flickriver.com).	90
9-2	Illustration of the lemniscate crane model implemented in SDC Verifier and FEMAP.	91

9-3	Detail model of the A-frame which is used to illustrate the calculation procedure for the remaining fatigue life of STS cranes.	91
9-4	Visualisation of the implementation of one FEM load (which describes the gravity load of the supported structure in one crane position).	92
9-5	Example of a FEM load definition in SDC verifier (which describes the gravity load of the supported structure in one crane position).	92
9-6	Definition of the load sets in SDC verifier.	93
9-7	Definition of the used load group in SDC verifier.	93
9-8	Visualization of the locations where the constraints are applied (constrained elements are displayed in red).	94
9-9	Implementation of the classification which represents the allowable stresses according to the EN 13001 crane standard.	95
9-10	Overview of the welds in this model.	95
9-11	Overview of the implementation of the fatigue check using SN curves.	96
9-12	Utilization factor for fatigue in the X direction.	97
9-13	Utilization factor for fatigue in the Y direction.	97
9-14	Utilization factor for fatigue in the XY direction.	98
9-15	Overall utilization factor for fatigue.	98
9-16	Overall utilization factor, zoomed in to show the element subjected to a stress singularity.	99
9-17	The overall utilization factor for fatigue using a limit value of 5.	99
9-18	The overall utilization factor for fatigue using a limit value of 5 (viewed from the back of the frame).	100
9-19	Number of cycles to reach an accumulated fatigue damage of 0.75, expressed in millions.	101
9-20	Number of cycles to reach an accumulated fatigue damage of 0.75, expressed in millions (viewed from the back of the frame).	101
9-21	Implementation of the fracture mechanics model in SDC Verifier.	102
9-22	This figure displays the critical crack size in metres across the structure.	104
9-23	This figure displays the critical crack size in metres across the structure.	104
9-24	This figure displays the remaining fatigue life across the structure.	105
9-25	This figure displays the remaining fatigue life across the structure.	105
9-26	This figure displays the remaining fatigue life across the structure.	106
B-1	Flowchart depicting the fatigue assessment method (first part).	116
B-2	Flowchart depicting the fatigue assessment method (second part).	117
B-3	Flowchart depicting the process of determining the inspection procedure (first part).	118
B-4	Flowchart depicting the process of determining the inspection procedure (second part).	119
B-5	Flowchart depicting the process of determining the repair procedure (first part).	120
B-6	Flowchart depicting the process of determining the repair procedure (second part).	121

D-1	Calculation of the geometry factor for a center crack in a plate subjected to bending or tensile loads.	126
D-2	Calculation of the geometry factor for a double-edge cracked plate subjected to bending or tensile loads.	127
D-3	Calculation of the geometry factor for a single edge cracked plate subjected to bending or tensile loads.	128
D-4	Calculation of the geometry factor for a circumferentially cracked cylinder subjected to bending or tensile loads.	129
D-5	Calculation of the geometry factor for a cracked hole subjected to normal and secondary stresses.	130
D-6	Calculation of the geometry factor for a cracked butt weld subjected to bending or tensile loads.	131
D-7	Calculation of the geometry factor for a fillet weld with weld toe crack subjected to bending or tensile loads.	132
D-8	Calculation of the geometry factor for a lap joint with a weld toe crack subjected to a tensile load.	133
D-9	Calculation of the geometry factor for a cruciform joint with a weld root crack and a transverse attachment with a weld toe crack subjected to a tensile load.	134
D-10	Calculation of the geometry factor for a cruciform joint (K-butt and fillet welded) with a weld toe crack subjected to a tensile load.	135

List of Tables

2-1	Overview of existing container weighing solutions [4]	17
2-2	Overview of methods that can be used to determine the (remaining) fatigue life.	20
3-1	Global areas of the crane that are prone to fatigue and the reasoning behind this assessment.	30
3-2	Summary of the types of defects that are associated with welded connections	30
4-1	Overview of the methods that are able to calculate the SIF.	39
4-2	Declaration of the symbols used in Equation 4-15.	40
5-1	Data used to verify the implementation of the crack growth calculations.	44
5-2	Data used to verify the calculation of the plastic radius.	45
5-3	Types of details for which the geometry factor is modelled in this research.	46
5-4	The benchmark values used in the sensitivity analysis.	48
5-5	Values used to determine the sensitivity of the model with respect to the yield strength.	49
5-6	Changes in the critical crack size and cycles to failure as a result of changes to the yield strength.	49
5-7	Values used to determine the sensitivity of the model with respect to the fracture toughness.	50
5-8	Changes in the critical crack size and cycles to failure as a result of changes to the fracture toughness.	50
5-9	Values used to determine the sensitivity of the model with respect to the crack growth constant.	51
5-10	Changes in the critical crack size and cycles to failure as a result of changes to the crack growth constant.	51
5-11	Values used to determine the sensitivity of the model with respect to the crack growth exponent.	52
5-12	Changes in the critical crack size and cycles to failure as a result of changes to the crack growth exponent.	52

5-13	Values used to determine the sensitivity of the model with respect to the maximum stress.	53
5-14	Changes in the critical crack size and cycles to failure as a result of changes to the maximum stress.	53
5-15	Values used to determine the sensitivity of the model with respect to the stress range.	54
5-16	Changes in the critical crack size and cycles to failure as a result of changes to the stress range.	54
5-17	Values used to determine the sensitivity of the model with respect to the geometry factor.	55
5-18	Changes in the critical crack size and cycles to failure as a result of changes to the geometry factor.	55
5-19	Values used to determine the sensitivity of the model with respect to the initial crack size.	56
5-20	Changes in the critical crack size and cycles to failure as a result of changes to the initial crack size.	56
5-21	Relative importance of the parameters with respect to the remaining fatigue life (sorted high to low).	57
6-1	Values for a_0 (in mm) used in Equation 6-1 [5]	64
6-2	Values for the scaling parameters used in Equation 6-1 [5]	64
6-3	Values for the crack sizes at POD values of 0.99 and 0.95	65
7-1	Overview of the advantages and disadvantages of the crack repair procedures. . .	73
8-1	Values of the fatigue specific resistance factor for different types of details as a function of accessibility and consequence of failure [6].	77
8-2	Values for the transition points, based on the specific resistance factor as defined by the EN 13001 design standard.	78
9-1	Values for the crack growth parameters that can be used in this model.	103

Chapter 1

Introduction

This research concerns remaining fatigue life assessment of existing Ship-to-Shore (STS) cranes. The first two sections of this chapter cover the relevance of this subject. The research goal is explained in the third section and section four concerns the scope of this research. This chapter concludes by discussing the structure of this report.

1-1 Background

STS cranes are widely used in ports all over the world in order to load and offload cargo vessels. These cranes are located at terminals, which connect two or more modes of transportation. The modes of transportation that are encountered at ports are vessels (deep-sea vessels, feeders and barges), trains and trucks. An example of a STS gantry crane is shown in Figure 1-1. The load is hoist and lowered by a trolley, which is able to drive along the boom. The boom in Figure 1-1 is the upper horizontal section, on which "APM Terminals" is painted.

Cranes are designed according to standards to provide a minimum level of safety. The NEN-EN 15011 standard for design of bridge and gantry cranes is an example of a standard that STS cranes in the Netherlands have to conform to [7]. This standard requires the manufacturer to design the crane for a finite service life, defined by the amount of moves (the number of times the trolley moves from the terminal to the vessel and back) that the crane is expected to perform.



Figure 1-1: Example of a STS gantry crane (source: www.flickr.com).

When a STS crane reaches its design fatigue life the steel structure is generally in reasonable condition, therefore STS cranes are often operated after the design fatigue life has expired. The actual service life of the crane is sometimes as much as twice the original design fatigue life. The condition of the crane therefore needs to be monitored in order to ensure that no safety concerns might arise due to the prolonged service life [8]. The condition of the structure can be monitored using calculations and/or inspection procedures. Special attention needs to be paid to fatigue cracks, because a major part of structural failures of STS cranes is caused by fatigue [9]

1-2 Fatigue in Structures of STS Cranes

Each move of the trolley along the boom of the crane forms a load cycle, these load cycles cause the material to fail at stress levels below the yield strength [10]. This phenomenon is called fatigue. Fatigue occurs when load cycles cause dislocations (defects in the lattice structure of the material) that are present in the material to accumulate. A crack is initiated at the location where these dislocations pile up and this crack subsequently grows until the material fractures [11].

An investigation into the causes of insurance claims from container terminals found that 13% of the claims originated from structural failures of STS cranes [12]. This figure does not include collision damage (which represents another 7.5% of all claims) to the crane. The amount of economic damage due to structural failures of STS cranes might therefore be reduced by regular assessment of the remaining fatigue life of the crane.

A recent incident involving a structural failure of a STS crane due to fatigue occurred on the 14th of May 2015. The boom of a crane collapsed due to fatigue failure of the forestay (see Figure 1-2). Apart from the damage cost, there was a loss of life [13]. This accident furthermore shows the importance of monitoring the remaining fatigue life of STS cranes.



Figure 1-2: Aftermath of the accident in Bremen, where a crane collapsed due to fatigue failure of the forestay (source: www.fleetmon.com).

1-3 Research Goal

As shown in the previous section, a fatigue failure of a structural member of a STS crane can have severe consequences. The fatigue life of the structure of a STS crane therefore needs to be assessed regularly in order to reduce the risk of fatigue failures. Kalmar (the division of Cargotec responsible for construction and service of STS cranes, amongst other things) currently uses fixed inspection intervals to monitor the condition of the crane with respect to fatigue cracks. The intervals between inspections are determined by experience only, because a comprehensive method to evaluate the remaining fatigue life of a specific STS crane is not available.

The time in which a crack in the structure of a STS crane grows to a critical size (the size of the crack at failure) cannot be estimated yet, so the inspection intervals need to be relatively short to account for this uncertainty. This is a significant disadvantage because operations at the terminals must be (partially) ceased each time an inspection of a STS crane takes place.

The second disadvantage of the current method is experienced by the customers of Kalmar as they don't know how long they can keep their crane in service, even when it passed an inspection (especially when the service life of the crane exceeds the design life).

The goal of this research is therefore to establish a method which is able to determine the remaining fatigue life of STS cranes. This calculation method must also be applicable to structures of STS cranes with service lives larger than the design fatigue life. The inspection regime and the after-inspection procedures need to be determined by the fatigue assessment method as well.

The following main research question is formulated:

What is the most appropriate method to assess the remaining fatigue life of steel structures of existing STS cranes?

This main research question is supported by the following subquestions:

- What types of methods can be used to monitor the remaining fatigue life?
- What are the fatigue critical areas of a general STS gantry crane?
- What fatigue crack sizes can be tolerated?
- How can crack sizes be predicted using models in which cracks are not explicitly modelled?
- How can the maximum allowable inspection interval be determined?
- What crack repair methods are suitable for steel structures of STS cranes?
- What information is required to determine the remaining fatigue life of a STS crane?

1-4 Scope

The method that is created to determine the remaining fatigue life applies to the steel structures of existing STS cranes (this method is not intended for use as a design tool). This method concerns fatigue only, as calculations for static strength or buckling strength are assumed to be performed correctly during the design stage.

When a crane is used after its design fatigue life has expired, some details might need to be adjusted in order to maintain the required reliability of the structure. The assessment method created to estimate the remaining fatigue life of STS cranes should be able to determine the location of these details, however it does not need to be able to perform a redesign of these details.

It is assumed that the stresses across the structures of existing STS cranes are known in advance. Stress calculation procedures are therefore out of the scope of this research and will not be reviewed.

Economic evaluations to determine whether STS cranes with large amounts of fatigue damage should be repaired or replaced will not be performed by this model as this is regarded as a different type of problem.

1-5 Structure of the Report

The first stage of this research concerns a review of the existing standards on fatigue life assessment and is described in Chapter 2. Standards on aircraft, bridges and offshore structures are evaluated as well because these structures are subjected to variable amplitude loading (which is the type of loading STS cranes are subjected to). This step is performed in order to determine whether one or more of these assessment methods can be used as a basis for the assessment method for the remaining fatigue life of STS cranes.

Before the fatigue assessment method for steel structures of STS cranes can be presented, the steps that are part of this model are discussed. The first step (which is covered in Chapter 3) is to identify the areas which are critical with respect to the fatigue life of the crane. These areas need to be identified because they require more attention when it comes to monitoring the fatigue life compared to non-critical details.

The next step of this research is to determine the remaining fatigue life of a STS crane in case it contains fatigue cracks. To complete this calculation both the speed at which the crack grows and the critical crack size need to be calculated. This calculation procedure is explained and validated in Chapter 4.

The implementation of the calculation procedure that is developed in Chapter 4 is verified in Chapter 5. The sensitivity of this calculation model with respect to its parameters will be investigated as well. The sensitivity is determined to determine the parameters that have the most influence on the (remaining) fatigue life of the crane.

To use the calculation model presented in Chapters 4 and 5, the location and size of fatigue cracks need to be known. In order to determine the location and size of fatigue cracks, the crane is subjected to an inspection. Chapter 6 therefore concerns the procedures that can be used to detect cracks and measure their size. The reliability of crack detection methods is discussed as well, as it influences the set-up of inspection regimes.

In case the structure of the STS crane reaches its calculated fatigue life, its fatigue life might be extended by repairing the fatigue cracks. The procedures which can be used to repair fatigue cracks at steel structures of STS cranes and their effects on the remaining fatigue life of the crane are investigated in Chapter 7.

The steps taken in the assessment method for the remaining fatigue life of STS gantry cranes are discussed in the previous chapters. The fatigue assessment method can therefore be discussed in Chapter 8. This method consists of calculation procedures for the remaining fatigue life, set-up of inspection methods and determination of the type of repair works.

The fatigue assessment method presented in Chapter 8 is visualized in Chapter 9. The fatigue assessment method is applied to an existing model of a crane to provide an example of fatigue assessment of existing STS cranes.

Chapter 10 contains the conclusion to this research. This chapter contains the answers to the research questions and provides recommendations for further research.

Standards on Fatigue Life Assessment

Bridges, offshore structures and aircraft are subject to variable amplitude loading (like cranes), therefore the fatigue life assessment methods for these structures are reviewed to determine whether one of these methods is suited to determine the remaining fatigue life of STS cranes. An overview of the different methods described in these standards is presented in this chapter, along with alternative methods. The fatigue life assessment methods are considered to determine whether one or more of these methods can provide a basis for the assessment method for the remaining fatigue life of existing STS cranes.

2-1 Standards on Inspection of Cranes

According to the EN 15011 design standard for cranes, the inspection intervals should be included in the operating manual and the intervals must be decided upon by the manufacturer of the crane [7]. Reference [14] advises to inspect the entire crane at fixed intervals, with a proposed time between inspections of three months.

The International Organisation for Standardization (ISO) standard 9927:1-2013 covers inspection procedures for cranes and is also based on fixed inspection intervals [15]. The inspection interval for regular inspections is three months (and an extensive regular inspection must be performed once a year).

However when an 'expert engineer' has estimated the remaining fatigue life and was in charge of the latest major inspection, the regular inspections can be dropped. The minimum requirements for an engineer to be a qualified 'expert engineer' are defined in ISO 9927:1-2013 [15]. In case the regular inspections are discarded, the condition of the crane must be thoroughly reassessed within five years.

2-2 Standards on Inspection Of Bridges

Different standards with respect to inspection of steel bridges exist, each applying a different method to determine the remaining fatigue life of the structure. These methods are explained in the following five subsections. Methods relating to inspection of bridges that are not included in standards are explained as well.

2-2-1 Fatigue Life Assessment by Classification

One standard on inspection intervals concerning steel bridges is the standard regarding inspection of fatigue prone details in Oregon (U.S.) [16]. The procedure in this standard requires the following information:

- Load range imposed on the structure
- Degree of redundancy of members which are prone to fatigue
- Tendency of material or particular details to cracking
- Condition of the details which are prone to fatigue
- Difference between experienced and predicted load cycles on the bridge

This procedure consists of two assessments; one assessment regarding the condition of the detail and one concerning the criticality of the detail. The assessment of the criticality of a detail is based on its fatigue category (which is defined by the standard) and the estimated number of stress cycles that the bridge will experience. The estimated number of stress cycles is determined using the Average Daily Truck Traffic (ADTT) figure which must be representative for the traffic volume across the bridge.

The details are inspected to assess their condition. The outcomes of these two assessments are used to categorize details of the bridge in specific classes. A specific fixed inspection interval is given for each class. The fatigue life is thus monitored by an inspection regime, where the intervals are determined using a classification system [16].

2-2-2 Fatigue Life Assessment According to the Eurocodes

The Eurocode standard which is applied in memberstates of the European Union (EN 1990) contains a different approach. This standard is used to evaluate the fatigue life in the design stage, the remaining fatigue life is in this case the difference between the amount of cycles that have been performed and the design fatigue life. The Eurocode standard for steel bridges specifies the magnitude of the loads, taking the trends in road transportation volumes into account [17]. Currently there is no agreement on the magnitude of these loads, as some nations have provided alterations to this load specification. The alterations concern prescribed loads which are higher than recommended in the Eurocode or traffic loads which are based on regional traffic data [17].

Two fatigue safety concepts can be applied according to the Eurocode; the safe-life concept and the damage tolerant design concept [17]. The damage tolerance concept is used for structures where fatigue failure is preceded by early warnings (in the form of fatigue cracks). This concept requires in service inspection of the structure in order to monitor and eventually repair the fatigue cracks. The inspection intervals according to this standard decrease over time to reflect the progressive nature of the fatigue process.

The safe-life concept can also be applied during the design stage, according to this concept failure of the any part of the structure during its design fatigue life must be prevented. This is different to the damage-tolerance concept (that may also be applied during the design stage), because local failure is permitted in the damage-tolerant concept as long as this does not lead to the collapse of the entire structure. The structure must remain stable upon local failure. The difference in methods is reflected by the allowable stress amplitude, which is lower for the safe-life concept.

The assessment of these methods is performed using S-N curves, which describe the relation between the number of load cycles and the corresponding allowable stress amplitude (see Figure 2-1). These curves are used to select an allowable stress amplitude for a given number of cycles that the structure will be subjected to during its service life.

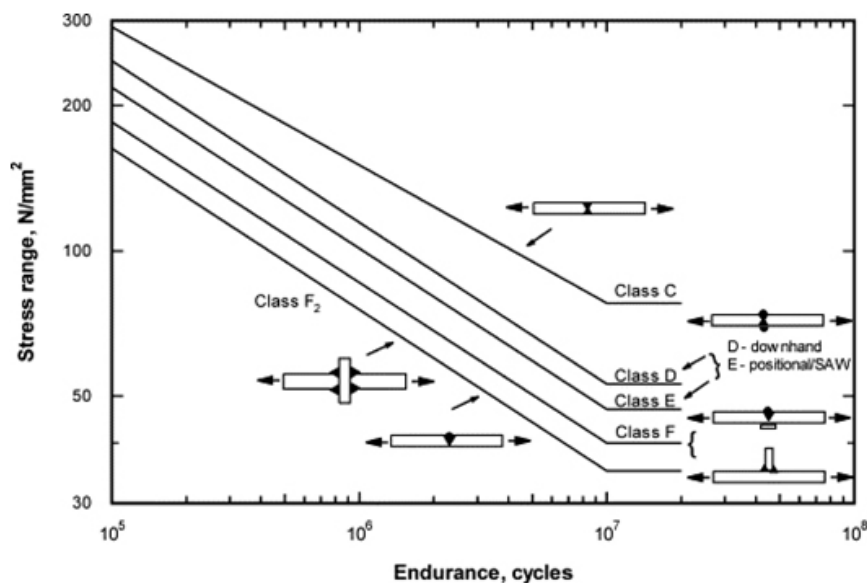


Figure 2-1: Example of S-N curves which describe the allowable stress range as a function of the amount of load cycles for different connection classes (source: www.twi-global.com).

The safe-life concept recognizes that fatigue cracks may not always be detected (because details are hard to reach or crack growth lives are short). Therefore the structures designed to the safe-life concept have a fixed fatigue life, after which the structure is taken out of service [17]. Structures designed to the damage tolerance concept can remain in service as long as the fatigue life is monitored adequately.

2-2-3 Fatigue Life Assessment Based on Crack Growth

A detailed procedure which is able to determine inspection intervals for steel bridges is explained in Reference [18]. The first step of this procedure uses S-N curves to determine the details which are critical with respect to fatigue failure. The S-N curves are also used to schedule the first inspection of these critical details.

When a crack could not be found upon inspection, it is assumed that the crack size is equal to the smallest crack size which can be accurately determined. The inspection interval is equal to the time it takes for the initial crack size to grow to a critical size (causing failure of the material). This is calculated by dividing the difference in initial and critical crack size by the crack growth rate. The crack growth rate is determined using the Paris equation (which is explained in Chapter 4). The calculation method for the critical crack size is not mentioned in this paper [18].

2-2-4 Fatigue Life Assessment by LEFM

A method to assess the fatigue life of bridges that is not yet included in a standard uses a Linear Elastic Fracture Mechanics (LEFM) model, which aims to extend the inspection intervals mentioned in current U.S. standards [19]. This method is similar to the previously discussed method, except that the critical crack size is calculated.

An initial crack size is chosen based on the type of construction detail and manufacturing methods used. The number of stress cycles in which the crack grows from the initial crack size to the final crack size (which is taken as a percentage of the critical crack size) is subsequently calculated. This number of cycles to failure is divided by the number of stress cycles that are imposed on the bridge each year in order to determine the inspection interval. It is expected that this method will eventually replace the current U.S. standards [19].

2-2-5 Fatigue Life Assessment Based on Data Analysis

Another method developed to monitor the fatigue life of railway bridges in India combines S-N curves with measurement data. This analysis requires the bridge to be fitted with strain gauges, which are used to determine the stress in the material as a function of time. From the measurement data the stress cycles are determined and the damage of each cycle is evaluated using a S-N curve with a 2.3 % probability of failure. The accumulated fatigue damage is calculated using the Palmgren-Miner rule (this rule is explained in Chapter 8).

The failure criterion is equal to an accumulated fatigue damage of one [20]. The remaining fatigue life is therefore defined as the number of cycles until the accumulated fatigue damage becomes equal to one. This method is created for real-time evaluation of the structure according to the safe-life concept.

Reference [21] contains an inspection method for bridges. This method covers the procedure for correct inspection of bridges and the manner in which the data is supposed to be processed. This detailed description of an inspection program set-up method can be used as a basis for inspection of STS cranes.

2-3 Standards on Inspection of Offshore Structures

This section concerns several standards with respect to the procedures that are used in the offshore industry to determine the (remaining) fatigue life. A number of these procedures are implemented in the design stage alone, while others can be used to determine the remaining fatigue life of existing structures.

Structures used in the offshore industry (such as platforms, semisubmersibles and Floating Production, Storage and Offloading (FPSO) vessels) are designed according to S-N curves. These curves are based on measurement data, which have a significant amount of scatter. The scatter is assumed to be normally distributed and two standard deviations are subtracted from the mean value of the dataset. This means that the S-N curves used in design of offshore structures are constructed with a 97,7 % probability of survival [22]. This figure is therefore considered as the minimum fatigue reliability of a structure used in the offshore industry.

2-3-1 Fatigue Life Assessment by LRFD

A method which can be used to determine the fatigue life of an offshore structure according to the Det Norske Veritas (DNV) is the Load and Resistance Factor Design (LRFD) method. The loads that are applied to the structure are multiplied by a safety factor to determine the minimum fatigue resistance of the structure. The safety factors reflect the uncertainty in the determination of loads and the uncertainty in material properties.

When the calculated fatigue resistance of the structure is higher than the calculated fatigue damage due to cyclic loads, the design meets its required service life [23]. This method is in effect equal to the safe-life concept and is also not suited to determine the fatigue life of existing structures. The working principle of this concept is visualized in Figure 2-2.

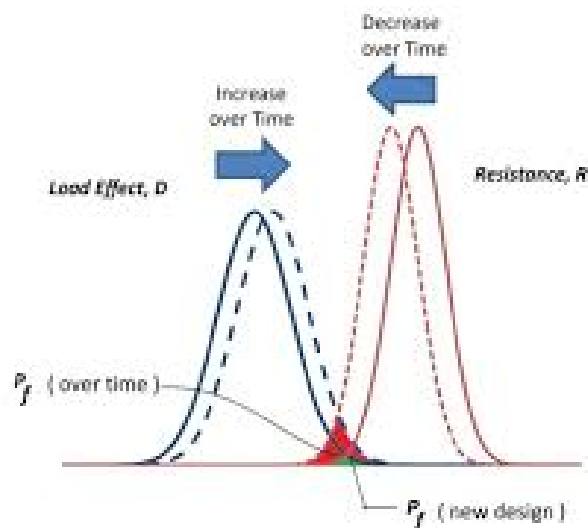


Figure 2-2: Example of the LRFD method, where the load effect and fatigue resistance curves are shown. (source: www.pwri.go.jp)

2-3-2 Fatigue Life Assessment Using SCF's

The fatigue life of offshore structures can also be evaluated using the Stress Concentration Factor (SCF) concept. These factors are applied to notches in the structure to calculate the stress directly at the notch. The stress at the notch is equal to the average stress over the cross-section of the material multiplied with the stress concentration factor.

The resulting notch stresses are subsequently compared to the allowable stresses (obtained using appropriate S-N curves) to determine the fatigue life of the detail under consideration. An overview of standard values for stress concentration factors for design details often used in the offshore industry is included in the DNV-RP-C203 design standard [24]. These factors can therefore be used to calculate the stresses by hand. This method is thus suited to directly determine the remaining fatigue life subject to the safe-life or damage-tolerant concepts. This method is therefore a relative quick fatigue life assessment method, because the SCF's and allowable stresses are tabulated in design standards.

The stresses at notches can also be determined by Finite Element Analysis (FEA) software. Recommendations for the implementation of Finite Element Method (FEM) models for offshore structures are given in Reference [25].

2-3-3 Fatigue Life Assessment Correcting for Measurement Error

A proposed DNV standard which concerns inspection of existing offshore structures is included in Reference [1]. This method uses S-N curves to plan the first inspection and to identify the construction details with the shortest fatigue lives (because these details need to be more frequently inspected than others).

The intervals between inspections are determined using fracture mechanics. The fracture mechanics models used in the offshore industry often ignore the crack initiation period and only regard the crack growth process. The crack initiation period is ignored because fatigue cracks at welds (especially weld toes) have a negligible crack initiation period compared to the crack growth period [1].

This method takes the distribution of crack size caused by measurement error into account. A distribution of the 'real' crack size is constructed using the known deviation of the measurement method. This crack size distribution translates to a distribution regarding the amount of cycles it takes for the crack to grow to a critical size. This 'time to failure' distribution is sampled at a pre-determined reliability to obtain the desired inspection interval [1]. The working principle of this method is illustrated in Figure 2-3.

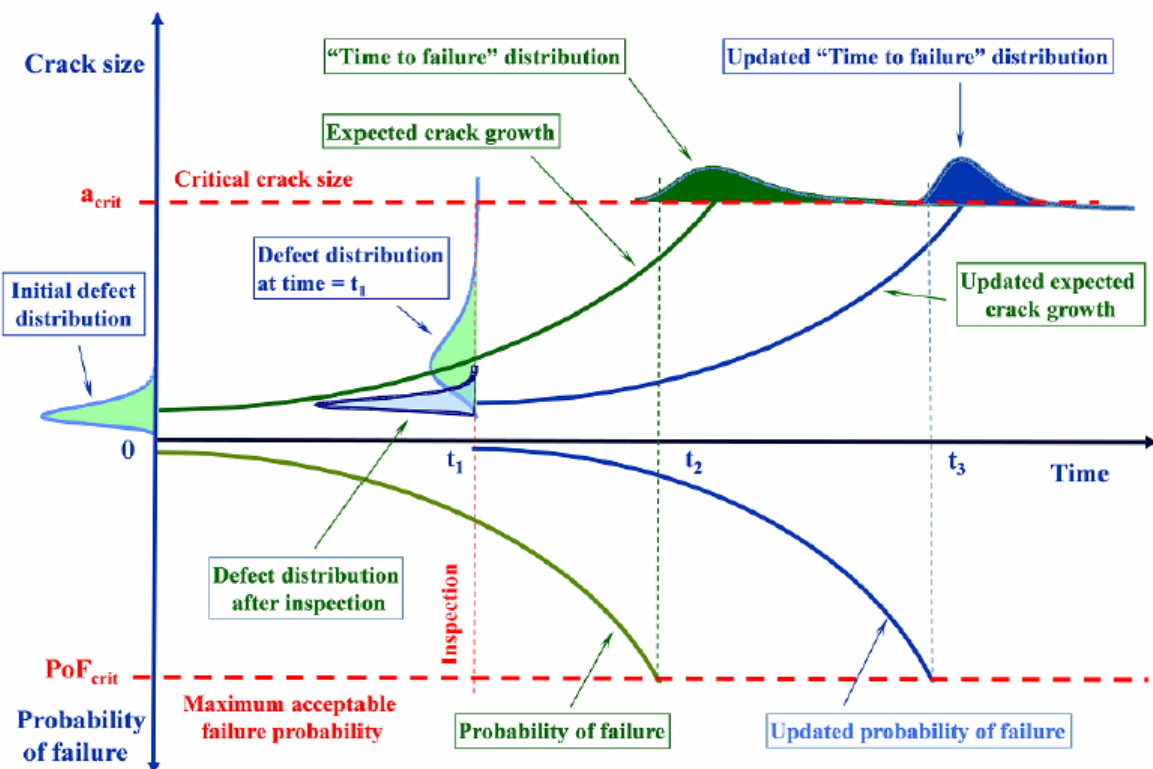


Figure 2-3: Illustration of the probabilistic method to determine the remaining fatigue life of offshore structures. The initial defect distribution is converted to a time to failure distribution (green line), which is sampled at a given value of the probability of failure to obtain the remaining fatigue life. The crack size distribution found at the inspection performed at t_1 deviates from the calculated distribution (blue line), therefore the remaining fatigue life is updated (source: [1])

Inspections are performed to find potential cracks and determine their length, the measured crack lengths are then compared to the calculated values. When the measured and calculated crack lengths deviate, the remaining fatigue life is updated. The subsequent inspection is scheduled when the crack length is calculated to exceed a threshold (for instance a percentage of the critical crack length).

2-3-4 Fatigue Life Assessment Accounting for Corrosion

Special consideration needs to be paid to the effect of corrosion on the fatigue life of offshore structures [26]. Although the corrosion rate of STS cranes is less than the rates which are common in the offshore industry, the inspection procedure of STS cranes generally includes checks on corrosion. When the STS crane is subject to a significant amount of corrosion, its fatigue life is reduced. The effect of corrosion on the remaining fatigue life of the crane should therefore be taken into consideration for cranes with large amounts of corrosion.

Reference [27] contains a method which is able to calculate the remaining fatigue life of members which are subject to corrosion. The first step expresses the hot spot stress function as a function of the corrosion rate. Corrosion is assumed to reduce the cross-sectional area and create additional stress concentrations (due to the increased surface roughness). The stress range therefore changes over time, which is accounted for by a time-dependent scale parameter. The final step expresses the safety margin for fatigue failure as a function of the geometry, the number of stress cycles per year, the crack size, the scale parameter and the material properties [27]. The safety margin can then be evaluated to obtain the service life at a given probability of survival.

2-4 Standards on Inspection of Aircraft

This section covers the methods that have been developed in order to assess the fatigue lives of aircraft. Inspection and maintenance procedures in the aviation industry are not performed to a universal standard. Instead, the airlines themselves provide the inspection and maintenance program, which needs to comply with the requirements set by the aircraft manufacturer [28]. The inspection requirements of the manufacturer in turn need to be approved by the Federal Aviation Authority (FAA) [29]. The guidelines provided by the FAA are therefore considered to be the industry standard for inspection and maintenance procedures for aircraft.

2-4-1 Damage Tolerant Design Philosophy

The airworthiness directives (which are the design standards aircraft have to conform to) adopted the damage-tolerant design philosophy early on [30]. A design is damage-tolerant when it is able to endure a limited amount of damage while the structure is in service. This philosophy therefore requires regular inspections to monitor the fatigue damage of the structure. When a crack is found with a length exceeding the repair threshold it should be repaired, otherwise the structure can remain in service.

The current certification procedure for aircraft requires the structures to be damage-tolerant except for the locations where this approach would cause unreasonably high penalties [31]. When supplied with data on material properties, loads applied to the structure and maintenance records, the crack growth rate can be calculated using a fracture mechanics model. The time between crack initiation and fatigue failure can then be calculated using the value for the crack growth rate [31].

The load spectrum that is used in the fatigue analysis of aircraft is standardized [32]. This spectrum consists of cycles with different load amplitudes, each cycle causing a different amount of fatigue damage. The contribution of the individual stress cycles are added together using the Palmgren-Miner rule, which ignores sequence effects (which means that dependence of the fatigue damage on the order in which the stress cycles are applied is not considered in the fatigue analysis) [33]. The Palmgren-Miner rule can be used to determine the amount of fatigue damage according to the damage-tolerant design concept.

The values for the material properties (like the yield strength and allowable stress range) are based on test data. However, data obtained from fatigue test specimens contains a lot of statistical variability (even under laboratory conditions). The test data is therefore fitted to a two-parameter Weibull distribution and subsequently sampled at a predetermined reliability to obtain the properties that can be used in the fatigue analysis using the damage-tolerant design concept [34].

When cracks are found in the structure, crack growth models are used to calculate the remaining fatigue life. This step is performed even when the structure is built according to the damage-tolerant design principle.

2-4-2 Widespread Fatigue Damage Concept

In 2013, the FAA amended the allowed procedures in order to account for Widespread Fatigue Damage (WFD). WFD occurs when multiple cracks are aligned with respect to each other. The loads that are imposed on the hull of the aircraft cause the cracks to grow towards each other. As a result, the stress across the uncracked area between the cracks increases, which in turn increases the crack growth rate. This process accelerates over time until the cracks merge, creating a large crack which can cause structural failure [29].

Due to this interaction, the maximum allowable crack lengths of individual cracks are lower when several cracks are present in the structure. The maximum allowable crack size is in this case not the size at which the member fails, but the size which causes the cracks to merge into a crack equal to the critical crack size.

A well known example of this type of fatigue failure is the accident involving Aloha Airlines flight 243 on April 28, 1988 [35]. Small fatigue cracks originated at rivet holes and merged to form a large fatigue crack across multiple holes. The following explosive decompression tore a large part of the skin off the aircraft. The aftermath of this accident is depicted in Figure 2-4.



Figure 2-4: Aftermath of the accident of flight 243, which was caused by a fatigue failure originating from multiple locations (source: www.nytimes.com)

A Limit of Validity (LOV) should also be defined (in flight hours, flight cycles or both) for which it is demonstrated with sufficient accuracy (by analysis, tests or maintenance records) that the aircraft meets the reliability target with respect to WFD failure. Consequently, an aircraft may not be operated once this LOV is reached [29].

2-4-3 Fatigue Life Assessment by Probabilistic Fatigue Reliability Calculations

Several procedures are developed to calculate the fatigue reliability of aircraft. One example is the method described in Reference [36]. The safe life of the structure with a prescribed reliability is determined in the first stage of this method. The safe life can be calculated when the median test life and the scatter factor for fatigue are known. The scatter factor for fatigue can be calculated assuming that the variation in fatigue lives follows a specific probability distribution. The next stage is to determine the confidence interval of the fatigue damage measurements themselves.

The safe life of the structure and the confidence interval of the measurements are subsequently used to determine the probability of survival [36]. The aircraft should be inspected when the probability of survival drops below a certain threshold. The aircraft is therefore operated at a minimum reliability with respect to fatigue failure. This method is currently not in use, because for this method to be effective a lot of tests are required which increase the cost of operating the aircraft.

2-5 Fatigue Damage Monitoring Methods

The previous sections concerned methods that were able to determine the service life of a structure using standardized load cases. Because the (rate of) fatigue damage of a structure highly depends on its loading, the remaining fatigue life might be more accurately determined when the loads are measured. The methods that can be used to monitor the fatigue damage of STS cranes are therefore discussed in this section.

2-5-1 Evaluating Crack Growth by Marking

One method which is not considered in standards on design and inspection of cranes, aircraft, bridges and offshore structures is marking of fatigue cracks. When a fatigue crack is detected, the end of the crack can be marked using a line (which should be clearly visible to the observer). The propagation of the crack with respect to this line can then be determined by visual inspection. An example of this method is shown in Figure 2-5. This figure shows bolted connections that are marked in order to determine whether the bolts have turned during operation or not.



Figure 2-5: Marking of bolted connections to determine whether the bolts have turned during operation (source: www.appliedbolting.com)

The crack growth rate can be determined when the growth distance (distance between the crack tip and the marking line) and the time (between time of measurement and time of marking) are known. The measured crack sizes and the crack growth rates can be used to verify a crack growth calculation method. When the measured crack growth rate is significantly larger than the calculated crack growth rate, the fatigue life assessment might be erroneous.

2-5-2 Evaluating Fatigue Damage by Load Measurements

In the design process (as well as the majority of fatigue life assessment methods), the loads on the structure are estimated based on standards. The design loads can be verified by measurements of the loads that are lifted by STS cranes. This information can subsequently be used to evaluate the fatigue damage using the Palmgren-Miner rule.

The loading of container cranes can be easily determined due to the discrete nature of the handling process. Reference [4] mentions four ways to determine the weight of the container at container terminals. These methods are displayed in Table 2-1 and are explained below.

Table 2-1: Overview of existing container weighing solutions [4]

Measurement Method	Description	Reported Accuracy (percentage of full scale measuring range)
1	Place load cell on hoist of STS crane.	3-5
2	Weigh the terminal equipment and subtract the tare weight of the vehicles.	0.2-0.5
3	Measure pressure in lift cylinders of reachstackers.	>5
4	Measure the load on the twistlocks.	0.5-1

The first method measures the weight of the container using load cells placed at the hoist system of the STS crane itself. The measurement needs to be performed at a fixed height, because the weight of the ropes will otherwise have a considerable influence on the measurement. This system needs to be recalibrated regularly and it is not as accurate as other systems [4].

The second method concerns weighbridges which are used to weigh the terminal equipment that drives over it. The tare weight of the vehicle needs to be subtracted to obtain the weight of the container. The third method for weighing containers measures the pressure in the lift cylinders of reachstackers. Although the boom extension is often accounted for, the accuracy of this method is poor due to friction in the hydraulic cylinders [4]. The final method measures the load on the twistlocks in order to determine the load of the container. This method is very accurate and can be retrofitted to each type of spreader[4].

An alternative method to measure the load of the container is to measure the load on an Automated Guided Vehicle (AGV). The mass of the container can be derived from measurements of the positions of the springs or dampers [37]. This method is not likely to be accurate because wind loads cannot be filtered out of the signal. The mass of the containers can be significantly overestimated when wind loads are high.

Automated container terminals use a Terminal Operating System (TOS) to control the container inventory. The properties (like the weight, type and size) of the containers are stored in this system as well. The TOS will determine which STS crane will move a specific container [38]. Based on the information from the TOS a dataset can be constructed which connects the cranes at a terminal to the containers that have been handled. The fatigue damage can be updated after each move or it can be updated based on a sample of this database.

The load measurement at other types of cranes (for instance cranes with a grab operation) cannot be performed at other types of terminal equipment. The measurements of the load applied to these cranes can be performed by installing loadcells at the hoist to measure the weight of the ropes, grab and payload.

An example of measurements on crane load spectra is included in Figure 2-6. This data shows that the load spectra of a container crane and a bulk handling crane are different. The range of the load spectrum of bulk handling cranes is smaller, but the loads are higher. This information can be used to increase the accuracy of the fatigue life calculation, because the relation between the load spectrum and the stresses in the structure is linear. The load spectrum can be therefore be used to more accurately determine the magnitude of the stress cycles in the structure, which leads to a more accurate value for the fatigue life of the crane.

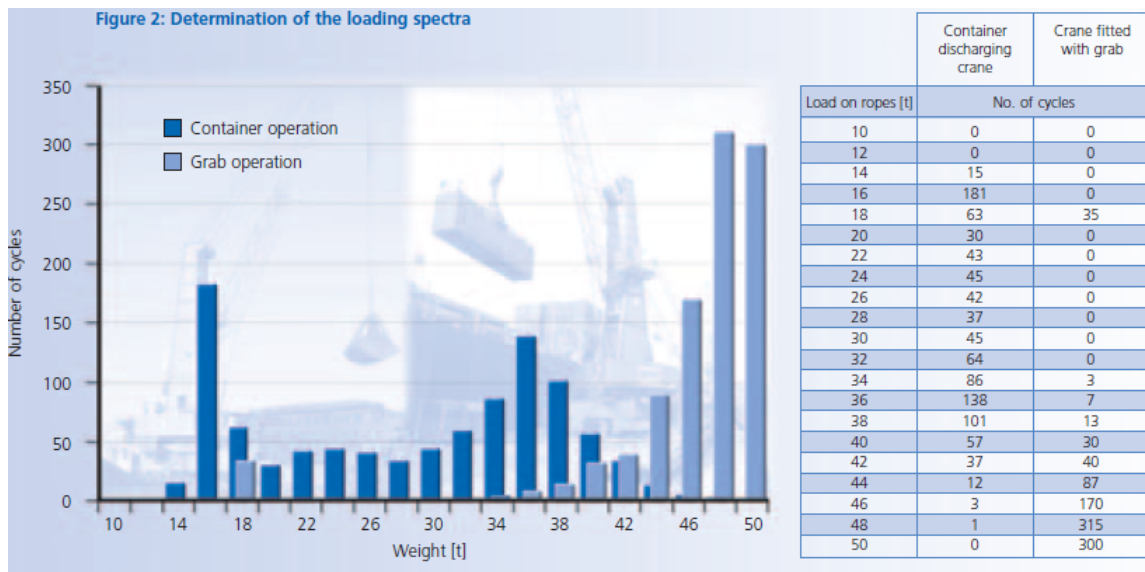


Figure 2-6: Illustration of loading spectra for container and grab cranes (source: [2]).

2-5-3 Evaluating Fatigue Damage Using Strain Gauges

The fatigue damage at a STS crane can also be determined using strain gauges. The strain gauges measure strain (percentage of elongation of the material) and use the relation between stress and strain to calculate the stress in the material.

The advantage of measuring stresses instead of applied loads is that the dynamic fluctuation of stresses can be measured as well. This means that the choice for dynamic load factors (used in the design standard for cranes to determine the stresses due to dynamic load fluctuations [6]) can be verified. Also, because the stress is measured (instead of derived) the data can directly be used in the fatigue life calculations.

The disadvantage of this method compared to the method of measuring the applied loads is that the stresses are measured locally. The data is therefore only representative of the part of the structure that is equipped with the strain gauge. This method is therefore mainly suited for checks of the most fatigue critical parts of the crane.

2-6 Overview

This section gives an overview of the fatigue life assessment methods that are discussed in this chapter. An overview of the assessment methods that are covered in this chapter is shown in Table 2-2.

Table 2-2: Overview of methods that can be used to determine the (remaining) fatigue life.

Method	Description	Reference
1	Fixed inspection intervals.	[15]
2	Engineering assessment of crane to determine amount of fatigue damage and remaining fatigue life.	[15]
3	Inspection interval determination using a classification system.	[16]
4	Safe-Life design philosophy (fatigue life is fixed at design stage).	[17]
5	Damage-Tolerant design philosophy; the structure is capable of handling a certain crack size. Remaining fatigue life is monitored by an inspection program.	[17]
6	Calculation of remaining fatigue life using a combination of S-N curves and a crack growth model.	[18]
7	Lifetime estimation using a crack growth model (both initial and final crack size are assumed to be known parameters).	[19]
8	Lifetime estimation using measurement data of the built structure to evaluate S-N curves.	[20]
9	Design method applying safety factors to the load and fatigue resistance to calculate the fatigue life of a structure.	[23]
10	Fatigue life calculation of details using stress concentration factors and S-N curves.	[24]
11	Remaining fatigue life calculation using a probabilistic method which accounts for measurement error.	[1]
12	Fatigue life estimation using a model which is able to account for the effect of corrosion on the fatigue life of the structure.	[27]
13	Damage-Tolerant design philosophy, where the remaining fatigue life is calculated by a fracture mechanics crack growth model.	[31]
14	WFD concept; the calculated critical size of a crack is adjusted to account for the event in which multiple cracks are in close proximity relative to each other.	[29]
15	Fatigue life estimation using a probabilistic method to calculate the fatigue reliability of a structure.	[36]
16	Crack size monitoring by marking of crack tips	
17	Fatigue damage monitoring by measuring the hoist load	
18	Fatigue damage monitoring by measuring stresses at the STS crane using strain gauges	

The methods which can be used to assess the fatigue life of steel structures can be roughly categorized as follows:

- Inspect the structure at fixed intervals.
- Fatigue life calculation in design stage (using the safe-life or damage-tolerant calculation methods).
- Fracture mechanics models; the remaining fatigue life is equal to the timeframe in which a crack grows to its critical size.
- Monitor the fatigue life by data analysis of the built structure.

Two types of methods are selected to assess the remaining fatigue life of existing STS gantry cranes. The first method uses the result of the fatigue life calculation that is performed in the design process [7]. Because the results of these fatigue life calculation are assumed to be available, it is convenient to use this information to determine the amount of fatigue damage when the crane is operated within its design fatigue life. When the service life of the crane exceeds the design fatigue life, another method is required to evaluate the remaining fatigue life. In this case a fracture mechanics model is deployed, which uses a crack growth model to calculate the remaining fatigue life of a structure.

Methods performing data analysis to estimate the (remaining) fatigue life of the structure are not considered in this research due to the high costs involved. These costs consist of the equipment cost (sensors and data acquisition system) as well as maintenance costs. The data still needs to be processed using S-N curves or a crack growth model to determine the remaining fatigue life of the structure. Therefore this type of assessment method is not considered to be an improvement over the aforementioned two types of methods.

Monitoring the fatigue life using fixed inspection intervals is not considered further because the remaining fatigue life cannot be determined. An assessment of the safety regarding operation of the crane can therefore not be made. This can only partly be overcome using short inspection intervals, but this means that downtime of the crane increases.

Identification of Fatigue Critical Details

In order to create a suitable method for the assessment of the remaining fatigue life of STS cranes, the areas which are critical with respect to the fatigue life of the structure need to be identified. The critical areas are identified because they need to be more frequently assessed due to the increased potential for fatigue failure.

First, an analysis is performed to identify the areas of the steel structure which experience high fluctuating loads. Large load fluctuations reduce the remaining fatigue life of the structure, thus the locations which are susceptible to large fluctuations need to be known in order to determine inspection intervals. The fundamental parts of steel structures of STS cranes are reviewed next to determine their failure modes with respect to fatigue. These failure modes need to be known in order to effectively set up inspection procedures.

3-1 General Fatigue Analysis of STS Gantry Cranes

At several locations across the structure of a STS gantry crane welds can only be applied at one side of the material, because it is not possible to weld from the inside of the structure. Examples of these locations are the connections at the forestay and the backstay (the locations of these parts are shown in Figure 3-1). As a result, the welds at the inside of these connections have a rough profile which enlarges the stress concentrations. Figure 3-2 shows this type of weld as viewed from the inside of the connection. The rough profile of the weld is clearly visible in this picture.

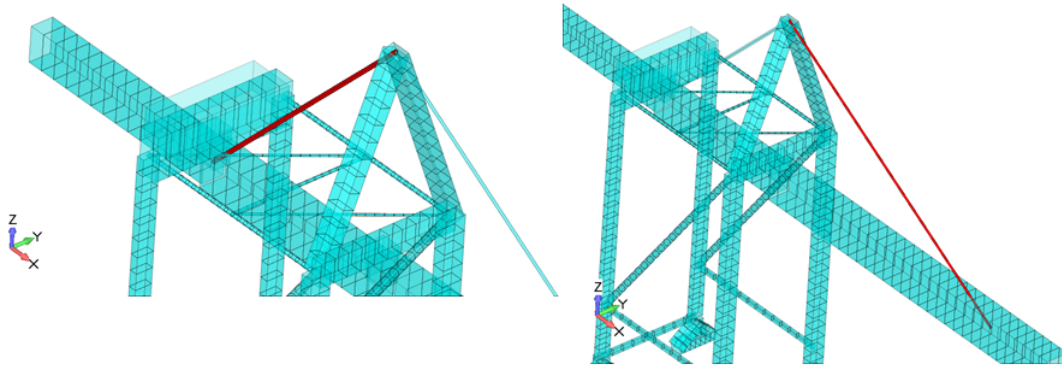


Figure 3-1: Indication for the location of and the the backstay (left) and the forestay (right) at STS gantry cranes.



Figure 3-2: A weld applied from the outside of the connection, as pictured from the inside of the structure (image provided by Cargotec).

The crack growth period becomes shorter when the stress concentration increases, therefore these connections are more susceptible to fatigue failure compared to welded connections which can be accessed from both sides. This needs to be accounted for during fatigue life assessment.

Another issue concerning the design and construction of STS cranes is mentioned in Reference [1]. This reference discusses the influence of heavily stiffened joints in steel offshore structures on the fatigue life. Heavily stiffened joints create large stress concentrations, this means that fatigue cracks can originate at several locations simultaneously [1]. Consequently, the fatigue life of the joint is reduced.

The previous considerations concerned specific types of constructional details which are likely to be affected by fatigue cracking. The remainder of this section concerns the fatigue sensitive areas of the general structure of a STS crane.

To illustrate the areas of STS cranes which are sensitive to fatigue failure, a FEM model of the steel structure of an existing STS crane is implemented in Femap and SDC Verifier. The loads that are applied to the model are in accordance with the FEM 1.001 design standard for hoisting appliances [39]. A fatigue utilisation check is programmed in SDC Verifier, this check displays the ratio of the stress in the structure and the allowable fatigue stress. The results of the analysis are shown in Figure 3-3.

A high ratio of the stress in the structure and the allowable fatigue stress indicates that the area is highly loaded with respect to fatigue. Fatigue cracks are therefore more likely to develop at these locations.

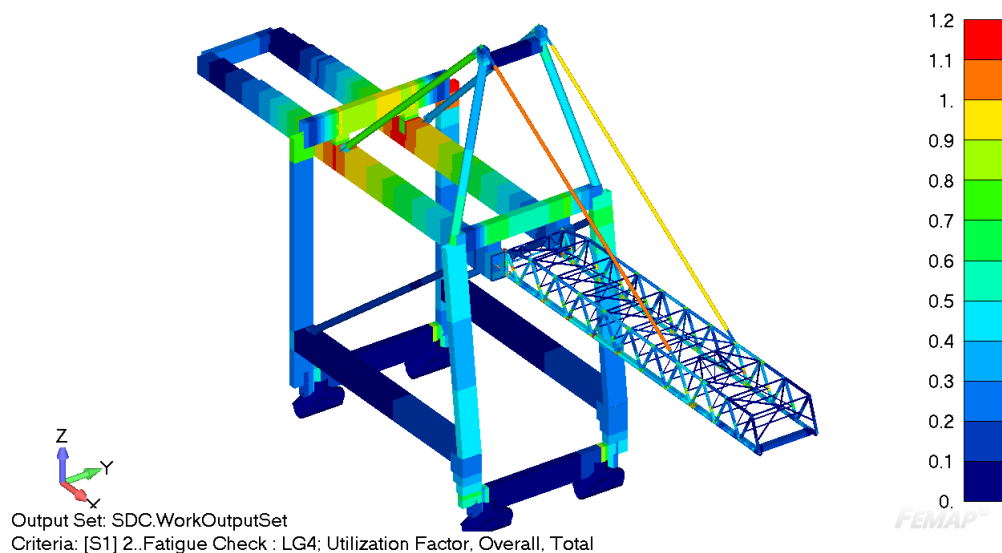


Figure 3-3: Result of the model used to illustrate the fatigue sensitive areas of the structure of a general STS gantry crane (image provided by SDC verifier).

As can be seen in this figure, the areas of STS cranes which are most sensitive to fatigue failure are:

- Connection between boom and forestay.
- Connection between boom and backstay.
- Connections between boom and the portal beams (beams connecting the top of the legs, running parallel to the quay wall).
- Base of the A-frame (triangular structure at the top of the crane).
- Connection between the legs and the portal beams.
- Connection between sill beam and the legs (the sill beam connects two bogie sets and runs parallel to the quay wall).

These areas are relatively sensitive to fatigue failure because they are subjected to relatively large load fluctuations. These load fluctuations are explained by the travel motion of the trolley. As the trolley (with or without payload) moves along the boom, the position of the load on the boom changes. The loads on the boom are transferred onto its supporting structure before they are transferred onto the legs of the crane. The members which are part of this loadpath are therefore subjected to these changing loads as well (which can be seen in Figure 3-3).

3-2 Fatigue Failure Modes of Fundamental Parts of Steel Structures

The steel structure of a STS crane consists of four fundamental parts (base material, welds, bolts and pins) according to the EN 13001 design standard. The steel structure is constructed using plates (often referred to as the base material) which are connected in one of three possible ways; welded connections, bolted connections and pinned connections. The failure modes of these fundamental parts with respect to fatigue failure are evaluated in this section.

3-2-1 Fatigue Failure Modes of the Base Material

Fatigue cracking of the base material is a failure mode that is especially of concern in components which are subject to Low Cycle Fatigue (LCF) [24]. Low cycle fatigue is characterised by high stress amplitudes, plastic deformation and a short fatigue life. Because STS cranes are designed for long fatigue lives (which implies that the structure is subject to relatively low stress amplitudes) fatigue cracking of the base material is of less concern.

Experience with STS crane inspections also shows that cracking of the base material is rare. Additionally, most of the fatigue cracks that are found in the base material are initiated at welds. However, fatigue cracking of the base material can occur when a material with initiated faults is used to construct the STS crane. Therefore this failure mode needs to be accounted for in the fatigue assessment method.

3-2-2 Fatigue Failure Modes of Welded Connections

The majority of fatigue cracks in welded steel structures originate at the welds because the welding process creates faults in the lattice structure (which is the arrangement of molecules relative to each other) of the base material near the weld. This area around the weld is called Heat Affected Zone (HAZ). When the lattice structure is subjected to fluctuating tensile stresses, the faults will move towards each other until a crack is initiated. This means that the crack initiation period in and around welds is negligible compared to the unaffected base material [1].

Fatigue cracks at welds often originate from the weld toe or the weld root. Figure 3-4 shows the locations of the root and toe for a butt weld. Weld root cracks are often considered to be more dangerous than weld toe cracks because they are only apparent when the crack has grown through the thickness of the weld (assuming the welds are only inspected from one side) [40].

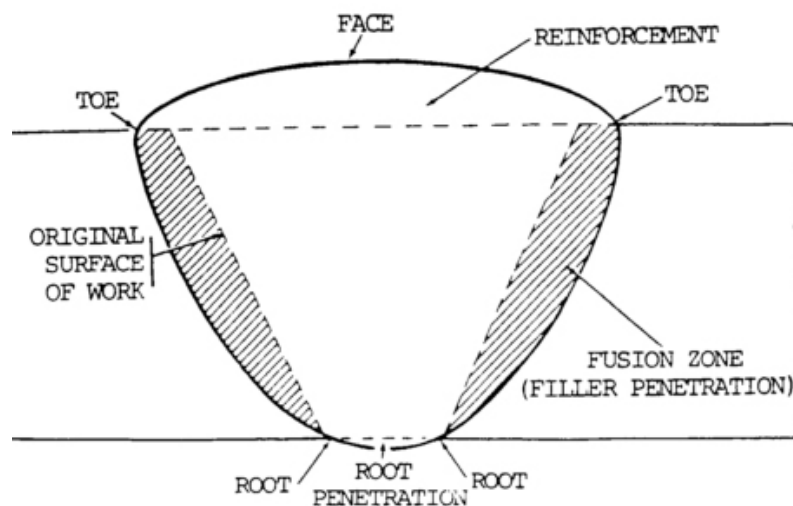


Figure 3-4: Location of the root and toe of a butt weld (source: www.weldersuniverse.com).

The surface of welds often have a rough profile compared to the base material, which creates stress concentrations. These stress concentrations further enhance crack growth, reducing the fatigue life of the welded connection even more [10]. Additionally, the welding process creates residual tensile stresses which reduce the fatigue life of the welded connection as well. These residual stresses are introduced when the area surrounding the weld cools down to the ambient temperature. The magnitude of the residual stress depends on the weld penetration, root opening distance and the number of passes of the welding tool [40].

When welds are not fully penetrated, a void is created at the weld root which acts as an initial crack. A root crack will then immediately develop when the material is subjected to fluctuating stresses. Slag intrusions which might be introduced during the welding process can also initiate fatigue cracks because the slag creates a local discontinuity in material properties of the weld.

3-2-3 Fatigue Failure Modes of Bolted Connections

Fatigue failures of bolts occur in three locations, the majority (65%) of fatigue fractures are located at the first thread which is engaged in the nut (which is the part of the nut closest to the bolt head) [10]. Another 20 % of the fatigue fractures occur at the thread runout and 15% of the fatigue failures occur at the radius (transition between shank and head). Figure 3-5 shows the terminology used for bolted connections in order to clarify the positions of the aforementioned locations.

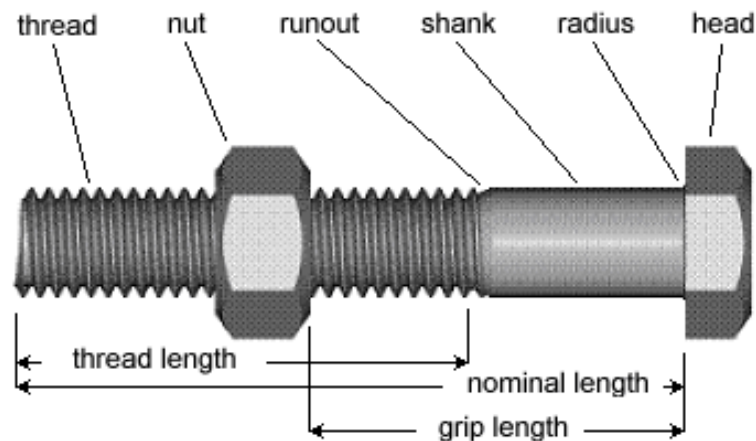


Figure 3-5: Terminology used in bolted connections (source: www.martinrobey.com).

Bolted connections of STS cranes are currently inspected on a random basis, because it is not practical to check every bolt of the crane. The inspection procedure determines whether the bolts have come loose or not. From experience gained by inspections of STS cranes it is determined that fatigue failure of bolts is extremely unlikely. The fatigue life of bolted connections are therefore only assessed when the service life of the crane is extended beyond the design fatigue life. The inspection procedure of bolted connections will be equal to the method currently used at Cargotec. This inspection method consists of tapping the bolt head with a hammer, the generated sound indicates whether the bolt has failed or not.

When bolted connections are overhauled, the bolts need to be replaced. Experience shows that when a bolt is removed and put back again, the fatigue life of the connection is severely reduced [10]. Therefore failed bolts should always be replaced instead of repaired.

3-2-4 Fatigue Failure Modes of Pinned Connections

Pinned connections allow for rotation about one axis, while the three translation directions as well as the remaining two axes of rotation are restrained. These connections are for instance used to construct the hinge points in the boom, so the boom can be raised when the crane is out of operation. Pinned connections are constructed using three plates and a shaft, the arrangement of these parts relative to each other is displayed in Figure 3-6.

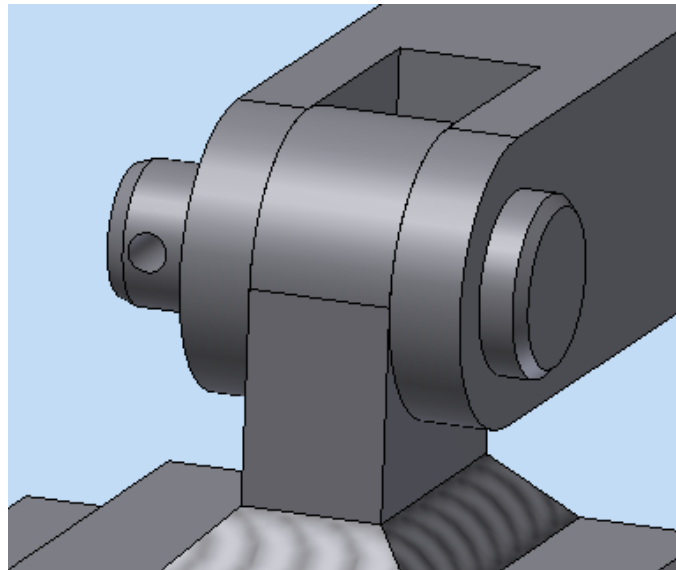


Figure 3-6: Depiction of an assembled pinned connection (source: www.synergiscadblog.com).

The pin itself is often an unnotched part (this means that this part does not contain stress concentrations), therefore this part is not sensitive to fatigue cracking. Sometimes a notch is created due to lubrication grooves, but these notches only have a small influence on the fatigue life of the pin. However, fatigue cracks can develop in the plates which are designed to lock the shaft into place.

Experience gained by inspections of STS cranes shows that fatigue cracking of the pins themselves does not occur. Therefore the fatigue life of the pins will not be monitored, they are only assessed when the service life of the crane is extended.

3-3 Conclusion

The global locations of the steel structure of STS gantry cranes which are prone to fatigue failure are listed in Table 3-1. This table also includes the reasoning behind the assessment. The term loadpath is used here to indicate that the location transmits relatively large fluctuating loads which are created by the movement of the trolley. These large fluctuating loads have a detrimental effect on the remaining fatigue life.

The connections of the forestay and backstay are also under consideration because they can only be welded from the outside, which means that the surface at the inside of these connections has a rough profile, which is detrimental to the fatigue life of the connection.

Table 3-1: Global areas of the crane that are prone to fatigue and the reasoning behind this assessment.

Location	Reason
Connection boom and forestay	Loadpath and inaccessible welds
Connection boom and backstay	Loadpath and inaccessible welds
Connection forestay/backstay and A-frame	Inaccessible welds
Connection between boom and portal beams	Loadpath
Base of the A-frame	Loadpath
Connection legs and portal beams	Loadpath
Connection sill beam and legs	Loadpath

It is determined that the majority of fatigue cracks at STS cranes are initiated at welded connections. The main types of weld defects which enable cracks to be initiated quicker or cracks to grow faster are listed in Table 3-2. Fatigue failure at welds is the most important failure mode when it comes to fatigue at STS cranes.

Table 3-2: Summary of the types of defects that are associated with welded connections

Defect Associated with Welds	Description
HAZ	Heat from the welding process creates faults in the lattice structure of the base material surrounding the weld.
Geometry of weld	The shape of the weld creates geometric stress concentrations.
Roughness of weld	Surface roughness of weld profile creates stress concentrations.
Residual tensile stresses	Tensile stresses introduced in and around welds which are initiated when the weld cools down.
Voids	Voids between weld and base material act as an initial crack.
Slag intrusion	Discontinuity in material properties introduced by slag intrusion acts as an initial crack.

A minor contribution of fatigue cracking at STS cranes comes from fatigue cracks in the base material. Fatigue cracking of bolts is not considered to be significant and cracks at pins (used in pinned connections) are not encountered in practice. The fatigue assessment method therefore focusses on fatigue cracks in welds and base material.

Crack Growth Calculations

A material will fail when a crack becomes equal to its critical crack size. So to determine the remaining fatigue life of an existing STS crane, the time that it takes for a crack to reach its critical crack size needs to be calculated. The calculations regarding the critical crack size and the crack growth rate are subject of this chapter.

4-1 Calculation of the Critical Crack Size

This section on the calculation procedure of the critical crack size is divided into four subsections. The first subsection explains the concept of the critical crack size. The second subsection concerns the Griffith equation for the critical crack size, which can be used to calculate the critical crack size for any given load.

The concept of the stress intensity factor is explained in the third subsection. This factor will be used in the calculations of the critical crack size and the crack growth rate (which is subject of the next section). The final subsection describes the stress approximation models which can be used to calculate the stresses in plates and the implications of these models with respect to the calculation of the critical crack size.

4-1-1 Theory Behind the Critical Crack Size

The steel used in STS cranes can be subjected to elastic and plastic deformation. With respect to fatigue, elastic deformation is associated with High Cycle Fatigue (HCF) while plastic deformation is associated with LCF. Cranes are designed for relatively high fatigue lives and the design codes prohibit stresses higher than the yield strength of the material [6]. Therefore, LEFM (which assumes linear elastic material behaviour) is suited to calculate the critical crack size and crack growth rate for the structure of a STS crane [41].

When a crack grows, the strain energy (which is stored in a body undergoing deformation) will be released. At the same time, energy is required to break the bonds between the atoms in the material. Therefore a crack will only grow when the released strain energy is at least equal to the energy required to break the atomic bonds [41].

The relation between the release of strain energy and the crack size is quadratic, while the energy used to break the atomic bonds is a linear function of the crack size [42]. The relation between the total energy associated with the crack and the crack size is therefore parabolic. The critical crack size is the crack size at which the total energy reaches its maximum.

For shorter crack lengths, the total energy increases for each increase in crack size (given a constant load). This means that input of energy is required for the crack to grow, therefore the crack growth process will be stable. When the crack size grows beyond its critical crack size, the total energy reduces for each increase in crack size (this means that energy is released during this stage of crack growth). The crack will grow without additional energy input and the crack growth process becomes unstable. This means that the velocity at which the crack grows becomes very large, leading to a sudden failure of the member [41].

Figure 4-1 displays a schematic plot of the energy input associated with breaking the atomic bonds (here called the surface energy) and the release of strain energy with respect to crack size. The total energy (sum of surface energy and strain energy) with respect to the crack size is displayed as well.

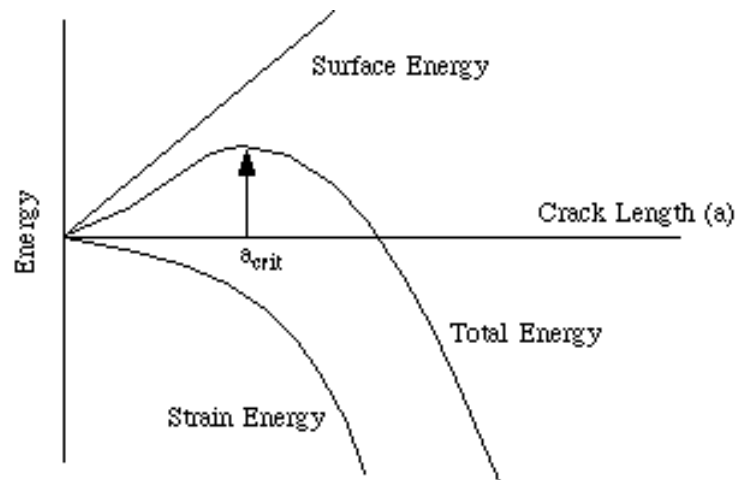


Figure 4-1: Schematic plot of the surface and strain energy as a function of crack size (source: <http://www.mse.mtu.edu/>).

4-1-2 Griffith Equation for the Critical Crack Size

The Griffith equation is an expression that can be used to calculate the critical crack size. This equation describes the derivative of the total energy with respect to crack size, which is set to zero so the crack size where the total energy is at its maximum can be calculated. Griffith assumed a through-thickness elliptical crack in a plate of infinite width and he formulated the critical crack length as Equation 4-1 [41]. In this equation γ represents the surface energy, σ_{fail} represents the tensile stress at which the material will fail (this is the maximum tensile stress in the structure for all loadcases) and E represents the Young's modulus. The stress at which the material fails is assumed to act in a direction normal to the crack.

$$a_{crit} = \frac{2\gamma E}{\pi \sigma_{fail}^2} \quad (4-1)$$

This equation assumes that all of the strain energy that is released will be used to break the bonds (no energy is dissipated in this case). Therefore this equation is appropriate for brittle materials (where the majority of released energy is used for crack growth), but leads to underestimation of the critical crack size for ductile materials (where a part of the available energy is dissipated) [41].

The critical strain energy release rate is introduced (G_c) to take energy dissipation into account. The critical strain energy release rate is the amount of released energy per unit of time at the moment the material fails. The critical strain energy release rate can subsequently be used to calculate the critical crack size using Equation 4-2 [41].

$$a_{crit} = \frac{G_c E}{\pi \sigma_{fail}^2} \quad (4-2)$$

The critical strain energy release rate of a material is often unknown, therefore Equation 4-3 is used. This equation relates the critical strain energy release rate to the critical stress intensity factor (K_c) [42].

$$G_c = \frac{K_c^2}{E'} \quad (4-3)$$

4-1-3 Stress Intensity Factor

The Stress Intensity Factor (SIF) expresses the stress concentration at the crack tip. Stress concentration factors (often used to evaluate the stress concentration at notches, holes etc.) cannot be used here because the SCF can only be evaluated for features with a finite radius of curvature [11]. The SCF concept is therefore not applicable to crack growth problems because the radius of curvature at the crack tip approaches zero.

The stress intensity at the crack tip induces a zone in which the stress is equal to the yield strength (which is the limit, because except for work-hardening of the material the stress cannot be higher than the yield strength). Therefore the material in the plastic zone will yield (deform plastically). The size of the plastic zone depends on the material properties and is therefore different for each material. Figure 4-2 shows a schematic representation of the plastic zone, along with a graph which displays the stress distribution.

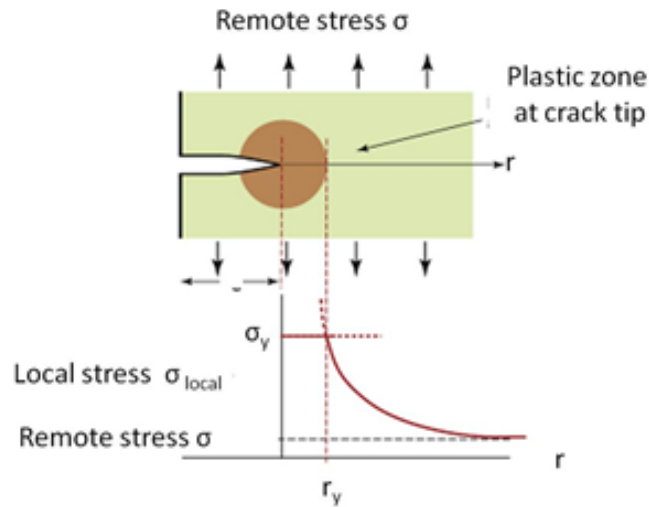


Figure 4-2: Schematic representation of the plastic zone around the crack tip (source: www.impact-solutions.co.uk).

Moving away from the plastic zone, the stress reduces to the remote stress (as can be seen in Figure 4-2). This stress function is described by the stress intensity factor. The stress intensity factor is shown in Equation 4-4. This is a function of a geometry factor (Y), the tensile stress (σ) and the crack length (a).

$$K_1 = Y \sigma \sqrt{\pi a} \quad (4-4)$$

The critical stress intensity factor is the stress intensity factor at which the material will fail, this approach can therefore be used to determine the critical crack size. The stress intensity factor can be used to calculate the crack growth rate as well, which is discussed in the next section on the calculation of crack growth.

4-1-4 Stress Calculations in Plates

A material is generally subjected to stresses in three orthogonal directions, however when the stress components along one axis are small their influence can often be neglected. This applies to plates because the stresses in the thickness direction are generally small compared to the in-plane stresses. Because the structure of STS cranes consists of plates, the stresses in the structure can be approximated using a 2D model. Two 2D stress approximation models are frequently used: plane stress and plane strain [41].

The plane stress model can be used when one dimension is relatively small compared to the other two dimensions (as is the case with thin plates) [43]. The stresses in the thickness direction are set to zero in this model. Only three independent equations remain, meaning that the stress state is now described in two dimensions. In equation 4-3, E' is equal to E when the plane stress approximation is used [41].

The plane strain model can be used when one dimension is relatively large compared to the other two dimensions (so this model is valid for thick plates). This model does not provide for elongation and shear in and normal to one direction [43]. This is applicable for thick plates because the strain in the thickness direction is considerably less than the strains in the other two directions. The plane strain model also contains three independent stress equations, however these equations are different compared to the equations for plane stress. This means that E' in Equation 4-3 is equal to $\frac{E}{1-\nu^2}$ (ν represents the Poisson ratio) when the plane strain approximation model is used [41]. The value for the critical stress intensity factor changes as well, because instead of K_c the value for K_{Ic} is used (which are different because the critical strain energy release rates for plane stress and plane strain are not equal).

The values of K_c and K_{Ic} are the critical stress intensity factors for plane stress and plane strain respectively. Reference [44] distinguishes between plane stress and plane strain using Equation 4-5. For plates where the thickness is equal or larger than this thickness, use of the plane strain model is valid.

$$t \geq 2.5 \left(\frac{K_{Ic}}{\sigma_y} \right)^2 \quad (4-5)$$

The plane stress approximation is applicable when the thickness of the material is smaller than the criterion in Equation 4-6 [44].

$$t < \left(\frac{1}{5.2} \right) \left(\frac{K_c}{\sigma_y} \right)^2 \quad (4-6)$$

For thicknesses between these limit values, a transition of the critical SIF occurs from fracture under plane stress into fracture under plane strain conditions. This is shown in Figure 4-3, where the fracture toughness is plotted as a function of the plate thickness. Two vertical lines are visible, these lines represent the critical SIF for plane stress (the left line) and the critical SIF for plane strain (the right line).

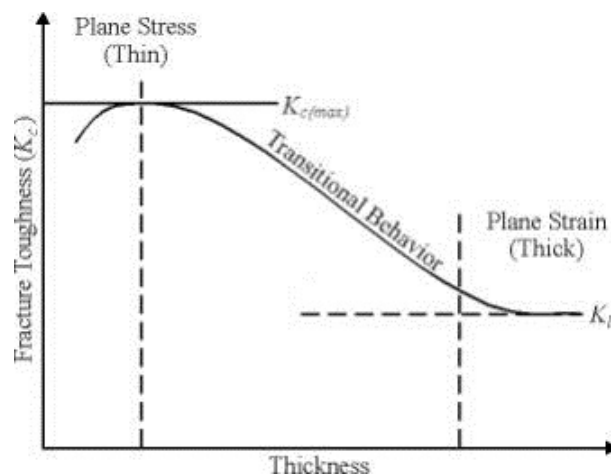


Figure 4-3: Plot of the fracture toughness as a function of plate thickness (source: <http://www.afgrow.net>).

The critical SIF for plane stress conditions (K_c) is a function of the geometry of the material [45]. This means that each feature will have a different value for the critical SIF for plane stress conditions. However, the critical SIF (K_{Ic}) at plane strain is a material property (its value does not depend on geometry) and its values for different types of materials are well-documented.

The resulting equations which are used to calculate the critical crack size for the steel structures of STS cranes are Equations 4-7 and 4-8.

For plane stress:

$$a_{crit} = \frac{K_c^2}{\pi Y^2 \sigma_{fail}^2} \quad (4-7)$$

For plane strain:

$$a_{crit} = \frac{K_{Ic}^2}{\pi Y^2 \sigma_{fail}^2} \quad (4-8)$$

4-2 Linear Crack Growth Calculations

The crack growth rate calculation, which is performed to be able to calculate the remaining fatigue life of a STS crane, is described in this section. The crack propagation for high cycle fatigue (which implicates linear elastic material behaviour) will be described using the SIF concept which is described in the previous section.

Because the implementation of this calculation procedure depends on the fatigue failure mode under consideration, the fatigue failure modes are discussed in the first subsection. The second subsection concerns the calculation of the stress intensity factor factor which is required to calculate the crack growth rate. The entire calculation procedure for the crack growth rate is described in the final subsection.

4-2-1 Fatigue Failure Modes

Three failure modes due to fatigue fracture exist (opening, in-plane shear and out-of-plane shear), these failure modes are illustrated in Figure 4-4. The stress intensity factor is a function of these failure modes, therefore the type of failure needs to be determined to be able to assess the remaining fatigue life of the crane once a crack is present.

Mode 1 fatigue fracture is the most dominant fatigue failure mode, the other two fatigue failure modes are rarely encountered at steel structures [1]. Only failure mode 1 will therefore be considered during the assessment of the propagation of fatigue cracks.

When a combination of crack loading modes is encountered, the stress intensity factor can be calculated using the superposition principle [46]. This means that the influence of the SIF's can be added together to determine the crack growth rate due to the multiple failure modes. This procedure will not be evaluated in this research because this is not required for fatigue assessment of steel structures of STS cranes.

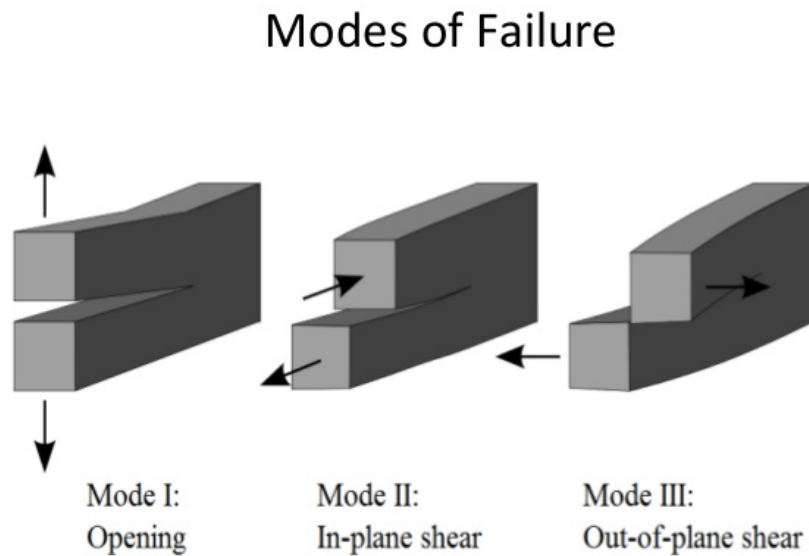


Figure 4-4: Illustration of the three failure modes for fatigue (source: <http://www.slideshare.net>).

4-2-2 Calculation of the Stress Intensity Factor

Calculation of the stress intensity factor is an important part of the crack growth calculation procedure. This factor can be obtained through literature, calculated using weight functions or calculated using FEM models.

The stress intensity factor can be found in literature for relatively simple constructional details. A number of publications list the SIF as a function of the geometry (see for instance references [47], [48] and [49]). Two options arise in this case; either the SIF itself or the geometry factor is given. When the geometry factor is given, Equation 4-9 can be solved to obtain the the SIF.

$$K_I = Y \sigma \sqrt{\pi a} \quad (4-9)$$

Another method that can be used to determine the stress intensity factor for specific geometries employs weight functions. The product of the weight function ($h_I(x, a)$) and the stress distribution across the crack ($\sigma(x)$) is integrated along the crack length (a) to calculate the SIF, see Equation 4-10. The weight function depends on the failure mode and the geometry, examples of weight functions can be found in literature [50].

$$K_I = \int_0^a \sigma(x) h_I(x, a) dx \quad (4-10)$$

The previous methods assumed that the crack is straight, however this might not always be the case. Therefore a perturbation method is developed to determine the SIF for cracks which are curved [50]. The perturbation method is a mathematical tool to approximate the solution of a problem which cannot be solved analytically. This method first develops a solution for a straight crack. The deviation of the curved crack with respect to the solution for the straight crack is subsequently estimated and these solutions are combined to reach the approximate solution for the curved crack.

The SIF can also be calculated for all crack types using FEA, for which three methods are available (the direct method, the indirect method and the cracked element method) [51]. The direct method uses the simulated stresses around the crack to calculate the SIF using Equation 4-11. R is the radius and θ represents the angle of the cartesian coordinate system that is used in this analysis. The function $f_{ij}(\theta)$ is determined by the FEA software.

$$K_I = \sigma_{ij} * \frac{\sqrt{2 * \pi * r}}{f_{ij}(\theta)} \quad (4-11)$$

The indirect method uses the relationship between the compliance and elastic energy to calculate the SIF. A fine mesh is not necessary because high accuracy of the calculated crack tip stress is not required. The procedure is included in Equation 4-12, where the load (P), the thickness (B), crack length (a), Youngs modulus (E) and compliance (C) are used to calculate the SIF.

$$K^2 = \frac{P^2}{2B} \frac{\partial C}{\partial a} E \quad (4-12)$$

The cracked element method uses special elements which allow a stress singularity at the crack tip. This method does not calculate the SIF directly, but simulates the crack growth rate. The crack surface is modelled by releasing a double-noded line which represents the crack. For each stress cycle the crack growth rate is calculated and the nodes are released accordingly, creating a larger crack. This procedure is repeated until the material fractures.

Table 4-1 shows a brief overview of the methods which can be used to calculate the stress intensity factor. The first three methods can be used without the need to explicitly model the cracked member, while the other three models can only determine the SIF when the crack is modelled in a FEM software package.

The first method is more suited for use in the assessment model than the second method because the amount of data on the SIF and geometry functions is larger than the amount of data on weight functions. The third method is dismissed because experience shows that the cracks found during inspections run along straight lines, therefore this model only adds unnecessary complexity. For crack growth analysis which are performed without FEM software, the first method will therefore be used.

When FEM software is used to determine the remaining fatigue life for a crack at a specific location, the fifth and sixth method can be used to calculate the crack growth rate. The fifth method is recommended because a fine mesh is not required to obtain reliable results. However, when a detailed crack growth simulation is desired the sixth method should be used. When FEM software is used to determine the remaining fatigue life of a structure without knowledge of the location and size of the crack, the first method is required because it is not viable to model cracks at each node.

Table 4-1: Overview of the methods that are able to calculate the SIF.

Method	Description
1	Choose the SIF or geometry function from a suitable table
2	Calculate SIF using weight functions
3	Use perturbation method to calculate the SIF for curved cracks
4	FEM- direct method (using stress field around the crack tip to calculate the SIF)
5	FEM- indirect method (using relation between compliance and elastic energy)
6	FEM- cracked element method (using special element type which allows stress singularity at the crack tip)

4-2-3 Crack Growth Rate Calculation Procedure

The crack growth rate in steel structures of STS cranes can be calculated by the Paris law (given in Equation 4-13) because this law is applicable for LEFM problems [41]. C and m are material parameters and ΔK can be calculated using equation 4-9 where instead of the stress (σ), the stress range ($\Delta\sigma$) is implemented.

$$\frac{da}{dN} = C * (\Delta K)^m \quad (4-13)$$

For high values of ΔK , the crack growth rate will be higher than the value predicted by the Paris law. This occurs when the crack size is larger than the critical crack size. Similarly, the crack growth rate will be lower than the predicted value for low values of ΔK . Figure 4-5 shows the crack growth rate plotted against the SIF, the region in which the Paris law is applicable is indicated as the power law region.

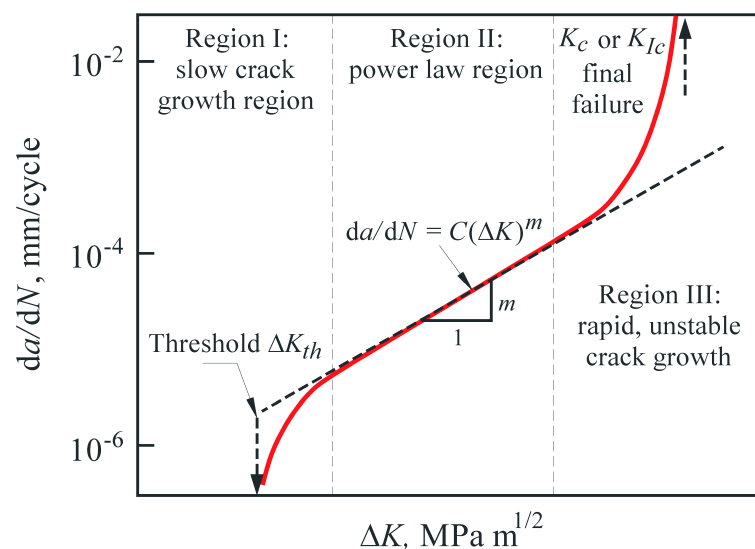


Figure 4-5: Crack growth rate plotted against the SIF, the crack growth rate is in red and the Paris law is represented by the dotted line (source: www.totalmateria.com).

A threshold value ΔK_{th} is used in adaptations of Equation 4-13 to discard the values of the SIF for which the crack growth rate is low [41]. However, this value is sensitive to the ratio of the minimum and maximum stresses that are encountered during one stress cycle [44]. The threshold is also influenced by the profile of the microstructure of the material [52]. Therefore each detail of the steel structure of a STS crane will have a different threshold value. Tabulating the values for ΔK_{th} for each geometry, material type and lading condition is considered impractical for the purpose of the assessment method, therefore the threshold value will not be included in the crack growth model. This means that the results of this model will be conservative for components which are subjected to minor loads.

The expression for the stress intensity factor is entered into the previous equation to obtain Equation 4-14. $\frac{da}{dN}$ represents the crack growth as a result of a load cycle with an amplitude of $\Delta\sigma$.

$$\frac{da}{dN} = C * (\Delta\sigma * Y * \sqrt{\pi * a})^m \quad (4-14)$$

After rearranging the terms and integrating both sides of the previous equation, an expression arises for the expected number of load cycles that can be performed between initial crack length and final crack length. This expression is included in Equation 4-15 and the declaration of the used symbols is presented in Table 4-2.

$$N_f - N_i = \frac{1}{1 - \frac{m}{2}} \frac{1}{C \Delta\sigma^m Y^m \pi^{\frac{m}{2}}} (a_{crit}^{1-\frac{m}{2}} - a_{eff}^{1-\frac{m}{2}}) \quad (4-15)$$

Table 4-2: Declaration of the symbols used in Equation 4-15.

Symbol	Description	Unit
m	Material parameter	-
C	Material parameter	$MPa^{-m} * m^{1-\frac{m}{2}}$
Y	Geometry Factor	-
$\Delta\sigma$	Stress range	MPa
a_{crit}	Critical crack length	m
a_{eff}	Effective initial crack length	m
N_f	Number of stress cycles at failure	-
N_i	Number of initial stress cycles	-

4-3 Non-Linear Crack Growth Calculations

The previous section concerned a model for elastic material behaviour, calculation of problems with non-linear behaviour must therefore be performed by a separate model. Non-linear behaviour occurs when the structure is subjected to low cycle fatigue or large structural deformations. The issue of non-linear crack growth calculation is discussed in this section, the first subsection concerns LCF problems and the second subsection covers large structural deformations.

4-3-1 Low Cycle Fatigue

Low cycle fatigue is characterised by a short fatigue life and stress cycles close to (or beyond) the yield limit. Because of the high stresses, stress and strain are not linearly related anymore. Therefore the problem becomes nonlinear and the fatigue damage accumulation cannot be described by stress analysis. Instead, strain is used to calculate the remaining fatigue life using the Coffin-Manson relation (see Equation 4-16) [53].

$$\frac{\Delta\varepsilon}{2} = \frac{\sigma_f}{E} (2 N_{fail})^b + \varepsilon_f (2 N_{fail})^c \quad (4-16)$$

When the strain range ($\Delta\varepsilon$), the fatigue strength coefficient (σ_f), the elastic modulus (E), fatigue ductility coefficient (ε_f), the fatigue strength exponent (b) and the fatigue ductility exponent (c) are known, the cycles to failure (N_{fail}) can be calculated. These parameters can be determined using test data analysis (for instance using the method described in Reference [54]). When test data is unavailable, generic data for steel (see Reference [55]) can be used.

The regime of fatigue failure (LCF or HCF) is determined by the number of load cycles that can be executed until the material fails. The boundary between the two regimes is often considered to be between $N = 1 \cdot 10^4$ and $N = 1 \cdot 10^5$ cycles [53].

To determine whether STS cranes are subjected to LCF, the European Standard (13001-3-1: cranes- general design) issued in 2012 is consulted. This standard states on page 19: "The use of theory of plasticity for calculation of ultimate load bearing capacity is not considered acceptable within the terms of this standard" [6]. This means that the yield stress should not be exceeded. For static stress analyses, the yield strength is supplied with a safety factor so that the material will not deform. This has to be verified for each loadcase as described in EN 13001-2:2010 [56].

Also, the SN-curves that are used to calculate the fatigue life in the design standard are not specified in the LCF regime. This implicates that LCF design of details in cranes is prohibited according to this standard.

This means that LCF does not occur at STS gantry cranes when the structure is designed according to the relevant design standards. Therefore the LCF regime will not be taken into account by the fatigue assessment model.

4-3-2 Structural Deformations

For crack sizes which are large compared to the uncracked geometry, the structure can deform in the vicinity of the crack. An example of this case is shown in Figure 4-6. When the structure deforms, the assumption of linear elastic material behaviour is violated and a model allowing for plasticity has to be deployed. In this case Equation 4-16 can be used to calculate the remaining fatigue life. Alternatively, an analysis accounting for plastic material behaviour can be performed using FEM-software [57].



Figure 4-6: Example of large deformations as a result of a fatigue crack. LEFM models are not valid in this case (image provided by Cargotec).

A method that can be used to determine the remaining fatigue life of a structure subjected to a large crack is Extended Finite Element Method (XFEM). This method holds an advantage over conventional FEM procedures because in this case the model does not have to be remeshed each time the crack propagates. With XFEM, the mesh can be created independent from the crack geometry. Therefore this type of software is often used to simulate fracture of materials [58].

The load across the steel structure might be redistributed in case the structure is subject to large deformations [1]. This means that when large deformations are detected at a structural detail of a STS crane during an inspection, the influence of this deformation on the rest of the structure needs to be determined. However, it is apparent that repair works are required eventually. So to reduce potential downtime of the crane, the assessment stage can be skipped in order to start preparations for repair works right away. Therefore nonlinear calculation models are not required for a fatigue assessment of steel structures of STS cranes.

Implementation of Calculation Model

This chapter concerns the implementation of the model which calculates the remaining fatigue life of steel structures of existing STS cranes. This calculation model can be found in Appendix C. The first section of this chapter describes the verification process of the calculation model, where it is checked whether the implementation of the calculation procedures is correct. The second section concerns the sensitivity of the model with respect to changes of the input parameters, to determine which parameters have the most influence on the remaining fatigue life of the structure.

5-1 Verification of the Calculation Model

This section describes the verification process of the calculation model and is divided into three subsections. The implementation of the crack growth model is verified in the first subsection. Calculation of the plastic radius is included in the second subsection and the final subsection concerns the calculation procedure of the geometry correction factor.

5-1-1 Verification of Fracture Mechanics Model

The implementation of the crack growth calculation procedure is verified using two worked examples made available by Plymouth university, the data used to verify this model is presented in Table 5-1. When the output of the model matches the result of the worked examples, the calculation model is considered to be implemented correctly. The values of the first worked example show only a minor difference (0.2%) which can be attributed to rounding errors [59].

The values of the calculated and given values for the remaining fatigue life at the second worked example deviate by 1.2%. This can be explained by the difference in the value of the exponent, which is calculated by the model to be 0.125 but rounded in the worked example to 0.13. The worked example was recalculated using the original value for the exponent, this caused the difference between the values to diminish [60]. The model can therefore be considered to be correctly implemented.

Table 5-1: Data used to verify the implementation of the crack growth calculations.

Parameter	Example 1	Model	Example 2	Model
Maximum stress [MPa]	200.4	200.4	310	310
Fracture toughness [$MPa * m^{0.5}$]	25	25	165	165
Geometry factor [-]	0.7	0.7	1.12	1.12
Minimum stress [MPa]	0	0	172	172
Initial crack length [m]	$1.5e*10^{-3}$	$1.5*10^{-3}$	$7.6*10^{-3}$	$7.6*10^{-3}$
Material constant C	$6.25*10^{-12}$	$6.25*10^{-12}$	$1.36*10^{-10}$	$1.36*10^{-10}$
Material constant m [-]	4	4	2.25	2.25
Critical crack length [m]	$10.2*10^{-3}$	$10.1*10^{-3}$	$71.9*10^{-3}$	$71.89 *10^{-3}$
Cycles to failure [-]	23,723	23,768	87,992	86,822

5-1-2 Plastic Radius Calculation

As described in Chapter 4, the size of the plastic zone is characterised by the plastic zone radius. Because the plastic zone is not included in the verification of the crack growth calculations, verification of this calculation is performed separately. The plastic zone radius is used to determine whether it is valid to use the plane strain model and to determine the effective crack length.

The formula for the plastic radius in case the material is subjected to plane stress is listed in Equation 5-1, the formula for plane strain is shown in Equation 5-2 [44]. Chapter 4 discusses the relation between these equations and the minimum thickness for the plane strain model to be valid.

$$Rp = \left(\frac{1}{2\pi} \right) \left(\frac{K_c}{\sigma_y} \right)^2 \quad (5-1)$$

$$Rp = \left(\frac{1}{6\pi} \right) \left(\frac{K_{ic}}{\sigma_y} \right)^2 \quad (5-2)$$

The calculation of the plastic radius is verified using the example on pages 190-194 of Reference [44] and the data is included in Table 5-2. The values of the minimum thickness for which the plane strain model is valid are in agreement with each other. The values for the plastic radius are similar as well, therefore the implementation of the calculation procedure for the plastic radius is considered to be correct.

Table 5-2: Data used to verify the calculation of the plastic radius.

Parameter	Example	Model
Yield strength [MPa]	1700	1700
Fracture toughness [$MPa * m^{0.5}$]	110	110
Thickness of plate [m]	0.1	0.1
Plane strain minimum thickness [m]	0.010	0.011
Plastic radius [m]	2e-4	2.2e-4

5-1-3 Calculation of the Geometry Correction Factor

The critical crack size and the crack growth rate depend on the geometry, this is reflected by the geometry correction factor. These factors have been developed for various types of geometries and loading conditions. An example of a compendium of geometry factors can be found in Reference [61]. The geometry factors are generally calculated for the case of a single crack, for adaptations to account for multiple interacting cracks the reader is referred to Reference [62] (for the case of several aligned cracks) or Reference [50] (for a cascade of cracks). Experience shows that the occurrence of multiple interacting cracks is rare at STS cranes, therefore only geometry factors for single cracks are considered.

Not all geometry factors are considered in this research, the geometry factors for cracks in plates and cracks in cylinders are evaluated because a general STS gantry crane consists of a combination of cylindrical cross sections and cross sections constructed out of rectangular plates. Because the members in the structures of STS are generally welded together, the geometry factors relating to welded connections are evaluated as well.

The geometry factors are calculated using Microsoft Excel, the type of details and loading conditions of the modelled factors are listed in Table 5-3. Apart from the references that are listed in this table, Reference [63] is used to provide an illustration for the calculation of the geometry factor of butt welds. Images of the excel file that is used to calculate the geometry factors can be found in Appendix D. One example of the calculation procedures for the geometry factor is provided in Figure 5-1.

Table 5-3: Types of details for which the geometry factor is modelled in this research.

Type of detail	Type of Load	Reference
Center-cracked plate	Bending stress	[64]
Center-cracked plate	Tensile stress	[64]
Plate with single edge crack	Bending stress	[64]
Plate with single edge crack	Tensile stress	[64]
Double-edge cracked plate	Bending stress	[64]
Double-edge cracked plate	Tensile stress	[64]
Circumferentially cracked cylinder	Tensile stress	[65]
Circumferentially cracked cylinder	Bending stress	[65]
Double cracked hole in infinite sheet	Tensile and shear stress	[?]
Single cracked hole in infinite sheet	Tensile and shear stress	[?]
Butt weld with weld toe crack	Tensile stress	[66]
Butt weld with weld toe crack	Bending stress	[66]
Fillet weld with weld toe crack	Tensile stress	[67]
Fillet weld with weld toe crack	Bending stress	[67]
Lap Joint with weld toe crack	Tensile stress	[68]
Transverse attachment weld toe crack	Tensile stress	[68]
Cruciform joint weld root crack	Tensile stress	[69]
Cruciform joint K-butt weld toe crack	Tensile stress	[68]
Cruciform joint fillet weld toe crack	Tensile stress	[68]

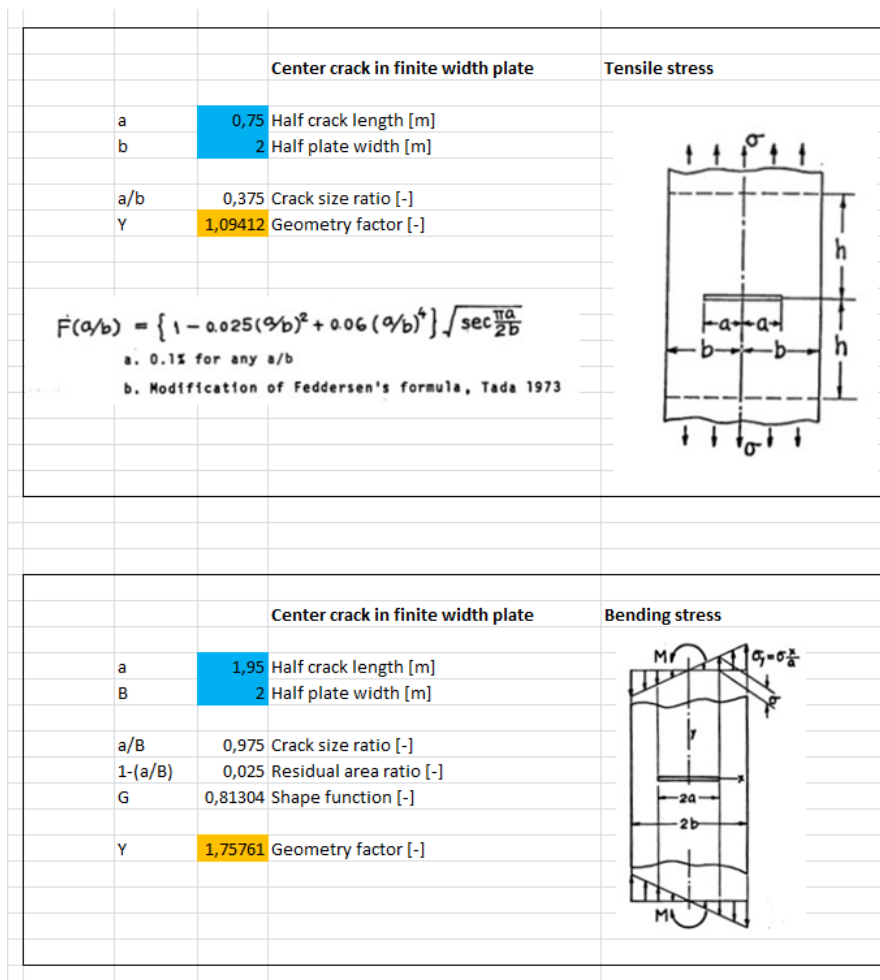


Figure 5-1: Example of the geometry factor calculation model. In this case the geometry factor for a center crack in a plate subjected to bending or tensile loads is calculated.

The geometry factor for cruciform joints depends on the location of the crack, which is either at the weld root or the weld toe. The location of the crack initiation point is in this case determined by the penetration depth of the weld [70]. For relatively small penetration depths a weld root failure is more likely, while for relatively large penetration depths a weld will fail at the weld toe. This makes it possible to predict the weld failure mode beforehand and select the correct geometry factor accordingly.

It is assumed that the relevant dimensions for the detail under consideration are known (from design drawings or measurements). The geometry factor can subsequently be calculated when the defect size is known. The selected defect size can range from the detection threshold to a relatively large crack (to obtain conservative estimates on the remaining fatigue life).

For cracks in plates, the plate width is an important parameter. For large structures, the plate width is equal to the spacing between two subsequent stiffeners. Finally, it should be noted that when the crack size is small compared to all other dimensions of the detail under consideration, the geometry factor is equal or close to one [11].

5-2 Sensitivity of the Model

The sensitivity of the model with respect to changes of the input parameters is investigated in order to determine which parameters have the most influence on the remaining fatigue life of the structure. The deterministic sensitivity of this model is determined by adding and subtracting 10, 25 and 50 percent to and from the benchmark value of the individual parameters.

The effects of changes to the input parameters are investigated separately. This means that when the sensitivity of one parameter is investigated the other parameters remain equal to their benchmark values. The benchmark value for the yield strength of the material is 355 MPa, equivalent to the yield strength of S355 steel [71]. The value for the fracture toughness is equal to the fracture toughness for mild steel ($50 \text{ Mpa} * m^{0.5}$) [72]. The maximum stress is set to 150 MPa and the minimum stress is set to 50 MPa, the stress range is therefore 100 MPa.

The initial crack size is chosen to be 10 mm and the geometry factor is set to 1.12 (this is the value for a center crack in a large plate). The crack growth data is taken from reference [73], which lists the crack growth data for welds in air. The exponent is equal to 3.1 and the material constant C is equal to $3.3e-13 \text{ Mpa}^{-m} * m^{(1-m/2)}$. The benchmark values for the sensitivity analysis are summarised in Table 5-4.

The critical crack size of the benchmark calculation is equal to 28.2 mm. The benchmark value for the number of cycles to failure is 1.99e6.

Table 5-4: The benchmark values used in the sensitivity analysis.

Parameter	Value	Unit
Yield strength	355	MPa
Fracture toughness	50	$\text{Mpa} * m^{0.5}$
Material constant m	3.1	-
Material constant C	3.3e-13	$\text{Mpa}^{-m} * m^{(1-m/2)}$
Maximum stress	150	MPa
Minimum stress	50	MPa
Initial crack length	10	mm
Geometry factor	1.12	-
Critical crack size	28.2	mm
Cycles to failure	1.99e6	-

5-2-1 Influence of Yield Strength

The sensitivity of the model with respect to changes to the yield strength of the material is investigated first. The values used to determine the sensitivity of the model with respect to changes to the yield strength are listed in Table 5-5.

Table 5-5: Values used to determine the sensitivity of the model with respect to the yield strength.

Yield strength	Value [MPa]
Benchmark-50%	177,5
Benchmark-25%	266,25
Benchmark-10%	319,5
Benchmark	355
Benchmark+10%	390,5
Benchmark+25%	443,75
Benchmark+50%	532,5

The results of this evaluation are displayed in Table 5-6. It becomes evident from this table that an increase in yield strength increases the remaining fatigue life as well. This effect can be attributed to changes in small scale plastic yielding. The plastic radius (and thus the effective crack length) becomes smaller once the yield strength increases. This means that the difference between the current effective crack size and the critical crack size becomes smaller, which in turn reduces the remaining fatigue life (the crack growth rate remains constant).

Table 5-6: Changes in the critical crack size and cycles to failure as a result of changes to the yield strength.

Yield strength	Critical crack size [mm]	Change in critical crack size	Cycles to Failure	Change in cycles to failure
Benchmark -50%	28.19	-	1.35e6	-32.2%
Benchmark - 25%	28.19	-	1.80e6	-9.5%
Benchmark -10%	28.19	-	1.93e6	-3.0%
Benchmark	28.19	-	1.99e6	-
Benchmark +10%	28.19	-	2.04e6	+ 2.5%
Benchmark + 25%	28.19	-	2.09e6	+5.0%
Benchmark + 50%	28.19	-	2.14e6	+7.5%

5-2-2 Influence of Fracture Toughness

The sensitivity of the crack growth process with respect to changes to the fracture toughness is investigated next. The values used to determine the sensitivity of the model with respect to changes to the fracture toughness are listed in Table 5-7.

Table 5-7: Values used to determine the sensitivity of the model with respect to the fracture toughness.

Fracture Toughness	Value [$Mpa * m^{0.5}$]
Benchmark-50%	25
Benchmark-25%	37.5
Benchmark-10%	45
Benchmark	50
Benchmark+10%	55
Benchmark+25%	62.5
Benchmark+50%	75

The results of this analysis are displayed in Table 5-8. These results show that the fracture toughness of the material influences the critical crack size, which increases for any increase in the fracture toughness. The number of cycles to failure are also influenced by this effect because this value depends on the difference between the initial crack size and the critical crack size.

For each increase in the fracture toughness, the critical crack size becomes larger. This means that the remaining fatigue life increases as well. This explains the negative remaining fatigue life in the first row of Table 5-8, where the critical crack size is smaller than the simulated initial crack size. As can be seen from this table, the influence of the fracture toughness on the remaining fatigue life is generally smaller than its influence on the critical crack size.

Table 5-8: Changes in the critical crack size and cycles to failure as a result of changes to the fracture toughness.

Fracture Toughness	Critical crack size [mm]	Change in critical crack size	Cycles to Failure	Change in cycles to failure
Benchmark -50%	7.05	-75.0%	-1.18e6	-159.3%
Benchmark - 25%	15.86	-43,7%	1.01e6	-49.2%
Benchmark -10%	22.84	-19.0%	1.68e6	-15.6%
Benchmark	28.19	-	1.99e6	-
Benchmark +10%	34.12	+21.0%	2.23e6	+12.1 %
Benchmark + 25%	44.05	+56.3%	2.49e6	+25.1%
Benchmark + 50%	63.44	+125.0%	2.76e6	+38.7%

5-2-3 Influence of Crack Growth Parameters

The final material parameters that have an influence on the remaining fatigue life are the parameters used in the Paris equation (the crack growth constant C and the crack growth exponent m). The influence of the crack growth constant C is evaluated using the parameters that are displayed in Table 5-9.

Table 5-9: Values used to determine the sensitivity of the model with respect to the crack growth constant.

Crack growth constant C	Value [$Mpa^{-m} * m^{(1-m/2)}$]
Benchmark-50%	1.65e-13
Benchmark-25%	2.475e-13
Benchmark-10%	2.97e-13
Benchmark	3.3e-13
Benchmark+10%	3.63e-13
Benchmark+25%	4.125e-13
Benchmark+50%	4.95e-13

The results of the analysis are shown in Table 5-10. This parameter only influences the crack growth rate, for each increase of the crack growth constant the remaining fatigue life reduces.

Table 5-10: Changes in the critical crack size and cycles to failure as a result of changes to the crack growth constant.

Crack growth constant C	Critical crack size [mm]	Change in critical crack size	Cycles to Failure [-]	Change in cycles to failure
Benchmark -50%	28.19	-	3.98e6	+100%
Benchmark - 25%	28.19	-	2.65e6	+33.2%
Benchmark -10%	28.19	-	2.21e6	+11.1%
Benchmark	28.19	-	1.99e6	-
Benchmark +10%	28.19	-	1.81e6	-9.0%
Benchmark + 25%	28.19	-	1.59e6	-20.1%
Benchmark + 50%	28.19	-	1.33e6	-33.2%

The next analysis concerns the crack growth exponent m , using the values shown in Table 5-11. This parameter is used in the Paris equation to calculate the time in which a crack grows to its critical size as well. Because the sensitivity of the two parameters of this equation is evaluated separately, it might appear that these are independent parameters. The reader is therefore reminded that this is not the case and that these parameters need to be selected from the same dataset at all times.

Table 5-11: Values used to determine the sensitivity of the model with respect to the crack growth exponent.

Crack growth exponent m	Value [$Mpa * m^{0.5}$]
Benchmark-50%	1.55
Benchmark-25%	2.325
Benchmark-10%	2.79
Benchmark	3.1
Benchmark+10%	3.41
Benchmark+25%	3.875
Benchmark+50%	4.65

From the results of this analysis (which are displayed in Table 5-12) it can be concluded that the crack growth exponent has a large influence on the calculations regarding the remaining fatigue life. When the crack growth exponent is reduced, the remaining fatigue life increases significantly.

It is evident that the crack growth exponent has a large influence on the outcome of a fatigue analysis, therefore this parameter must be selected with great care.

Table 5-12: Changes in the critical crack size and cycles to failure as a result of changes to the crack growth exponent.

Crack growth exponent m	Critical crack size [mm]	Change in critical crack size	Cycles to Failure [-]	Change in cycles to failure
Benchmark -50%	28.19	-	3.15e8	+15729.1%
Benchmark - 25%	28.19	-	2.49e7	+1151.3%
Benchmark -10%	28.19	-	5.46e6	+174.4%
Benchmark	28.19	-	1.99e6	-
Benchmark +10%	28.19	-	7.27e5	-63.5%
Benchmark + 25%	28.19	-	1.61e5	-91.9%
Benchmark + 50%	28.19	-	1.31e4	-99.3%

5-2-4 Influence of Maximum Stress

The calculation procedure also contains two parameters describing the load on the detail under consideration, the maximum stress and the stress range. This subsection concerns the sensitivity of the calculation procedure with respect to changes to the maximum stress. Because the sensitivity of the stress range is to be evaluated separately, the minimum stress is 100 MPa lower than the maximum stresses which are displayed in Table 5-13.

Table 5-13: Values used to determine the sensitivity of the model with respect to the maximum stress.

Maximum Stress	Value [MPa]
Benchmark-50%	75
Benchmark-25%	112.5
Benchmark-10%	135
Benchmark	150
Benchmark+10%	165
Benchmark+25%	187.5
Benchmark+50%	225

The results of this analysis are displayed in Table 5-14. For lower values of the maximum stress, both the critical crack size and the remaining fatigue life increase. This effect can be explained by the increasing difference between the current and critical crack sizes. The crack growth rate in this example is unchanged because this is governed by the difference in maximum and minimum stress (which is kept constant).

Table 5-14: Changes in the critical crack size and cycles to failure as a result of changes to the maximum stress.

Maximum Stress	Critical crack size [mm]	Change in critical crack size	Cycles to Failure [-]	Change in cycles to failure
Benchmark -50%	112.78	+300.1%	3.57e6	+79.4%
Benchmark - 25%	50.12	+77.8%	2.79e6	+40.2%
Benchmark -10%	34.81	+23.5%	2.31e6	+16.1%
Benchmark	28.19	-	1.99e6	-
Benchmark +10%	23.30	-17.3%	1.66e6	-16.6%
Benchmark + 25%	18.04	-36.0%	1.17e6	-41.2%
Benchmark + 50%	12.53	-55.6%	3.3e5	-83.4%

5-2-5 Influence of Stress Range

This subsection concerns the sensitivity of the model with respect to the stress range that the construction is subjected to. The maximum stress is kept constant during this analysis, the stress range is adjusted by raising or lowering the minimum stress. The stress ranges that are evaluated can be seen in Table 5-15.

Table 5-15: Values used to determine the sensitivity of the model with respect to the stress range.

Stress Range	Value [MPa]
Benchmark-50%	50
Benchmark-25%	75
Benchmark-10%	90
Benchmark	100
Benchmark+10%	110
Benchmark+25%	125
Benchmark+50%	150

The fatigue failure condition (the critical crack size) is not a function of stress range (as can be seen in Table 5-16). The increase in crack growth rate for each increase of the stress range causes the remaining fatigue life to be reduced for each increase of the stress range. The results show that the magnitude of the stress range has a significant influence on the remaining fatigue life of the detail under consideration.

Table 5-16: Changes in the critical crack size and cycles to failure as a result of changes to the stress range.

Stress Range	Critical crack size [mm]	Change in critical crack size	Cycles to Failure [-]	Change in cycles to failure
Benchmark -50%	28.19	-	1.71e7	+759.3%
Benchmark - 25%	28.19	-	4.85e6	+130.2%
Benchmark -10%	28.19	-	2.76e6	+38.7%
Benchmark	28.19	-	1.99e6	-
Benchmark +10%	28.19	-	1.48e6	-25.6%
Benchmark + 25%	28.19	-	9.96e5	-49.9%
Benchmark + 50%	28.19	-	5.66e5	-71.6%

5-2-6 Influence of Geometry Factor

The geometry of the detail where the crack is located has an influence on the critical crack size and the remaining fatigue life. The values used to evaluate the sensitivity of the calculation model with respect to changes to the geometry factor is displayed in Table 5-17.

Table 5-17: Values used to determine the sensitivity of the model with respect to the geometry factor.

Geometry Factor	Value [-]
Benchmark-50%	0.56
Benchmark-25%	0.84
Benchmark-10%	1.008
Benchmark	1.12
Benchmark+10%	1.232
Benchmark+25%	1.4
Benchmark+50%	1.68

The results of this evaluation are displayed in Table 5-18. These results show that increasing the geometry factor leads to a reduced critical crack size, which means that the remaining fatigue life is reduced as well. The remaining fatigue life is further compromised by the fact that the increased geometry factor leads to a higher crack growth rate. Increasing the geometry factor therefore leads to a crack that grows faster to smaller critical size.

Table 5-18: Changes in the critical crack size and cycles to failure as a result of changes to the geometry factor.

Geometry Factor	Critical crack size [mm]	Change in critical crack size	Cycles to Failure [-]	Change in cycles to failure
Benchmark -50%	112.78	+300.1%	3.06e7	+1437.7%
Benchmark - 25%	50.12	+77.8%	6.81e6	+242.2%
Benchmark -10%	34.81	+23.5%	3.21e6	+61.3%
Benchmark	28.19	-	1.99e6	-
Benchmark +10%	23.3	-17.3%	1.24e6	-37.7%
Benchmark + 25%	18.04	-36.0%	5.85e5	-70.6%
Benchmark + 50%	12.53	-55.6%	9.39e4	-95.3%

5-2-7 Influence of Initial Crack Size

The last experiment to determine the sensitivity of the crack growth model with respect to changes of the used variables concerns the initial crack size. The values used to evaluate the influence of the initial crack size on the remaining fatigue life are displayed in Table 5-19.

Table 5-19: Values used to determine the sensitivity of the model with respect to the initial crack size.

Initial Crack Size	Value [m]
Benchmark-50%	0.005
Benchmark-25%	0.0075
Benchmark-10%	0.009
Benchmark	0.010
Benchmark+10%	0.011
Benchmark+25%	0.0125
Benchmark+50%	0.015

The results are shown in Table 5-20, which makes clear that the remaining fatigue life increases for smaller initial cracks. For smaller cracks, the difference between the current crack size and the critical crack size becomes larger. The unchanged crack growth rate therefore means that the remaining fatigue life increases as the initial crack size decreases. However, this effect was not as high as indicated by earlier publications, which list this parameter as the most influential with respect to the remaining fatigue life [1].

The reason for this difference to the literature is likely the result of the influence of the geometry factor. The geometry factor is a function of the crack size as well, the observations regarding crack growth might therefore be the combined result of the influence of the geometry factor and initial crack size.

Table 5-20: Changes in the critical crack size and cycles to failure as a result of changes to the initial crack size.

Initial Crack Size	Critical crack size [mm]	Change in critical crack size	Cycles to Failure [-]	Change in cycles to failure
Benchmark -50%	28.19	-	3.93e6	+97.5%
Benchmark - 25%	28.19	-	2.74e6	+37.7%
Benchmark -10%	28.19	-	2.25e6	+13.1%
Benchmark	28.19	-	1.99e6	-
Benchmark +10%	28.19	-	1.76e6	-11.6%
Benchmark + 25%	28.19	-	1.47e6	-26.1%
Benchmark + 50%	28.19	-	1.07e6	-46.2%

5-2-8 Summary of the Sensitivity Analysis

The results are sorted by their average influence on the remaining fatigue life, which is displayed in Table 5-21. It is determined that the influence of the crack growth exponent or geometry factor is larger than the influence of the yield strength or crack growth constant. It is shown that the remaining fatigue life can be significantly over- or underestimated even with relatively small fluctuations of the major parameters. This needs to be considered when the results of a fatigue analysis are interpreted.

Table 5-21: Relative importance of the parameters with respect to the remaining fatigue life (sorted high to low).

Relative importance	Parameter
1	Crack growth exponent m
2	Geometry factor
3	Stress range
4	Fracture toughness
5	Maximum stress
6	Initial crack size
7	Crack growth constant C
8	Yield strength

Measurement of Crack Sizes

The structure of the crane will be inspected at predetermined intervals to obtain information on its condition. This chapter concerns the methods that can be used to detect cracks during these inspections. The methods that can be used to detect and measure cracks are described in the first section. The second section concerns the influence of the selected crack detection method on the inspection regime.

6-1 Crack Detection and Measurement Methods

The methods that are considered for crack detection and measurement in this research are Non-Destructive Testing (NDT) methods. These methods are able to detect a crack without the need to damage the structure, which means that the crane can resume operation directly after inspection. The NDT methods considered in this research are listed below (and will be described in the remainder of this section):

- Visual inspection
- Magnetic particle inspection
- Colour penetration test
- Radiographic inspection
- Ultrasonic inspection
- Eddy current technique
- Acoustic analysis

Visual inspection is performed by an engineer who looks closely at all parts of the structure under consideration, which means only surface cracks can be detected. The result of this inspection procedure largely depends on the skill and experience of the people performing the inspection [74]. Crack sizes can be established using a ruler or tape measure. This method is often used because it is a relatively quick method.

Magnetic particle inspection can be performed to detect surface cracks at ferromagnetic materials. The formation of a magnetic field will be distorted around cracks, which can be visualized using a layer of magnetic particles (see Figure 6-1). Once the paint coating is removed, magnetic particles are applied to the surface and the section under consideration is magnetized using a large magnet. A pile-up of magnetic particles is an indication of a crack. This inspection method is able to accurately detect surface cracks which are 2 mm long [75].

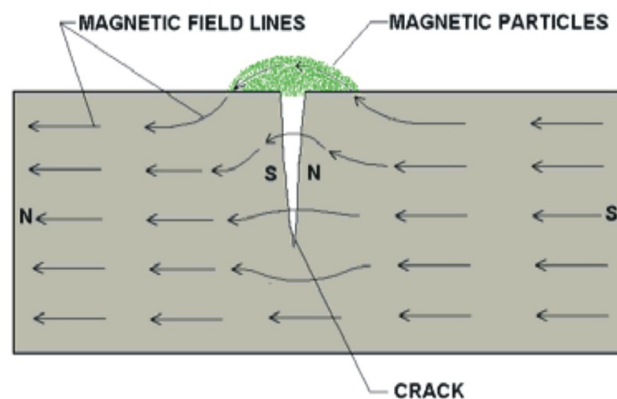


Figure 6-1: Schematic representation of crack detection by magnetic particle inspection (source: www.industrialndt.com).

For non-ferromagnetic materials the colour penetration test can be used to indicate a crack which is not visible to the eye. The crack can be visualized by spraying a dye onto the surface. The surface is subsequently cleaned and a developer is applied in order to reveal the location where the dye has penetrated the structure (indicating a crack). This method is able to detect a surface crack which has a depth of three times the surface roughness [75]. The process of this NDT method is depicted in Figure 6-2. This method requires removal of the paint coating as well.

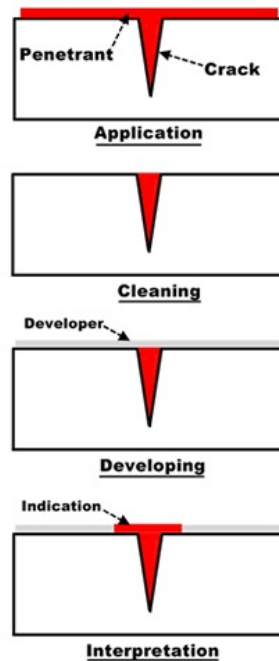


Figure 6-2: Schematic representation of the color penetration test (source: www.asnt.org).

Subsurface cracks can be detected using radiographic inspection, where a source emits radiation through a cross section. A detector is placed at the other side of the material and constructs a two dimensional image of the cross section based on the level of radiation that it receives (see Figure 6-3). This image displays the cracks and other discontinuities as spots. The accuracy of this method depends on the half-life of the radioactive source, experience of the operator, the characteristics of the material and the thickness of the material. It is possible to detect a crack with a length of 1 mm in a plate with a thickness up to 56 mm [75].

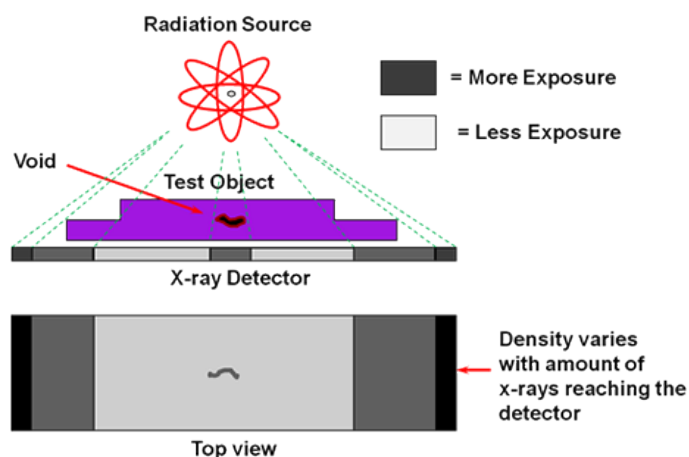


Figure 6-3: Schematic representation of the radiographic inspection method (source: www.iprt.iastate.edu).

Ultrasonic inspection can also be used to measure subsurface cracks. This type of inspection methods emits ultrasonic waves in the material and displays the reflections of these waves (at the back face of the material or at internal defects) on a screen. The working principle of this inspection method is shown in Figure 6-4. When a crack is detected and its direction is known, its size can be measured when the ultrasonic tester is held at an angle [75]. The paint layer must be removed before this method can be used.

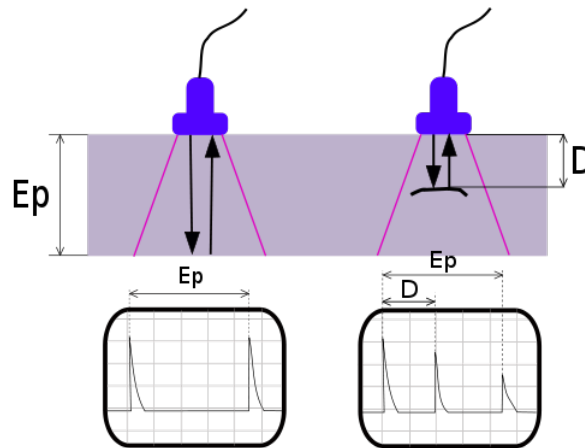


Figure 6-4: Schematic representation of the ultrasonic inspection method (source: www.elumeco.com).

Eddy current inspection detects cracks by evaluating fluctuations in the magnetic field in thin plates. A small probe is supplied with an alternating current, which creates a magnetic field around the probe. When this probe is placed near a conductive material, eddy currents are generated in the material (as can be seen in Figure 6-5). Variations of the magnitude and phase of these eddy currents indicate the presence of any discontinuities (like cracks) [76].

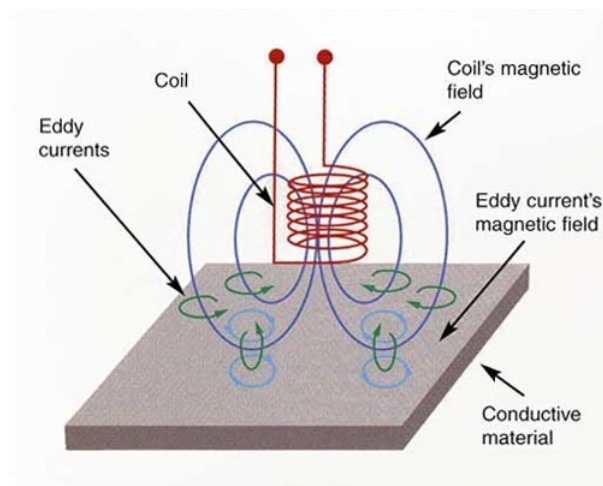


Figure 6-5: Visualisation of the formation of eddy currents (source: www.nde-ed.org).

Acoustic inspection methods measure the soundwaves that are emitted by growing cracks. When the speed of sound in the specimen is known, the rate of crack growth can be established using frequency analysis of the soundwaves emitted by the growing cracks. This analysis can also be performed by emitting soundwaves into the specimen and evaluating the frequencies at a specific distance away from the source. The location of the crack needs to be known in advance, these methods are therefore only able to monitor crack growth and are unable to detect the location of a crack [75].

6-2 Influence of Crack Detection Method on Inspection Regime

The ability to detect a crack depends on the selected NDT method, which in turn influences the required inspection regime. The ability to detect a crack is described by the smallest crack size which can be detected with sufficient reliability [18]. This section displays the detectable crack sizes for various NDT methods. This information is subsequently used to select a suitable NDT method for inspections of steel structures of STS cranes.

The reliability of an inspection method is described by the Probability of Detection (POD). The POD describes the likelihood of detecting a crack as a function of the crack size. Guidelines on calculation procedures for the POD of an inspection method can be found in Reference [77]. Figure 6-6 displays POD curves for visual inspection of structures subjected to cyclic loads. These curves are constructed using data from Reference [5] for various degrees of accessibility of the area that needs to be inspected.

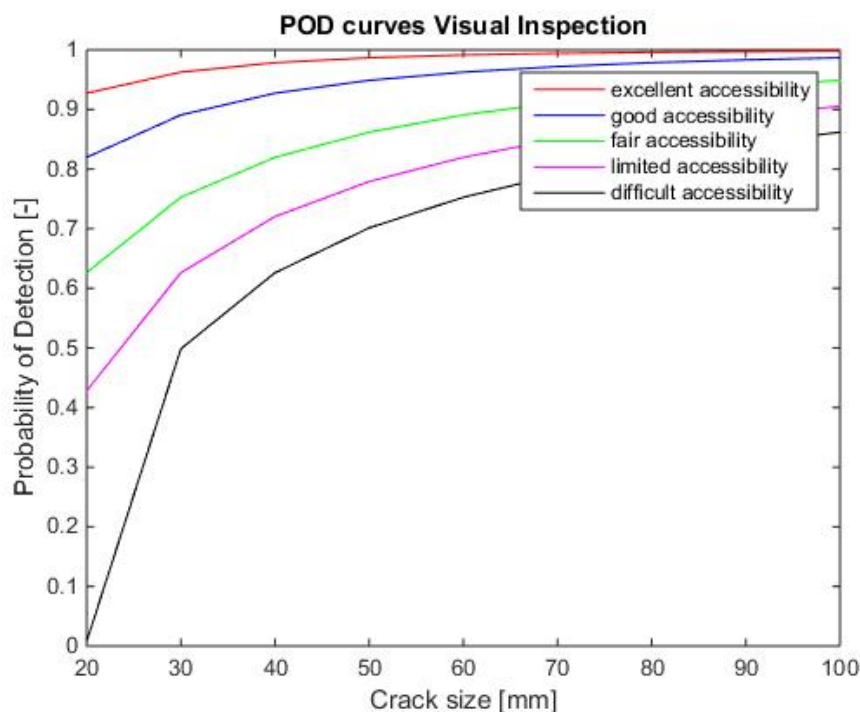


Figure 6-6: Example of POD curves for visual inspection for varying degrees of accessibility of the structure.

The data regarding the POD for NDT equipment is assumed to be supplied by the equipment manufacturer. When this is not the case Equation 6-1 can be used to establish an estimate for the POD for different types of NDT methods [5]. a represents the crack size in mm, λ and α are scaling parameters and a_0 represents the crack size where detection is impossible.

$$POD = 1 - e^{-\left(\frac{a-a_0}{\lambda-a_0}\right)^\alpha} \quad (6-1)$$

The values for a_0 for different types of NDT methods are presented in Table 6-1 [5]. The parameters describing the eddy current method, magnetic particle inspection and alternating current field measurement (a method similar to the eddy current inspection method) can be regarded as being equal [1] and are therefore not separately entered into the table. The values for the scaling parameters for different types of NDT methods are displayed in Table 6-2.

Table 6-1: Values for a_0 (in mm) used in Equation 6-1 [5]

Accessibility	Visual Inspection	Radiographic Inspection	Colour Penetration Test	Ultrasonic Inspection	Eddy Current Technique
Excellent	2.54	1.524	0.762	0.508	0.889
Good	5.08	3.048	1.524	1.016	0.889
Fair	10.16	6.096	3.048	2.032	0.889
Limited	15.24	9.144	4.572	3.408	0.889
Difficult	20.32	12.19	6.096	4.064	0.889

Table 6-2: Values for the scaling parameters used in Equation 6-1 [5]

Parameter	Visual Inspection	Radiographic Inspection	Colour Penetration Test	Ultrasonic Inspection	Eddy Current Technique
α [-]	0.5	0.5	0.5	0.5	1.78
λ/a_0 [-]	2.0	2.5	2.17	3.0	2.23

The scatter in the scaling parameters describing the POD for visual inspection is large, because the reliability of this method largely depends on the people performing the inspection. A study comparing the performance of 12 inspectors working in the aviation industry found a detectable crack size range of 0.16 to 0.91 inch (which equals a range of 4.06 to 23.11 mm) at a POD of 0.9 [74]. Therefore any published POD values for visual inspection need to be used with caution.

Because the crack initiation period at welds is negligible, it is assumed that cracks are always present at the structures of STS gantry cranes. This means that when cracks are not detected, their size is expected to be equal to the crack size which cannot be detected (the expected crack size is thus equal to the a_0 parameter of the NDT equipment that is used during the inspection).

STS cranes are often subjected to visual inspection because it is a relatively quick method and the paint layer does not have to be removed. When the required POD value is smaller than the critical crack size an inspection method needs to be selected that is able to reliably detect smaller cracks. A suitable method for inspection of an existing STS crane therefore might involve a combination of visual inspection and another NDT method. The inspection methods that should be used are selected on their POD values with respect to the critical crack size of the area that is to be inspected.

The boundary between different NDT methods is set at the crack size which corresponds to a POD of 0.99 (using data from Tables 6-1 and 6-2). The selection of the NDT method is related to the critical crack size of the member that is to be inspected. When the critical crack size is below the chosen threshold (POD equal to 0.99) another method is selected which is able to detect potential cracks with the desired level of reliability.

The values for the crack sizes at two POD values are displayed in Table 6-3. Apart from the crack size at a POD of 0.99, the crack size at a POD of 0.95 is displayed in order to show that the choice for a POD value has a significant influence on the decision making process regarding the inspection methods to be used. The values for the POD's are evaluated for the case in which the accessibility of the structure can be marked 'excellent'.

Table 6-3: Values for the crack sizes at POD values of 0.99 and 0.95

Method	Crack size at POD of 0.99 [mm]	Crack size at POD of 0.95 [mm]
Visual inspection	56.4	25.3
Color penetration test	19.7	8.8
Eddy current technique	3.5	2.9
Ultrasonic inspection	22.0	9.6
Radiographic inspection	50.0	22.0

This means that for critical surface crack lengths above 60 mm, the visual inspection method will be used. According to the engineering department at Kalmar, this is a reasonable number because they rule that an inspector must be able to detect cracks in order of 30 to 40 mm. This statement is supported by the crack size corresponding to a POD value of 0.95, which is equal to 25 mm.

For critical surface crack lengths between 20 and 60 mm, the colour penetration test will be employed. When necessary, the eddy current technique or magnetic particle inspection can be used to detect even smaller cracks, as they have similar POD curves.

For cracks which are not visible (like cracks at the inside of connections or cracks originating from weld roots), the ultrasonic inspection method can be employed for critical crack lengths above 22 mm. For critical crack lengths lower than 22 mm, the eddy current inspection method can be used.

Radiographic inspection is outperformed by all inspection methods bar visual inspection, therefore this method will not be used to inspect STS cranes.

Repair Methods for Cracks in Steel Structures

The remaining fatigue life of STS cranes (which is calculated using the model discussed in Chapter 4) can be extended when fatigue cracks are repaired. This chapter therefore concerns repair methods for fatigue cracks in steel structures of STS cranes. The crack repair methods are listed in the first four sections and an overview of these methods is presented in the last section.

The methods that are considered are:

- Load path redundancy
- Reduction of SWL
- Gouge-and-weld method
- Drilling crack arrest holes near the crack tip
- Adding doubler plates

7-1 Load Path Redundancy and Reducing the SWL

Two methods are developed which mitigate the effect of fatigue cracks without repairing the crack. The first method uses redundant load paths to limit the consequences of a random fatigue failure. When the structure of an STS crane has redundant load paths, the loads can be redistributed across the structure in case one element fails [8]. Figure 7-1 shows a schematic representation of this concept, several connections can be seen which are able to transmit loads from one structural member to another. When one connection fails, the loads will be redistributed to the other connections.

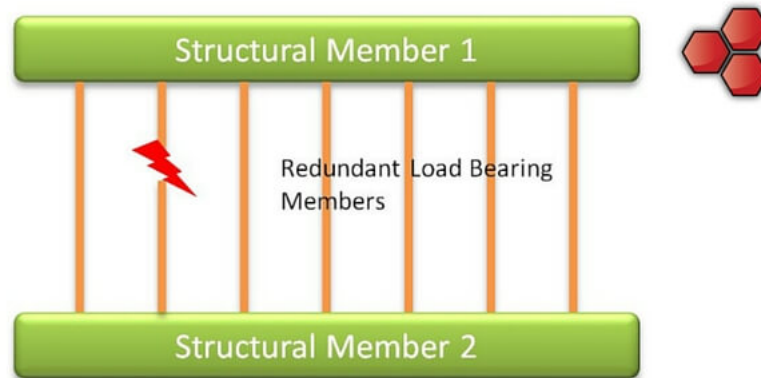


Figure 7-1: Schematic representation of the load path redundancy concept (source: www.stressebook.com).

The use of this method implies a redesign of (existing) STS gantry cranes, because the structure that supports the boom generally does not contain redundant load paths. This method will therefore be of limited use to mitigate the effect of fatigue cracks at STS gantry cranes.

Another way to increase the fatigue life of a STS crane without the need to perform repair works is reducing the Safe Working Load (SWL) of the crane. When the SWL of a STS crane is reduced, the maximum stress and the stress range are reduced as well. The reduction of the maximum stress means that the critical crack size becomes larger and due to the reduction of the stress range the crack growth rate becomes lower. The fatigue life of the STS gantry crane therefore increases without physically altering the steel structure [8].

The SWL of any STS gantry crane has a minimum value in order to comply with the demands set by the owner of the crane. The applicability of this method is therefore limited, because the crane would become ineffective if the SWL drops below a minimum value. This effect has to be taken into account when deciding on the use of this method.

7-2 Gouge-and-Weld Method

The preferred method which is deployed by Kalmar to repair cracks in steel structures of STS gantry cranes is the gouge-and-weld method, where the crack is repaired by plugging it with a weld. The crack is gouged prior to welding because the distance between the crack faces is generally too small to create a satisfactory full penetration repair weld [78].

During the gouging process, the material surrounding the crack is heated locally (for instance using an arc or a flame). The material then melts and is subsequently blown away using a high-velocity gas stream. The gouging tool is moved across the surface to create a groove which can subsequently be filled with a weld. The gouging process is depicted in Figure 7-2. When carbon electrodes are used, carbon is introduced in the material during gouging. The groove resulting from the gouging process must therefore be ground carefully.

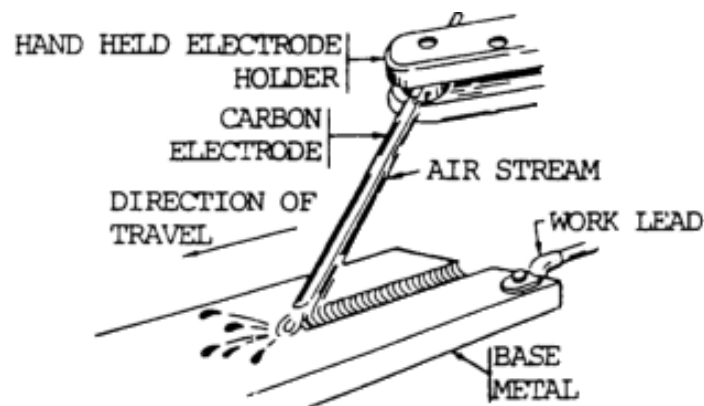


Figure 7-2: Schematic representation of the gouging process (source: www.alloyavenue.com).

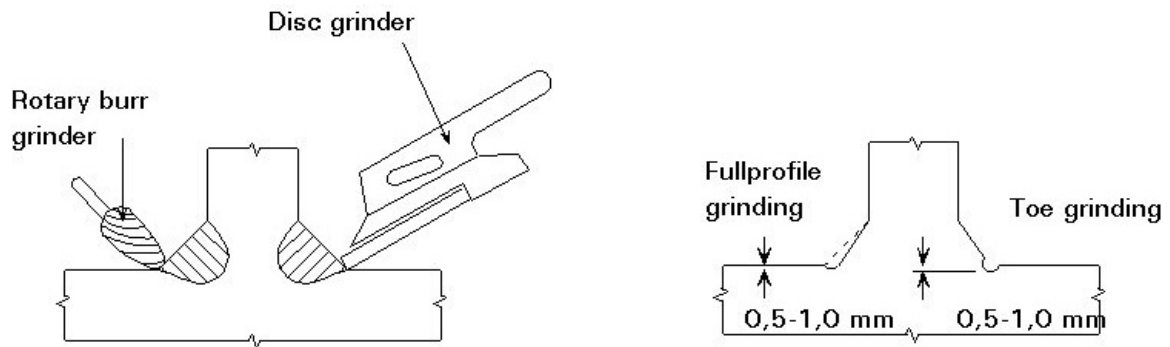
The location of the crack tip is generally difficult to spot because the distance between the crack faces at the tip diminishes. Therefore the length of the gouged groove is in general somewhat larger than the apparent crack length to make sure the entire crack is gouged away. Guidelines on the extra amount of material that needs to be gouged away could not be found in literature. The gouging depth must be at least equal to the maximum crack depth in order to remove the crack entirely.

This method can be applied to repair cracks in the base material and cracks at welded connections. When the repair weld is applied to a cracked plate, the fatigue life of the structure is reduced unless the fatigue strength of the weld is improved (or the local cyclic stress amplitudes are reduced) [78]. The weld should be ground level to the base material in order to reduce the notch factor resulting from the repair weld.

When the repair weld is applied to cracked welded connections, the repair should in theory last as long as the original joint. However, this is often not the case as the repair weld is made in less favourable conditions than the original weld. When the quality of the repair weld does not match the quality of the original weld, the fatigue life of the repair will be lower than the fatigue life of the original joint [78].

The repair weld causes tensile residual stresses as well as notches, which are both detrimental to the fatigue life of the structure. To counteract these effects, two categories of weld improvement methods exist; geometry modification methods and residual stress methods. Geometry modification methods alter the profile of the weld in order to reduce the stress concentration imposed by the geometry of the weld. Residual stress methods reduce the tensile residual stresses by introduction of compressive stresses.

The geometry of the welded connection can be improved by burr or disc grinding. These devices are used to create an undercut at the weld toe in order to remove crack-like defects or slag intrusions and to reduce the SCF resulting from the weld profile [79]. A schematic representation of these grinding methods is displayed in Figure 7-3. Another method to improve the weld geometry is weld toe remelting, which uses TIG or plasma welding equipment to remelt the weld toe. The fatigue life of the weld is enhanced because the weld transition becomes smoother (which reduces the SCF associated with the weld geometry) [79].



(a) 1 -Rotary burr grinding, 2 -Disc grinding (b) 3 -Full profile grinder, 4 -Toe grinding

Figure 7-3: Schematic representation of the grinding processes (source: www.fgg.uni-lj.si).

Examples of residual stress methods are hammer peening, shot peening and Post Weld Heat Treatment (PWHT). Hammer peening introduces compressive residual stresses at the surface of the weld toe by deforming it using a solid tool [79]. Shot peening deforms the surface of the weld toe by blasting it with small steel spheres. PWHT reduces (and redistributes) the tensile residual stresses by reheating the material after welding [80].

The exact welding procedure that should be used to repair cracks in steel structures depends on the geometry of the damaged detail. A number of repair procedures are listed in the standard governing repair works to existing structures in the offshore sector (see Reference [81]). The requirements with respect to tolerances, welding procedures and post-welding treatments are described in this standard. These repair welding procedures can be used as a guideline for repair works to the steel structures of STS gantry cranes as well.

A similar method can also be used to repair cracked plates, where a damaged segment is cut out (for instance by gouging) and a new plate is welded into place. The repaired part might not be as strong as the original part due to the stress concentrations at the edges of the repair plate. The welds also introduce residual tensile stresses and a HAZ, which was not accounted for in the design stage. These effects need to be considered during calculations on the remaining fatigue life after applying repair welds to cracked base material.

7-3 Drilling Crack Arrest Holes

Crack arrest holes can be drilled at the crack tip to remove the plastic zone, which diminishes the crack growth rate. This concept is displayed in Figure 7-4, where crack arrest holes are drilled at the crack tips of a center crack. In order to sufficiently stop crack growth the crack arrest hole should be larger than a specific minimum size [82]. Guidelines to determine this minimum diameter for crack arrest holes can be found in Reference [83].



Figure 7-4: Two crack arrest holes are used to stop a center crack which is initiated at a welded detail (source: www.alwayscivil.blogspot.com).

To further reduce crack growth, an insert can be embedded in the crack arrest hole in order to create a residual compressive stress. This local compressive stress will slow down the crack growth process even further, thus extending the fatigue life of the repaired detail [84]. An example of such an insert is a cylinder (slightly larger than the crack arrest hole) which is shrink-fitted to the hole. Use of tensioned bolts as inserts is not recommended because this only leads to a marginal increase of the remaining fatigue life [82].

Another way to reduce crack growth is to use crack arrest holes that have an optimised shape [85]. The optimised holes are not necessarily circular, which means they might be relatively difficult to apply in practice.

This repair method is predominantly used as a temporary repair, as the crack will reinitiate after a number of load cycles. The crack reinitiates because the average stress at the cross-section increases as a result of the hole. The hole also creates a notch, meaning that the stress in the material surrounding the hole increases with respect to the average stress at the cross-section. The number of load cycles until reinitiation of the crack depends on the dimension of the hole, the finish of the hole and the magnitude of the load.

7-4 Doubler Plates

A method often used to repair cracks in the aviation industry is the application of doubler plates. First, the material surrounding the crack is removed to eliminate the plastic zone at the crack tips. Subsequently, a plate is placed on top of the resulting gap in the structure and is fastened by bolts or welds. A schematic view of this principle can be seen in Figure 7-5.

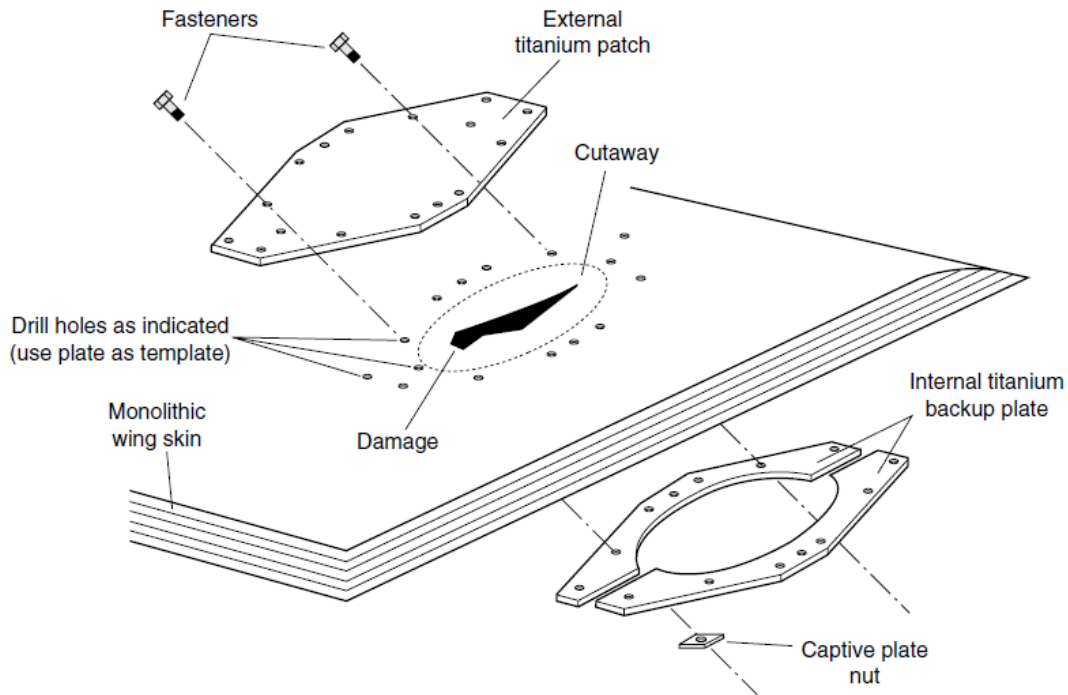


Figure 7-5: Example of a repair using a doubler plate which is fastened by bolts (source: www.dsiac.org).

The doubler plates increase the local cross-sectional area, which reduces the stress in the material surrounding the crack. However, the doubler plates also create an additional notch due to the local increase in total plate thickness which cancels a part of the stress reduction. The downside of this method is that the crack might be reinitiated at the cutaway which may not be initially detected due to the plate blocking the view.

7-5 Overview of Crack Repair Methods

Table 7-1 displays the main advantages and disadvantages of the aforementioned crack repair procedures. The load path redundancy method will not be used in this research due to its limited applicability with respect to STS cranes. The reduction of the SWL as a measure to counteract the presence of fatigue cracks will not be considered either, because it will only lower the crack growth rate. This means that the crack ultimately needs to be repaired using another method, reducing the SWL only extends the timeframe in which these repairs need to be performed.

For the repair of cracked welds, the crack arrest hole and the gouge-and-weld methods are considered. For crack repairs in the base material, the use of doubler plates is considered as well. The remaining fatigue life and the inspection interval after repair need to be calculated, taking the effects of the selected repair method on the fatigue life of the crane into account.

Table 7-1: Overview of the advantages and disadvantages of the crack repair procedures.

Method	Advantage	Disadvantage
Load path redundancy	Consequences of random fatigue failure are reduced	Method implies a redesign of (existing) cranes
Reduction of SWL	Adjustments to the structure are not required	Method can only be implemented when reduction of SWL is justified considering the performance objectives of terminal operator
Gouge-and-weld	Repaired welded connections are theoretically as strong as the original welded connections	Repair weld can create extra notch and residual tensile stresses, which reduce the remaining fatigue life after repair
Drilling crack arrest holes	Quick and low-cost method	Crack is able to reinitiate, which must be accounted for by the inspection regime
Mounting doubler plates	Average stress at crack decreases, which reduces the driving force of the crack growth process	Crack is able to reinitiate and is hard to detect due to nature of repair

Fatigue Life Assessment Method

This chapter describes the method that is developed to assess the remaining fatigue life of STS gantry cranes. The structure of the fatigue assessment method is explained in the first section and the steps that are incorporated in this method are explained in the subsequent four sections.

Evaluation of the fatigue damage during the design fatigue life is performed using SN-curves, this process is discussed in section two. The third section covers the set-up of inspection procedures to monitor the fatigue damage of the steel structures of STS cranes. Section four describes the calculation procedure for the remaining fatigue life using a crack growth model and this chapter concludes with a discussion on the selection of a suitable repair method, which might be required when the remaining fatigue life of the crane is considered to be insufficient.

8-1 Structure of the Assessment Method

The flowchart of the fatigue assessment method is displayed in Figure 8-1 (A larger version of this image is included in Appendix B).

The flowchart shows the steps that are taken in the assessment method for the remaining fatigue life of steel structures of existing STS cranes. The set-up of inspection procedures and repair works are shown in separate flowcharts, because these procedures are equal at each stage. The flowchart to determine the required inspection procedure is included in section three, while the flowchart governing the selection of repair methods is presented in section five.

The data that is required to assess the remaining fatigue life is collected in the first step of the assessment method. The collected data comprises of the stresses in the structure of the crane, usage of the crane and the properties of the materials that are used in the structure of the crane. This data is used to evaluate the cumulative fatigue damage using SN-curves and fracture mechanics.

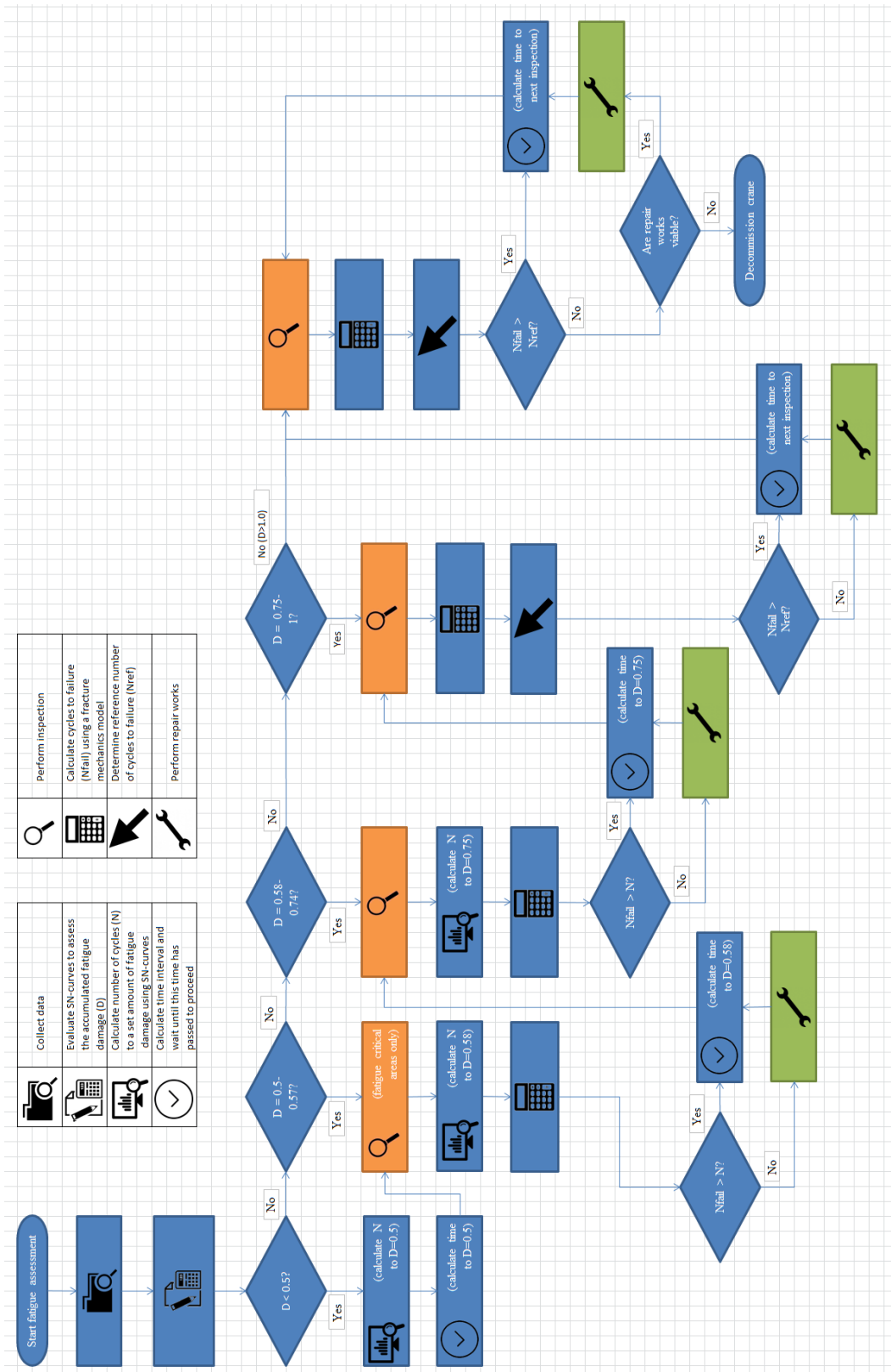


Figure 8-1: Flowchart of the fatigue assessment model for steel structures of existing STS gantry cranes.

The fatigue assessment method consists of five stages. The transition between two subsequent stages is governed by the fatigue specific resistance factor as defined by the EN 13001 design standard [6]. The values of the fatigue resistance factor with respect to the accessibility and the consequence of failure of the detail under consideration are displayed in Table 8-1. Non-failsafe structures are designed to the safe-life design concept, while fail-safe structures are designed according to the damage-tolerance design concept. Within the structure of a single STS crane, both concepts can be applied. For those elements of the structure where a failure does not have any consequences regarding the structural stability of the crane or the position of the load, the damage-tolerant design principle is used while for other details the safe-life approach is in effect.

Table 8-1: Values of the fatigue specific resistance factor for different types of details as a function of accessibility and consequence of failure [6].

	Fail-safe	Non-Failsafe (without hazards to persons)	Non-Failsafe (with hazards to persons)
Accessible detail	1.0	1.1	1.2
Detail with poor accessibility	1.05	1.15	1.25

For the majority of details used in cranes, the accumulated fatigue damage is proportional to the stress range to the third power (according to the design standard [6]). The fatigue specific resistance factor is therefore also put to the third power. Because the fatigue resistance factor is a safety function regarding fatigue failure of STS cranes, the transition between stages is chosen to be the inverse of the specific resistance factor to the third power. The values for fail-safe operation are not used, because fatigue life monitoring of non-failsafe details is dominant (the inspection intervals are shorter for non-failsafe details, which means that fail-safe details are checked moreoften than theoretically required).

The fatigue critical areas are assumed to have the highest fatigue resistance factor (1.25), which means that these locations need to be inspected when the accumulated fatigue damage equals 0.5. The rest of the structure is considered to have a fatigue resistance factor of 1.2 (equivalent to an accessible structure where failure creates hazards to persons). This means that a detail needs to be inspected when the accumulated fatigue damage equals 0.58. The details are also inspected at a accumulated fatigue damage of 0.75 (for a fatigue resistance factor of 1.1, equivalent to an accessible structure where failure does not create hazards to persons) to account for details with low crack growth rates.

The four transition points are listed in Table 8-2, where the type of details under consideration are listed along with the accumulated fatigue damage corresponding to a transition between two stages in the fatigue assessment method.

Table 8-2: Values for the transition points, based on the specific resistance factor as defined by the EN 13001 design standard.

Type of details	Accumulated fatigue damage
Fatigue critical details	0.5
All details	0.58
All details	0.75
All details	1

This means that the first stage is in effect while the accumulated fatigue damage is lower than 0.5. This stage employs SN-curves to calculate the timeframe in which the fatigue damage is expected to equal 0.5. During this timeframe, no further action is warranted and the assessment procedure continues at stage two.

The second stage concerns the fatigue critical areas and is triggered when the accumulated fatigue damage ranges between 0.5 and 0.57. After inspection of these areas, the number of stress cycles in which the accumulated fatigue damage is expected to equal 0.58 is determined using SN-curves. The inspection results are subsequently entered into a fracture mechanics model to calculate the number of cycles to failure. The inspection interval is determined when the remaining fatigue life (as calculated by the fracture mechanics model) exceeds the prediction based on the calculation using SN-curves. When this is not the case, suitable repair works are selected and scheduled. After these repair works are executed, the interval to the next inspection is calculated and the assessment process moves on to the third stage.

The third stage is executed for an accumulated fatigue damage between 0.58 and 0.74. The process conducted in this stage is similar to the process in the previous stage, the only difference is that this stage concerns the analysis of all details instead of the critical details only. This stage concludes by calculating the time in which the accumulated fatigue damage is expected to equal 0.75.

Stage four is executed near the end of the design fatigue life of a STS crane (where the accumulated fatigue damage ranges from 0.75 to 1.0). This stage calculates the remaining fatigue life using a fracture mechanics model and its results are compared to a reference number of cycles. The reference number of cycles is derived from a predetermined minimum time interval in which the crane should be operational. When the predicted remaining fatigue life of the STS crane is insufficient, any structural deficiencies need to be repaired or upgraded. The inspection interval is determined before the fatigue assessment procedure moves onto the final stage, where the fatigue life is assessed after the design fatigue life has expired.

The final stage is an iterative process which starts with an inspection of the entire steel structure. The analysis of the remaining fatigue life is equal to the fatigue life calculation process in stage four. The only addition to this is that for each iteration a decision needs to be made if repair works are viable (in case repair works are required to reach the reference number of cycles). This step is included because even when the fatigue life is monitored well, a STS gantry crane will not have an indefinite service life. At some point in time the crane will have to be decommissioned, because the amount of work required to repair the fatigue damage to the structure becomes too large.

8-2 Evaluation of SN-curves

SN-curves are used to evaluate the accumulated fatigue damage and the amount of cycles it takes for a crane to reach a predetermined amount of fatigue damage. The SN-curves that are used in the assessment are taken from the design standard that is applicable to STS gantry cranes [6]. An example of SN-curves for steel and aluminium is displayed in Figure 8-2.

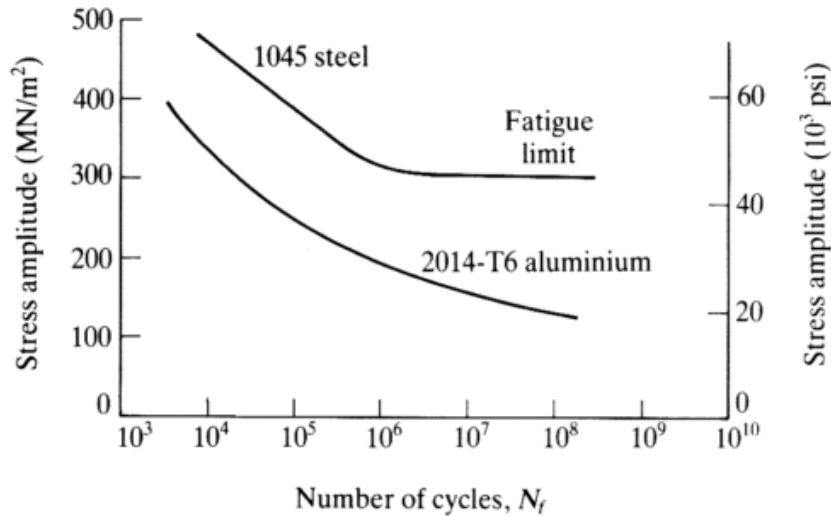


Figure 8-2: Examples of SN-curves for steel and aluminium (source: www.efunda.com).

The number of cycles that would lead to failure at a given stress amplitude can be established using the SN-curve. The SN-curve is defined in the standard by an allowable stress amplitude at a reference number of cycles and an exponent. The allowable stress and the exponent vary per detail. According to the design standard, the mean stress influence and sequence effects can be considered to be negligible [6]. This means that the fatigue damage accumulation can be calculated using the Palmgren-Miner rule (see Equation 8-1), which sums the fatigue damage (D) for all stress amplitudes (n). The fatigue damage for a stress amplitude i is equal to the ratio of the number of occurrences of that stress amplitude (n_i) and the number of cycles that would lead to failure at that stress amplitude (N_i).

$$D = \sum_{i=1}^n \frac{n_i}{N_i} \quad (8-1)$$

When the load history for each detail is described using one stress amplitude, the stress history parameter (used in the EN13001 crane design standard to represent the Palmgren-Miner rule) becomes equal to one. This means that the fatigue damage can be described by the stress amplitude with respect to the allowable stress amplitude. This can be seen in Equation 8-2, where UF is the utilisation factor with respect to fatigue, $\Delta\sigma$ represents the stress amplitude and $\Delta\sigma_{allow}$ represents the allowable stress amplitude at the reference number of cycles.

$$UF = \frac{\Delta\sigma}{\Delta\sigma_{allow}} \quad (8-2)$$

The design fatigue life of the crane expires when the accumulated fatigue damage as calculated by the Palmgren-Miner rule becomes equal to one. Therefore the SN-curves are not used for assessment of the remaining fatigue life of the structure of STS gantry cranes when the calculated accumulated fatigue damage exceeds 1.0.

8-3 Determining the Inspection Procedure

The flowchart depicting the process of determining the inspection procedure is depicted in Figure 8-3 (a larger version can be found in Appendix B). This process consists of three steps; selection of the inspection method, performing a global inspection of the structure and detection of fatigue cracks. These steps are explained in the following three subsections.

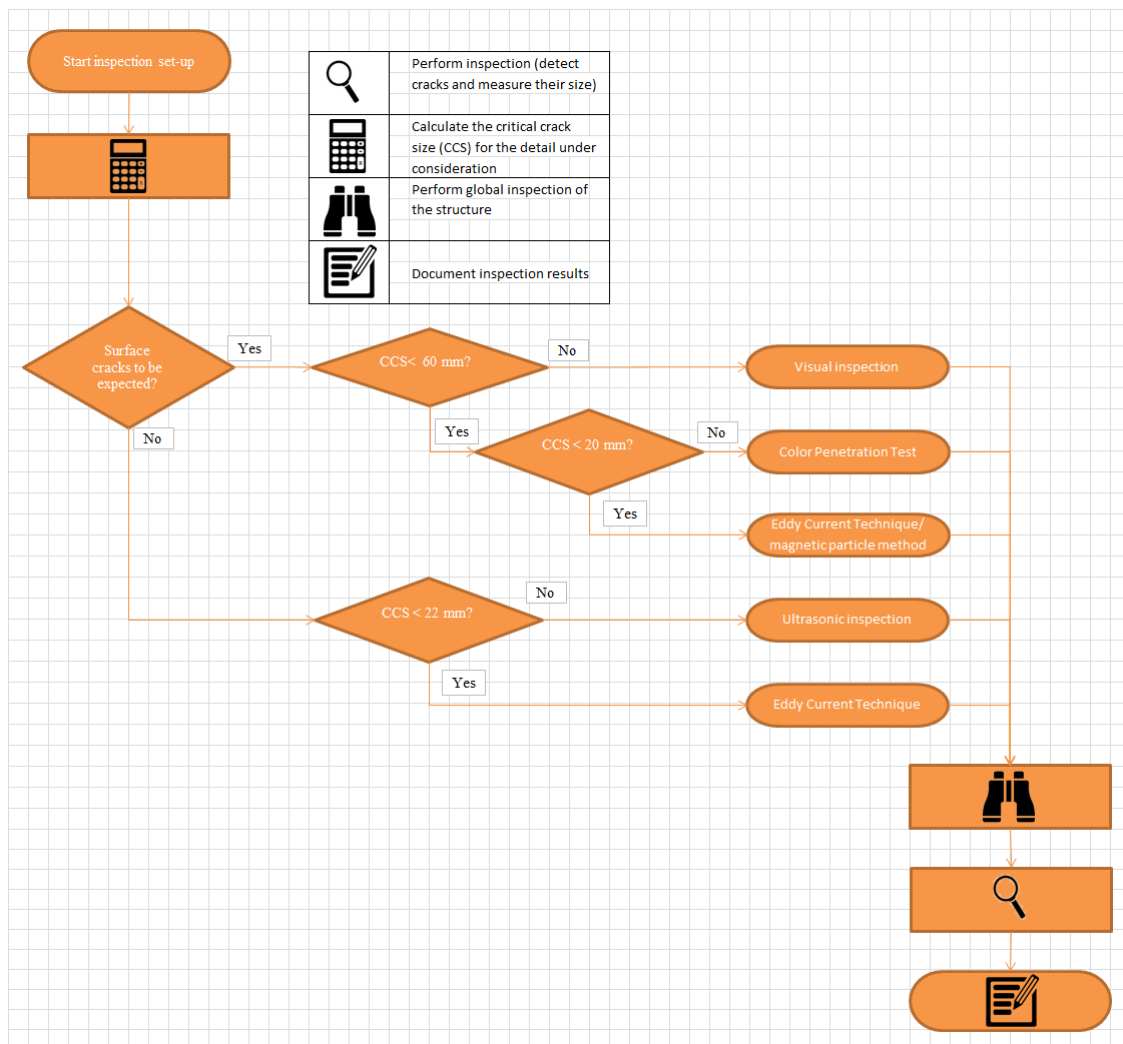


Figure 8-3: Flowchart of the process of determining the inspection procedure for steel structures of existing STS gantry cranes.

8-3-1 Selection of Inspection Method

The first step is to select the inspection methods that should be used to detect and measure fatigue cracks across the structure. This step is performed prior to the inspection itself. The selection of the inspection methods is related to the critical crack size (which is explained in Chapter 6). Apart from the critical crack size, the selection of the inspection method also depends on whether surface or subsurface cracks are to be expected.

Subsurface cracks can be expected for fillet welds for which the weld height is relatively small (less than 85 % of the main plate thickness). For small weld penetration depths, weld subsurface cracks are more likely as well. The likelihood of a root failure also increases when a weld is subjected to PWHT or very large stress amplitudes ("very large" is not further specified in the reviewed literature) [70]. Subsurface cracks can therefore be expected at small weld heights and penetration depths which are highly loaded in fatigue. Surface cracks are to be expected at other welds and plates.

Because the geometry and the load on each member are different, the critical crack sizes of the members are different. This means that the inspection methods are selected separately for each member or detail of the crane that is to be inspected.

8-3-2 Global Inspection of the Structure

The second step of the inspection procedure consists of a global inspection of the structure. This step is performed during the inspection in order to verify whether the crane is in its design condition. When this is not the case, the stresses which were calculated in the design process are not applicable. Three cases are considered; deviation with respect to the design specification, influence of accident damage and a change in load spectrum with respect to the design specification.

Deviations of the built structure with respect to the design specification often arise due to modifications of the crane by its owner. Examples of these types of (non-structural) adjustments are brackets for lighting or communication equipment, which can have a significant influence on the fatigue life of the entire structure [1]. Modification of the structure of the crane can result in local stress concentrations as well as small cracks, which are detrimental to the fatigue life of the structure.

An infamous example of structural collapse due to adjustments to the structure is the accident involving the offshore accommodation platform Alexander L. Kielland. The adjustment in this case concerned a hydrophone support which was set through a brace. The quality of the weld which connected the support to the brace was poor and resulted in significant cracking already during fabrication. The effects of the attachment of the support to the highly stressed bracing were not considered to be important and were therefore neglected in fatigue analyses [86]. Figure 8-4 shows the failed brace, where the hydrophone support from which the fatigue failure initiated is located at the fracture surface. This example highlights the necessity to verify that the crane is in its assumed specification.



Figure 8-4: The brace which failed as a result of a fatigue crack originating from the hydrophone support, which is still attached to the wreckage (source: www.olechris.page.tl).

The structure of the crane is also checked for (accident) damage. Damage to the structure can reduce the load bearing capacity and create local stress increases across the structure. This means that the fatigue life of the structure of a damaged crane can be (significantly) lower. Any signs of damage need to be evaluated in order to prevent the remaining fatigue life to be overestimated.

This also holds for repaired parts of the crane structure, because the repair works can also adversely affect the remaining fatigue life of the structure. For instance, a doubler plate can be welded to the structure in order to repair a damaged plate, which means that cracks can grow from these welds (reducing the fatigue life of that detail with respect to the design specification).

Finally, the crane load spectrum is reviewed in order to make sure the predictions regarding crack growth are correct [8]. This review can be performed by verifying that the specified lifting equipment is attached to the headblock. Alternatively, the load spectrum can be evaluated using load measurement methods (see Sections 2.5.2 and 2.5.3) when these are available at the time of inspection. The crane load spectrum can also be estimated using terminal operational data.

When the result of one of these checks indicates that the original stress analysis is (partly) incorrect with respect to the current operation of the crane, the stresses need to be recalculated in order to ensure the remaining fatigue life assessment yields correct results.

8-3-3 Detect and Measure Fatigue Cracks

The structure of the crane is subjected to inspection in the final step of the inspection procedure. The inspection is performed to detect and measure fatigue cracks. The inspection is performed according to the specification that is constructed in the first step. When fatigue cracks are found, their location is documented along with the size of the crack. This information is used to calculate the remaining fatigue life using a fracture mechanics model.

8-4 Calculation of the Remaining Fatigue Life Using Fracture Mechanics

Once the service life of the crane exceeds the design fatigue life, the remaining fatigue life is calculated using a fracture mechanics model (this calculation model is described in Chapters 4 and 5). The calculation model is provided with the loading of the detail under consideration, the material properties and the measured crack length in order to calculate the remaining fatigue life.

The susceptibility to fracture depends, unlike fatigue, on the type of material and even the particular heat of steel or lot of weld metal [3]. It is therefore preferable to obtain the material properties through material certifications provided by the crane manufacturer. The material parameters that are required by the model are the fracture toughness (for calculation of the critical crack size and the plastic radius), the yield strength (to calculate the plastic radius) and the crack growth parameters. When material properties are not available, standard values for these properties are used in the model.

The load on the detail under consideration can be taken from the results of the stress analysis that is performed during the design process of the crane. The maximum tensile stress determines the critical crack length and the difference between the maximum and minimum stress is a factor in the crack growth rate calculations.

The dimensions of the details can be found in design drawings, so the geometry factor can be determined when the crack size (which is obtained by inspection) is provided. Alternatively, the dimensions can be obtained by measurements of the built structure.

8-5 Selection of Repair Method

When the remaining fatigue life of the steel structure is considered to be insufficient, repair works need to be performed. The flowchart that is used to select a repair method is depicted in Figure 8-5 (a larger version can be found in Appendix B). Execution of the repair methods (described in detail in Chapter 7) is discussed in subsections one to four.

The first stage concerns a review of the documentation which holds information on the location and size of cracks as well as the timeframe in which these cracks need to be repaired. When a detail has a small calculated remaining fatigue life, urgent repair is required. In this case crack arrest holes are drilled to stop crack growth. After these holes are drilled, the detail will be redesigned to increase its fatigue strength. The crack arrest holes are drilled to make sure that the crane will not collapse during the time it takes for the cracked detail to be redesigned and modified. When crack arrest holes cannot be drilled, operations of the crane must be ceased until the cracked detail is modified.

For repair works which do not have to be performed imminently other repair procedures are used. Cracked pins or bolts are replaced with new parts. Cracked pins are replaced because repair works might introduce notches or material discontinuities which reduce the fatigue life of the repaired part compared to the original specification. Cracked bolts are replaced because it is cheaper and quicker than repairing cracks in bolts.

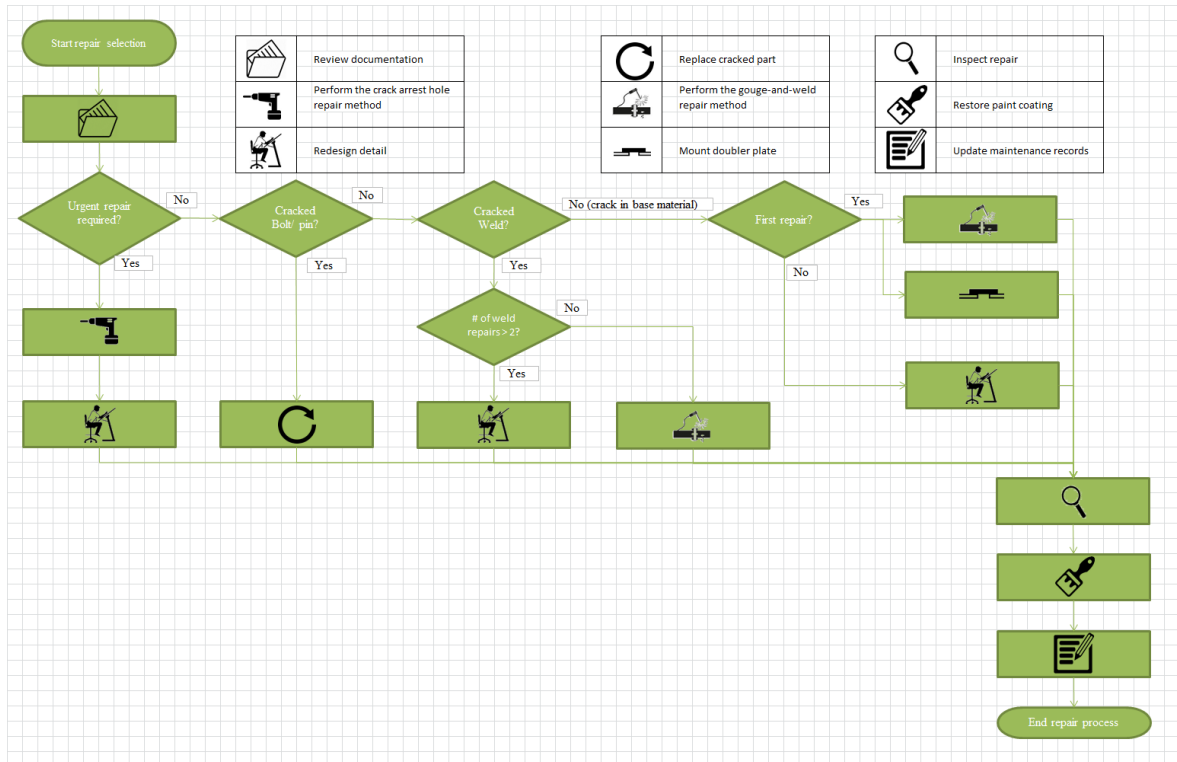


Figure 8-5: Flowchart of the process of determining the repair method for cracks in steel structures of existing STS gantry cranes.

Cracked welds are repaired by the gouge-and-weld method. This repair method can be used to repair cracks up to four times at the same location. However when cracks keep forming at the same location the fatigue strength might be inadequate. Therefore when a fatigue crack is found at the same location for the third time the detail needs to be redesigned to increase its fatigue strength.

In case the crack is found in the base material, it must be determined whether the location under consideration has been subject to repair works before. When the location has been previously repaired, the detail needs to be redesigned because the fatigue resistance of the structure appears to be inadequate. In case the location has not been repaired before, the crack can be repaired using a doubler plate or by replacing the plate (using the gouge-and-weld method around the circumference, gouging a section of the plate clear and welding a new section in place).

The choice between these two options depends on the location of the crack, accessibility of the detail, effect of the repair on the remaining fatigue life and the time available to perform the repair. The doubler plate method is preferred because this method performs better with respect to the remaining fatigue life of the repaired detail.

When the crack is repaired, the repaired section will be subjected to an inspection to determine whether the repair has been performed according to specification. When the detail fails the inspection, the repair has to be redone. When the detail passes the inspection, the paint coating (designed to shield the structure from corrosion) needs to be restored. The final step of the repair procedure concerns updating the crane documentation and maintenance records.

8-5-1 Gouge-and-Weld Method

The gouge-and-weld method is used to repair cracks in welded connections because the repair welds in theory have equal fatigue lives compared to the fatigue lives of the original welds [3]. However, the fatigue life of the repair weld is in practice lower because the conditions in which the repair is performed are often not as good as the conditions during construction of the crane.

This effect can be mitigated using post weld treatments to increase the fatigue life of the repair weld. The post weld treatments reduce the stress concentration at the weld (for example by disc grinding, burr grinding or weld toe remelting) or create compressive residual stresses (for instance by hammer peening, impact treatment or ultrasonic impact treatment) [3].

This repair method can be performed several times at each location. A study found that multiple cycles of repair (up to four) have no detrimental effect on the fatigue life of the repaired detail [3]. This fatigue assessment method only accounts for two repair welds at the same location. When a fatigue crack is formed after the second repair, the detail will be redesigned.

When this method is selected, the gouging and welding procedures need to be specified. In case post weld treatment need to be performed to increase the remaining fatigue life of the repair, execution of this treatment needs to be included in the repair specification.

8-5-2 Mounting Doubler Plates

To avoid applying repair welds in the base material, doubler plates can be used to repair cracks because they can be attached to the structure using bolts. A doubler plate is designed under the assumption that the area beneath the repair no longer carries any load. The load on the structure therefore determines the required cross sectional area of the doubler plate. The number of bolts required to fix the plate as well as their pattern finalise the dimensions of the plate.

Before the plate is mounted to the structure, the crack tips are provided with crack arrest holes to stop the crack growth process. The plate is subsequently used as a drilling template to make sure the holes for the bolts align. The surfaces are then cleaned and the doubler plate is bolted to the structure.

8-5-3 Drilling Crack Arrest Holes

Crack arrest holes act as a temporary measure in case a crack needs to be repaired imminently (see explanation in Chapter 7). This allows for a timeframe in which the crane can be kept operational until a redesign of a cracked detail is executed. Crack arrest holes can only be drilled when the reduction of the strength and stiffness of the structure does not become a hazard in itself.

This repair method starts with identifying the crack tips, using for instance the color penetration test. In case the crack has grown through the thickness, a small hole must be drilled to check whether the crack tip at the other side of the member is aligned [3]. When the location of the crack tip is determined, a minimum drill size needs to be selected using Equation 8-3. Where r indicates the minimum radius of the hole to be drilled, σ_y is the yield strength of the material and ΔK is the stress intensity factor range.

$$\sqrt{r} \geq \frac{\Delta K}{10.5 \sqrt{\sigma_y}} \quad (8-3)$$

After the crack arrest hole is drilled, the edges need to be ground smooth to reduce stress concentrations. An insert can also be mounted in the hole in order to create a compressive residual stress, which reduces the potential for the crack to reinitiate [3].

The location of the hole with respect to the crack tip is important. Ideally, the edge of the hole coincides with the crack tip. When this is not possible, the center of the hole must align with the crack tip in order to create a sufficient repair. The locations of the hole with respect to the crack tip are displayed in Figure 8-6.

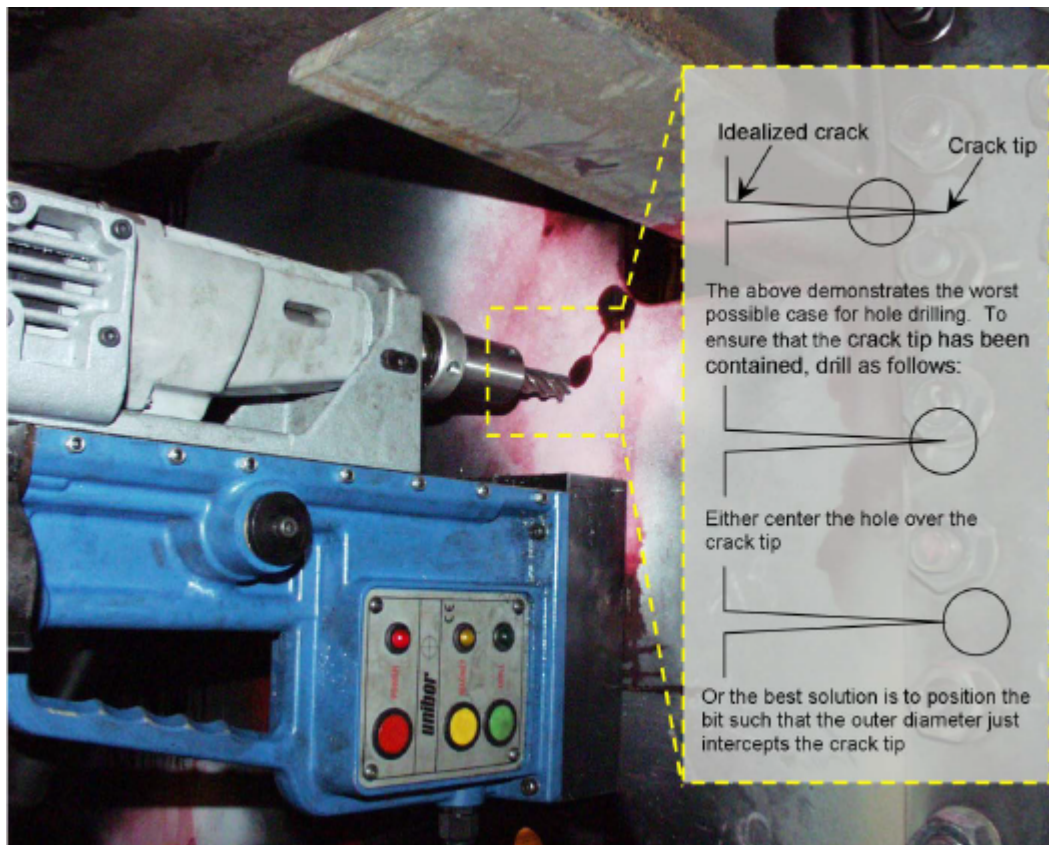


Figure 8-6: Illustration of the preferred location of crack-arrest holes (source: [3]).

8-5-4 Redesign of Detail

A cracked detail is redesigned when a repair is only considered to be effective when the stress range is reduced. The cracked detail is removed and replaced by a new design, which is engineered and manufactured to increase the fatigue strength of the existing crane.

The stress range across the detail can be reduced by increasing the cross sectional area (when the detail is subjected to normal stress) or increasing the moment of inertia (when the detail is subjected to bending stress). Alternatively, the geometry of the global structure can be adapted to redistribute the loads.

When the detail is redesigned to increase the fatigue strength, the effect of this change on other areas needs to be investigated. Strengthening of the detail should be performed according to the methods described in the design standard for STS gantry cranes [6].

FEM Example of Fatigue Life Calculation Method

This chapter serves to visualize the proposed method for assessment of the remaining fatigue life of the steel structures of STS gantry cranes. The remaining fatigue life in this example is evaluated using FEM software. A model of a crane is implemented in Femap and SDC Verifier to visualise the calculation procedure of the remaining fatigue life and the selection of appropriate inspection methods.

The example concerns calculations regarding fatigue only, other types of calculations (static strength or buckling) are not taken into account. The first section describes the set-up of the model, the second section serves to visualise the SN-curve method and the final section visualises the fracture mechanics method.

9-1 Set-up of Example FEM Model

This example concerns a model of a lemniscate crane, of which an example is included in Figure 9-1. These cranes are typically mounted on floating pontoons or barges to perform direct transshipment (which means that cargo is loaded from one vessel directly onto another).

The construction of the lemniscate crane is based on the four-link mechanism concept, which consists of a base and three arms (front, back and top). The front and back arms are used to hold the top arm in place with respect to the base and one of these arms (generally the back arm) is actuated by a hydraulic cylinder to move the mechanism. As a result, the top arm can be moved to and from the base of the crane. The top arm will remain (nearly) horizontal when the mechanism is moved to a new position [87].

FEMAP (Finite Element Modelling And Post-processing) is used to model and analyse the model using finite elements, this program is used as a pre-processor by the SDC Verifier software. SDC Verifier is developed to facilitate the process of verifying structural designs according to design standards and to generate reports containing the results of the analyses. Some of the standards are predefined in the software (FEM, DNV or DIN standards for instance) and others can be defined by the user. Because the standard used in this research (EN 13001) is not included in the software as a predefined standard, this standard will be user defined.

The versions of the software used in the analyses are listed below:

- FEMAP with NX Nastran v11.0 64-bit
- SDC Verifier 4.0 64-bit (trial version)



Figure 9-1: Example of an existing lemniscate crane (source:www.flickrriver.com).

Figure 9-2 shows an illustration of the lemniscate crane model in FEMAP. One part of this model is investigated further in this analysis; the A-frame. This frame connects the back arm to the base of the lemniscate crane. The model of the A-frame is shown in Figure 9-3.

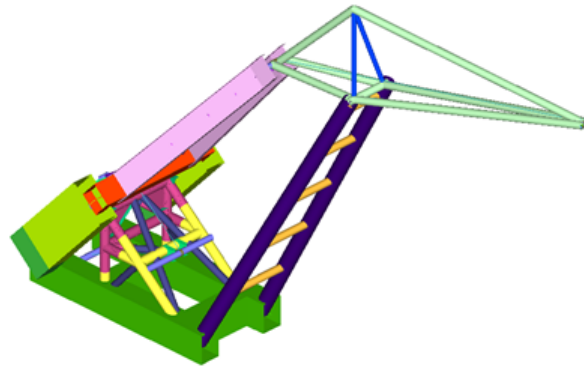


Figure 9-2: Illustration of the lemniscate crane model implemented in SDC Verifier and FEMAP.

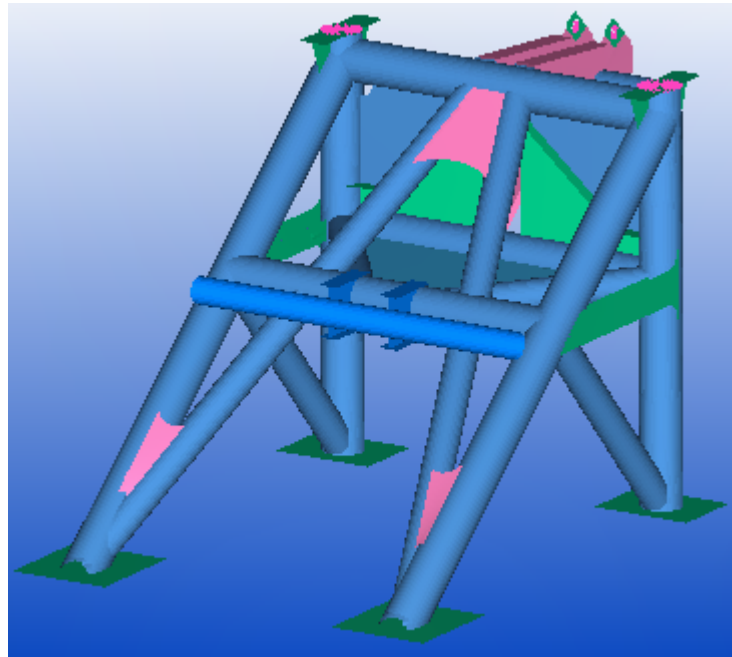


Figure 9-3: Detail model of the A-frame which is used to illustrate the calculation procedure for the remaining fatigue life of STS cranes.

Two configurations of the crane are modelled, one where the hydraulic cylinder is extended (which means that the crane is at its maximum outreach) and one where the cylinder is retracted. The loads on the frame are modelled using six individual loads, these are defined as the gravity load of the part of the structure that is supported by the frame, the effect of the hoist load and the slewing load (the load that acts on the crane as the crane rotates) in both crane positions.

The loads are applied to the model using spiders, which are stiff connections representing the interface with the rest of the crane. There are four interfaces between the A-frame and the mechanism of the crane. The applied loads which are the result of one load effect (for instance gravity) are combined to form an individual load. An individual load is defined in SDC verifier as a combination of FEM loads (which define the loads on the structure) and constraints (which define the boundary conditions). The definition of one of the six FEM loads is displayed in Figure 9-4, where the loads are highlighted using arrows. The implementation of this FEM load in SDC Verifier can be seen in Figure 9-5.

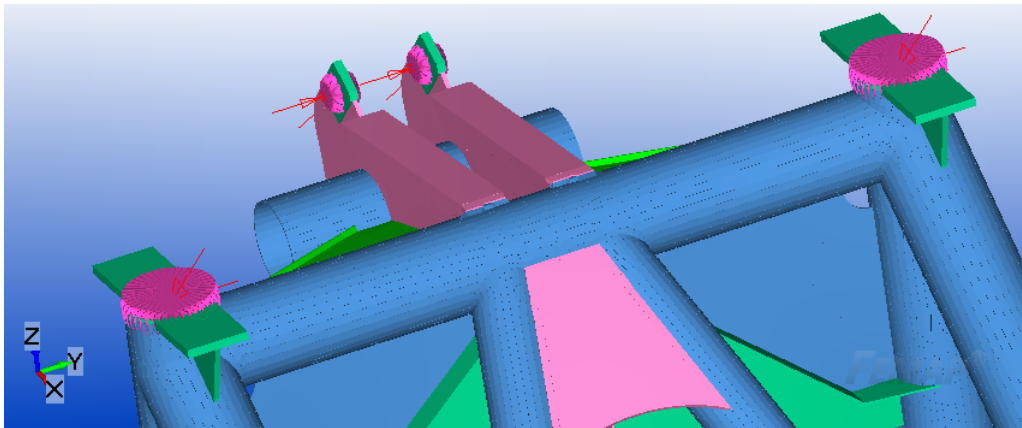


Figure 9-4: Visualisation of the implementation of one FEM load (which describes the gravity load of the supported structure in one crane position).

Node ID	Fx	Fy	Fz	Mx	My	Mz
119265	98737.914	199.703	75847.594	-41.681	115139.242	-35.189
9477	-345579.469		336479.875		-138231.797	
127630	-346385.25	140.78	335613.875	-56.312	-138554.109	
159489	98737.914	-199.703	75847.594	5	115139.242	35.189

Figure 9-5: Example of a FEM load definition in SDC verifier (which describes the gravity load of the supported structure in one crane position).

The individual loads are combined in load sets in order to calculate the effect of multiple individual loads acting on the structure simultaneously. Each load set therefore represents an event, for example: "the crane is rotating clockwise with the maximum hoist load and the boom in maximum outreach". The definition of the load sets in SDC is included in Figure 9-6. The two positions of the crane are indicated with A and C, the load on the crane is either "empty" or "full" and the direction of rotation is indicated by + and -. The six individual loads therefore equate to eight load sets.

	IL7..Gravity C,pinned	IL8..Content C,pinned	IL9..Side Load C,pinned	IL10..Gravity A,pinned	IL11..Content A,pinned	IL12..Side Load A,pinned
Empty C +	0.75		1			
Empty C -	0.75		-1			
Full C +	1	1.53	1			
Full C -	1	1.53	-1			
Empty A +				0.75		1
Empty A -				0.75		-1
Full A +				1	1.53	1
Full A -				1	1.53	-1

Figure 9-6: Definition of the load sets in SDC verifier.

The effects of the different load sets are evaluated in a load group. The load group serves to determine the most severe loading conditions for all elements. Figure 9-7 shows the definition of the load group as it is implemented in SDC. The load group contains all eight load sets and a safety factor (which is in this model 1.0).

	Safety Factor	IL7..Gravity C,pinned	IL8..Content C,pinned	IL9..Side Load C,pinned	IL10..Gravity A,pinned	IL11..Content A,pinned	IL12..Side Load A,pinned	LS1..Empty C +	LS2..Empty C -	LS3..Full C +	LS4..Full C -	LS5..Empty A +	LS6..Empty A -	LS7..Full A +	LS8..Full A -
Load Group 1	1							1	1	1	1	1	1	1	1

Figure 9-7: Definition of the used load group in SDC verifier.

One constraint is used in this model to calculate the stresses in the structure. The edges of the support plates of the frame are pinned, this means that the constrained nodes cannot be displaced in the three orthogonal directions but rotations remain possible. This definition of the constraint represents the welds that are applied to hold the frame to the base of the crane. The constrained elements are displayed in Figure 9-8.

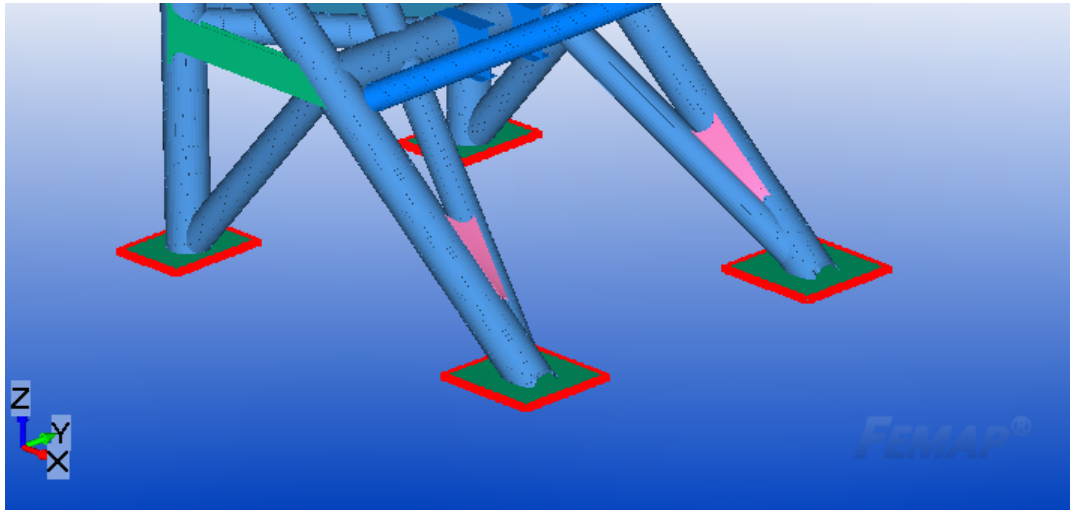


Figure 9-8: Visualization of the locations where the constraints are applied (constrained elements are displayed in red).

9-2 Visualisation of SN-curve Method

The standard that is referred to throughout this thesis is the EN 13001 crane standard, describing the limit states and proof of competence of steel structures. This standard is represented in SDC Verifier by a custom check, using characteristics that are assigned to the model properties. The characteristics are described in the first subsection and the results of the analysis are displayed in the second subsection.

9-2-1 Characteristic Values Used in the Analysis

Four characteristics are required to determine the fatigue life according to the EN 13001 standard; the allowable normal stress range, allowable shear stress range and the exponents of the SN-curves for normal and shear stresses. The values of these characteristics are provided by the standard. The allowable normal stress for the base material is 160 MPa according to the standard. The allowable shear stress for the base material is 112 MPa [6].

The values for welded details are provided as well. The allowable stress for welds which are loaded in the direction along the weld is 140 MPa. When the load is perpendicular to the weld, the allowable stress is 100 MPa. The allowable shear stress for welds and normal stress in case of intersecting welds are also equal to 100 MPa. The exponent for shear stress is equal to 5 and the exponent for normal stress is equal to 3 [6].

The listed fatigue characteristics for welded connections also depend on the weld quality. It is assumed that each type of detail is welded according to weld quality B, as defined in [6]. The values for the fatigue characteristics for welds are selected under this assumption.

The A-frame is considered to be a fatigue critical area because the connection to the back arm is subjected to relatively large load amplitudes. Failure of this frame would likely lead to a collapse of the crane, which in turn is a hazard to humans near the crane. Therefore the fatigue specific safety factor is set at 1.25.

The implementation of the values for the allowable stresses is displayed in Figure 9-9.

No.	Selection	Classification
1	All Entities	160
2	All Entities	112 (XY)
3	All welds	140 (X)
4	All welds	100 (Y)
5	All welds	112 (XY)
6	All welds intersections	100 (X)

Figure 9-9: Implementation of the classification which represents the allowable stresses according to the EN 13001 crane standard.

The location and orientation of the welds are determined using the weld finder tool provided by SDC Verifier. The welds that are applied in this model are visualized in Figure 9-10.

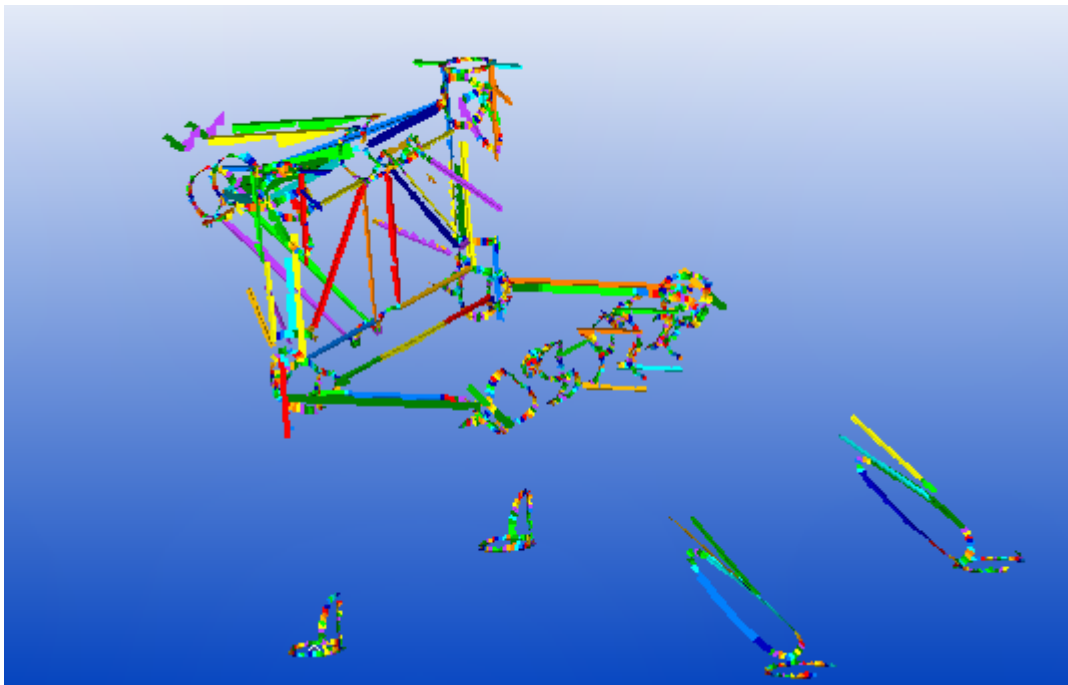


Figure 9-10: Overview of the welds in this model.

A custom check is implemented in SDC to assess the fatigue life based on the ratio between the calculated stress range and the allowable stress range. This ratio is called the utilization factor and is used as an expression for the fatigue life of the crane. This check is performed for the stresses in the X and Y directions (these are the in-plane stresses), the shear stress and the equivalent stress (which is performed according to the rule as defined in the EN 13001 standard). Subsequently, the maximum of the four calculated utilization factors is determined for each element.

The implementation of this fatigue check is displayed in Figure 9-11. This figure shows the definition of the two parameters used in this analysis. This check uses four characteristics: FAT_SF represents the fatigue safety factor, FAT_Class represents the allowable stress range, SN_m1 is the exponent of the SN-curve for normal stress and SN_m2 is the exponent for the SN-curve for shear stress.

Property	Value
Category	Elemental Custom Check
Selection	All Entities
Parameters	4
Alias (Parameter)	Delta S (Delta S)
Description	Calculation of the stress range [Pa]
All	(SMax- SMin)
X	(Smax.x-Smin.x)
Y	(Smax.y-Smin.y)
XY	(Smax.xy-Smin.xy)
Eqv.	(Smax.eqv-Smin.eqv)
Overall	Max(me.x,me.y,me.xy,me.eqv)
Alias (Parameter)	UF_SN (Utilization_Fatigue_SN)
Description	Utilization factor for fatigue based on EN13001 [-]
All	DeltaS*FAT_SF/ (FAT_Class*1000000)
Eqv.	pow(me.x,SN_m1)+pow(me.y,SN_m1)+pow(me.xy,SN_m2)
Overall	Max(me.x, me.y, me.z, me.xy, me.yz, me.zx, me.eqv)
Alias (Parameter)	UF_SN_Update (Utilization_Fatigue_SN_Update)
Description	Updated expression for the utilization factor for fatigue, taking stress singularities into account.
All	DeltaS*FAT_SF/ (FAT_Class*1000000)
Eqv.	pow(me.x,SN_m1)+pow(me.y,SN_m1)+pow(me.xy,SN_m2)
Overall	MIN(Max(me.x, me.y, me.z, me.xy, me.yz, me.zx, me.eqv),MAX_UF)
Alias (Parameter)	N_inspect_SN (N_inspect_SN)
Description	Calculation of the inspection interval using SN curves
All	(Dref/(pow(MAX(UF_SN_Update,0.2),3))) [*] Nref_SNcurve
Overall	MIN(me.x,me.y,me.xy,me.eqv)

Figure 9-11: Overview of the implementation of the fatigue check using SN curves.

9-2-2 Results of Implemented Fatigue Check

The results for the fatigue utilization factor are displayed in Figures 9-12, 9-13, 9-14 and 9-15. The overall result combines the results for normal stress (X and Y directions), shear stress (XY direction) and the equivalent stress (as defined by the EN13001 standard). The result for the overall utilization factor is equal to the utilization factor for equivalent stress, therefore the results for the equivalent stress are omitted in this section.

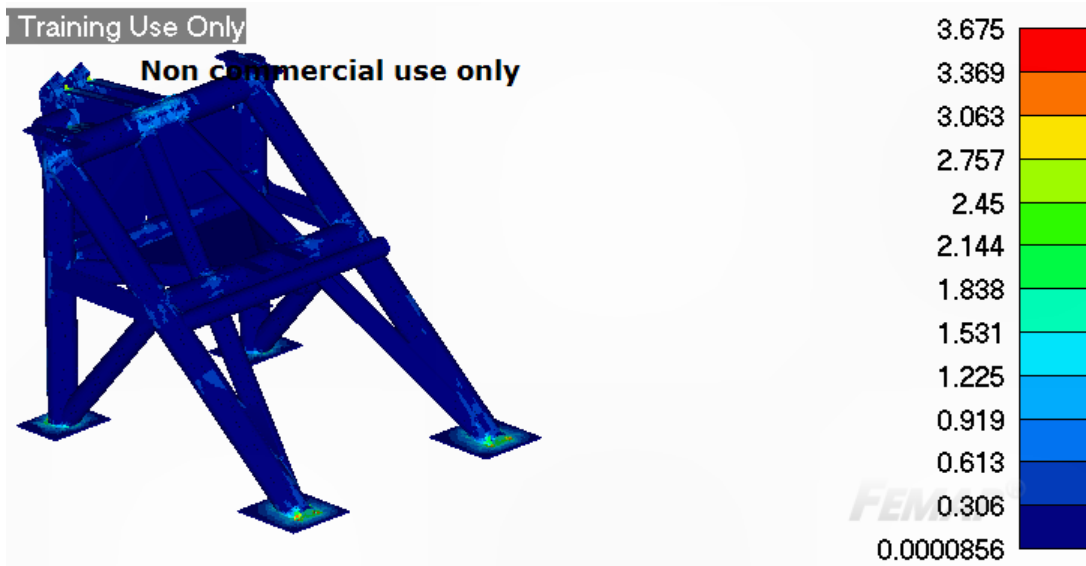


Figure 9-12: Utilization factor for fatigue in the X direction.

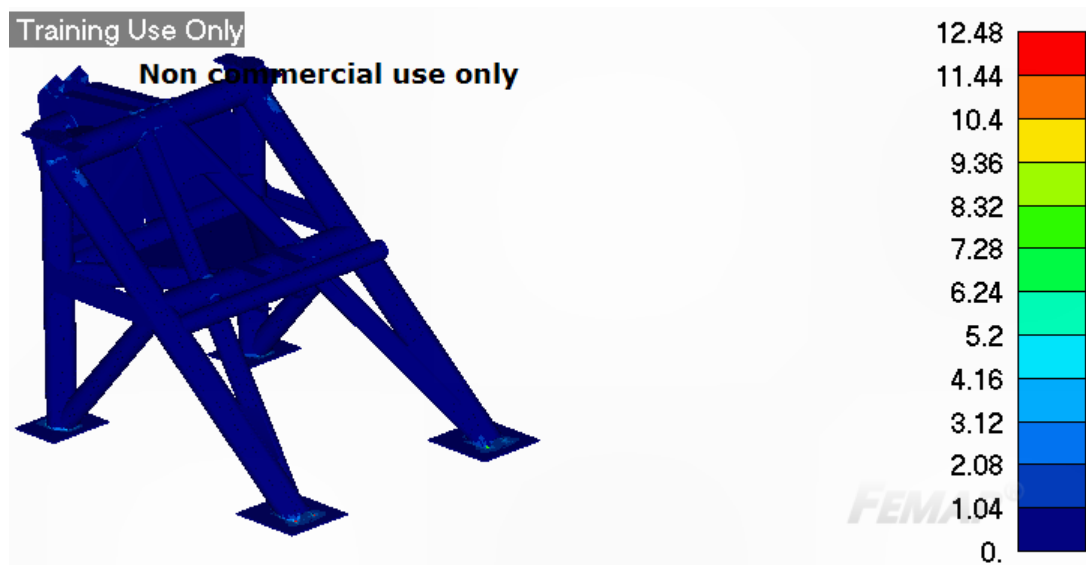


Figure 9-13: Utilization factor for fatigue in the Y direction.

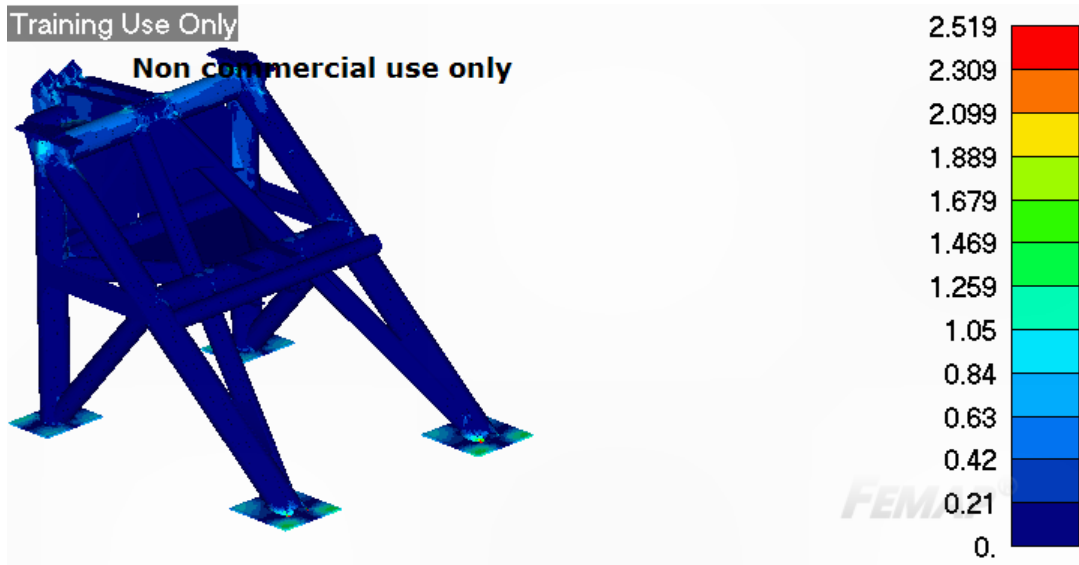


Figure 9-14: Utilization factor for fatigue in the XY direction.

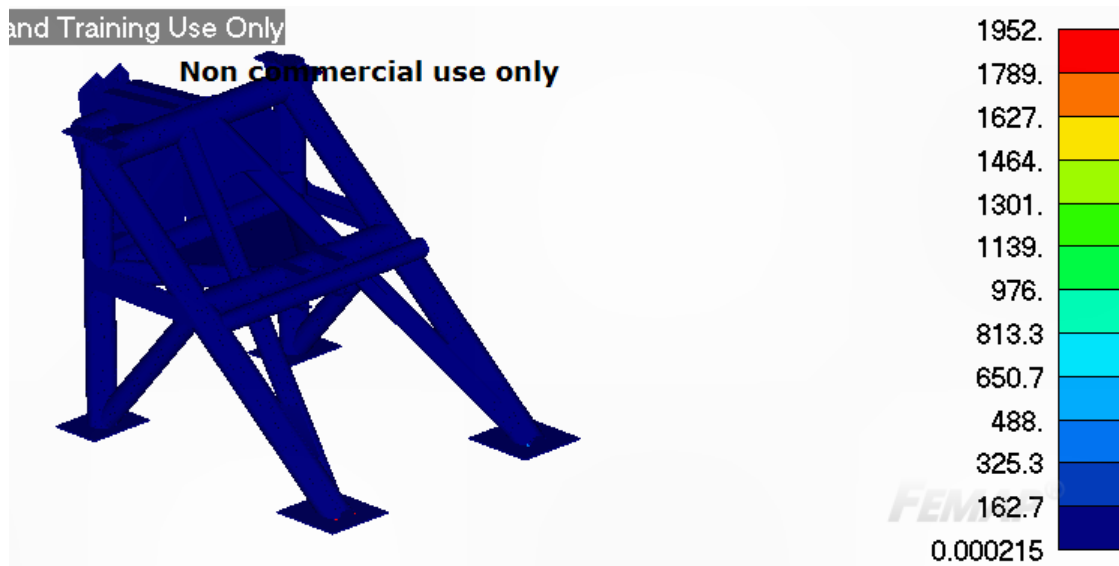


Figure 9-15: Overall utilization factor for fatigue.

The high maximum value for the overall utilization factor implies that the fatigue life is short. When zooming in on the structure, it becomes clear that this value is caused by a few elements which are subject to stress singularities (see Figure 9-16). The value for the stress at a stress singularity is theoretically infinite due to a discontinuity of the geometry at this point. The stress at these locations is therefore much larger than the allowed stress, which equates to higher utilization factors and a reduced fatigue life.

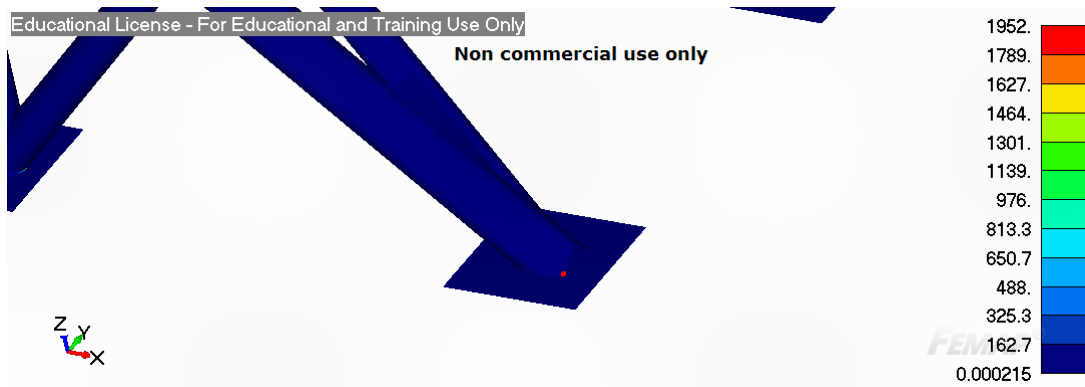


Figure 9-16: Overall utilization factor, zoomed in to show the element subjected to a stress singularity.

The utilization factor for fatigue is limited in order to take these stress singularities into account. This operation therefore makes it easier to interpret the results of the fatigue analysis using SN-curves. The utilization factor is limited at a value of 5, which means that the design fatigue life of the crane would be just 12.000 load cycles. Higher limit values are considered to be irrelevant because a limit value of 5 already yields a conservatively low fatigue life

The results of this modification are included in Figures 9-19 and 9-20. As can be seen in these figures, the areas which are heavily loaded with respect to fatigue are the connections of the base plate to the legs and the connections of the support structure of the back arm to the back legs.

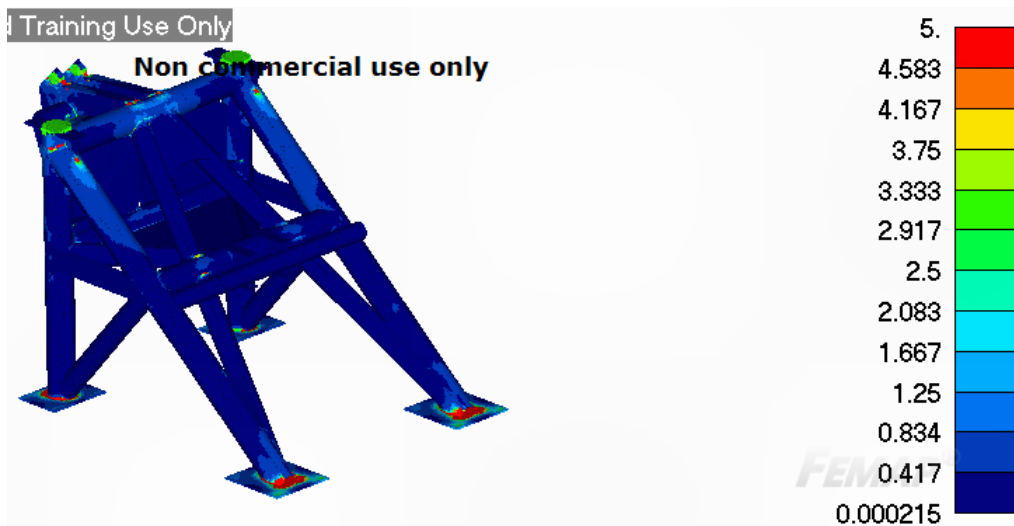


Figure 9-17: The overall utilization factor for fatigue using a limit value of 5.

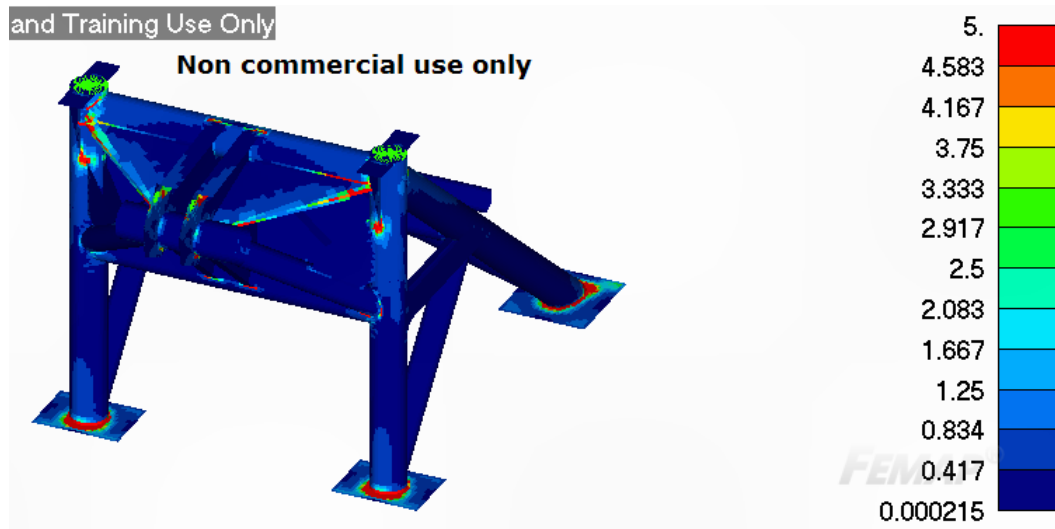


Figure 9-18: The overall utilization factor for fatigue using a limit value of 5 (viewed from the back of the frame).

The final step in this procedure is to calculate the time it takes for the accumulated fatigue damage to reach a predetermined value (modelled by the D_{ref} value). The total amount of cycles to reach a certain amount of accumulated fatigue damage depends on the fatigue utilization factor and the reference number of cycles (set by the EN 13001 standard at 2 million cycles). The results are included in Figures . These figures show the number of cycles (expressed in millions) that it takes for the details to reach an accumulated fatigue damage of 0.75. The areas which are displayed in red can endure a relatively high number of cycles until the reference amount of accumulated fatigue damage is reached. The blue areas can endure a lower number of cycles to reach the same value for the accumulated fatigue damage.

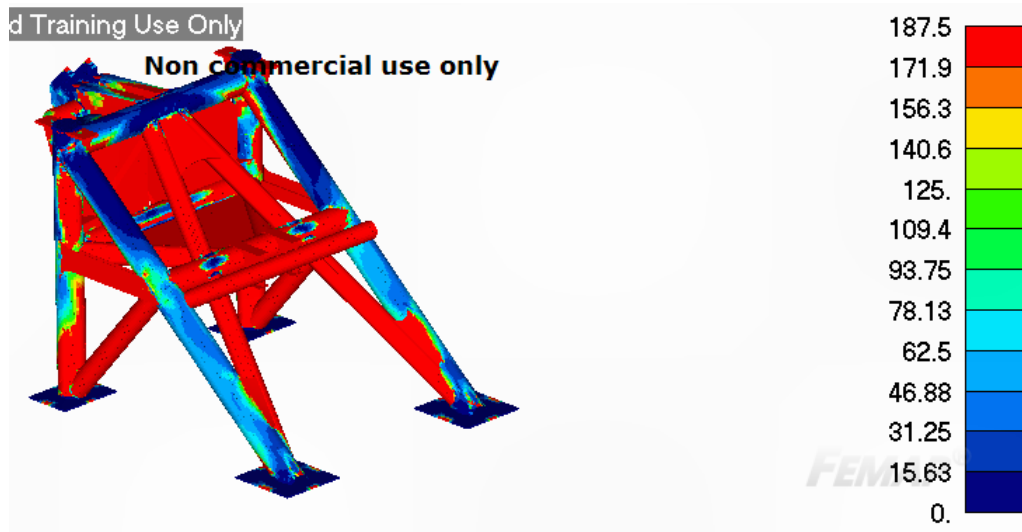


Figure 9-19: Number of cycles to reach an accumulated fatigue damage of 0.75, expressed in millions.

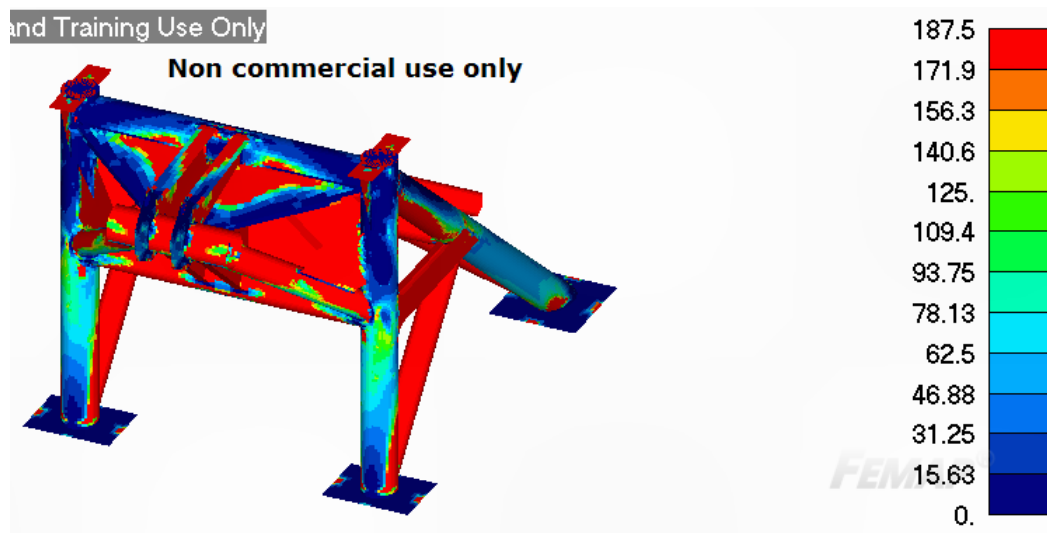


Figure 9-20: Number of cycles to reach an accumulated fatigue damage of 0.75, expressed in millions (viewed from the back of the frame).

The results of this analysis can be used to schedule the required inspections while the accumulated fatigue damage is below 1.0. The number of cycles that are already performed by the crane are subtracted from the total number of cycles required to reach a predetermined value for the accumulated fatigue damage. This difference is subsequently divided by the amount of cycles per unit of time to calculate the inspection interval.

9-3 Visualisation of Fracture Mechanics Method

This section concerns the implementation of the fracture mechanics method which is able to calculate the remaining fatigue life of the steel structure of the crane when it is subjected to fatigue cracks. The implementation of this model in SDC verifier is discussed in the first subsection. The second subsection covers the results of this check.

9-3-1 Implementation of Fracture Mechanics Model in SDC Verifier

The implementation of the fracture mechanics model in SDC verifier can be seen in Figure 9-21. This check calculates the minimum critical crack size (in order to prevent excessive large values for parts which have a low maximum stress), the overall critical crack size, the remaining fatigue life and displays the areas which can be inspected using visual inspection. The result for the remaining fatigue life is limited at 1.000.000.000 cycles to prevent unrealistic large values for the remaining fatigue life.

Property	Value
Category	Elemental Custom Check
Selection	All Entities
Parameters	5
Alias (Parameter)	MAX Stress (Maximum stress)
Description	Calculation of the maximum stress [MPa]
All	SMax/1000000
Overall	AbsMax(me.x, me.y, me.z, me.xy, me.yz, me.zx, me.eqv)
Alias (Parameter)	MaxCCS (Maximum Crack length)
Description	Calculation of the maximum crack size (the crack size at stress cutoff limit) [m]
All	$\text{Pow}(\text{Kic}, 2) / (\text{PI} * \text{Pow}(\text{Y}, 2) * \text{Pow}(\text{Sset}/1000000, 2))$
Overall	Min(me.x, me.y, me.z, me.xy, me.yz, me.zx, me.eqv)
Alias (Parameter)	CCS (Critical Crack Size)
Description	This check calculates the critical crack size [m]
All	$\text{if}(\text{Smax} > \text{Sset}, (\text{Pow}(\text{Kic}, 2) / (\text{PI} * \text{Pow}(\text{Y}, 2) * \text{Pow}(\text{SMax}/1000000, 2))), \text{MaxCCS})$
Overall	Min(me.x, me.y, me.xy)
Alias (Parameter)	RFL (Remaining Fatigue Life)
Description	This parameter calculates the remaining fatigue life [cycles]
All	$(1 / (1 - (\text{m_Class}/2))) * (1 / (\text{C_Class} * \text{POW}(((\text{FATcheck.DeltaS}/1000000), \text{m_Class}) * \text{POW}(\text{Y}, \text{m_Class}) * \text{POW}(\text{PI}, (\text{m_Class}/2)))) * (\text{POW}(\text{CCS}, (1 - (\text{m_Class}/2))) - \text{POW}(\text{ICS}, (1 - (\text{m_Class}/2))))))$
X	$(1 / (1 - (\text{m_Class}/2))) * (1 / (\text{C_Class} * \text{POW}((\text{FATcheck.DeltaS.x}/1000000), \text{m_Class}) * \text{POW}(\text{Y}, \text{m_Class}) * \text{POW}(\text{PI}, (\text{m_Class}/2)))) * (\text{POW}(\text{CCS}, (1 - (\text{m_Class}/2))) - \text{POW}(\text{ICS}, (1 - (\text{m_Class}/2))))))$
Y	$(1 / (1 - (\text{m_Class}/2))) * (1 / (\text{C_Class} * \text{POW}((\text{FATcheck.DeltaS.y}/1000000), \text{m_Class}) * \text{POW}(\text{Y}, \text{m_Class}) * \text{POW}(\text{PI}, (\text{m_Class}/2)))) * (\text{POW}(\text{CCS}, (1 - (\text{m_Class}/2))) - \text{POW}(\text{ICS}, (1 - (\text{m_Class}/2))))))$
XY	$(1 / (1 - (\text{m_Class}/2))) * (1 / (\text{C_Class} * \text{POW}((\text{FATcheck.DeltaS.xy}/1000000), \text{m_Class}) * \text{POW}(\text{Y}, \text{m_Class}) * \text{POW}(\text{PI}, (\text{m_Class}/2)))) * (\text{POW}(\text{CCS}, (1 - (\text{m_Class}/2))) - \text{POW}(\text{ICS}, (1 - (\text{m_Class}/2))))))$
Overall	MIN(me.x, me.y, me.xy, 1000000000)
Alias (Parameter)	CCS_Plot (Plot_ccs)
All	$\text{if}(\text{CCS} > 0.06, 1000, 1)$
Overall	Min(me.x, me.y, me.xy)

Figure 9-21: Implementation of the fracture mechanics model in SDC Verifier.

The stress cutoff parameter is a lower bound to the stress results and therefore provides an upper bound to the critical crack size, so this size does not become unrealistically large. The stress cutoff parameter is in this case equal to 15 MPa. The stress cutoff parameter is modelled as a material characteristic. Other material characteristics are the crack growth parameters and the fracture toughness of the material.

The fracture toughness for mild steel is equal to $140 \text{ MPa} \cdot \sqrt{m}$ [88]. The geometry factors are determined using the equations described in Appendix D. The initial crack size is set at 5 mm, this value is applied across the entire structure.

The crack growth parameters for various types of steel are listed in Table 9-1. This model is assumed to be constructed of low carbon steel, which has properties equivalent to S355 steel. These values are therefore selected in this analysis.

Table 9-1: Values for the crack growth parameters that can be used in this model.

Description	Crack Growth Constant	Crack Growth Exponent	Reference
Welds in steel structures	3.3 e-13	3.1	[73]
S355	2.11e-15	3.7447	[89]
S690	2.261e-13	3.1255	[89]
18 G2A	2e-12	3	[90]
40 H	3.96e-12	2.97	[90]
20 G	2e-11	3	[90]
A533	2e-11	2.2	[90]

9-3-2 Results of Fracture Mechanics Calculations

This section lists the results of the fracture mechanics calculations. The critical crack sizes are included in Figures 9-22 and 9-23. The critical crack sizes are different depending on the location of the structure, as can be seen in these figures.

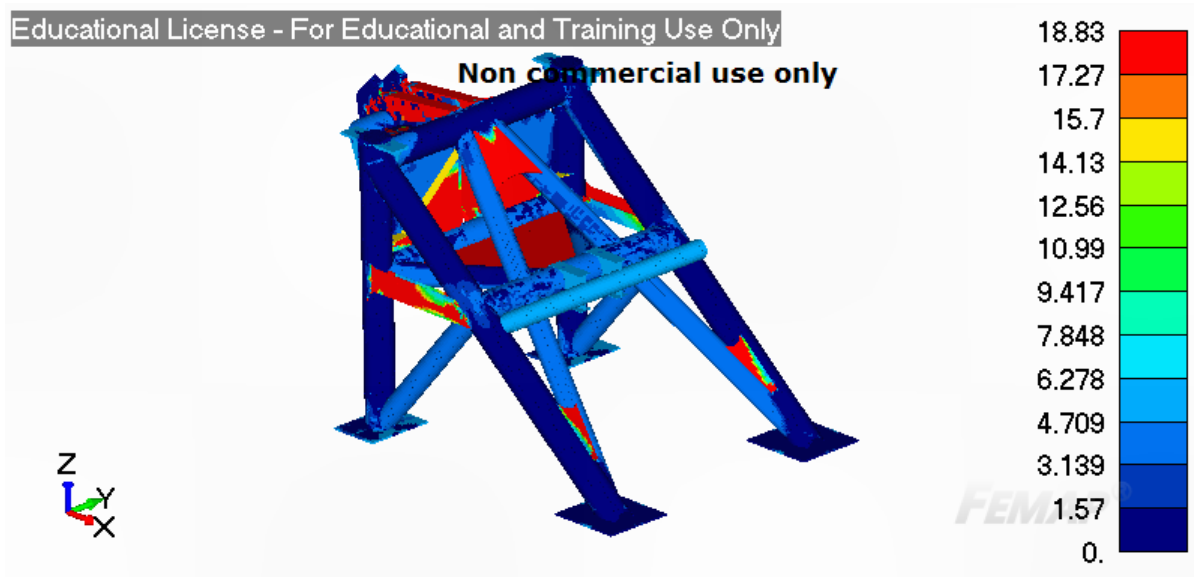


Figure 9-22: This figure displays the critical crack size in metres across the structure.

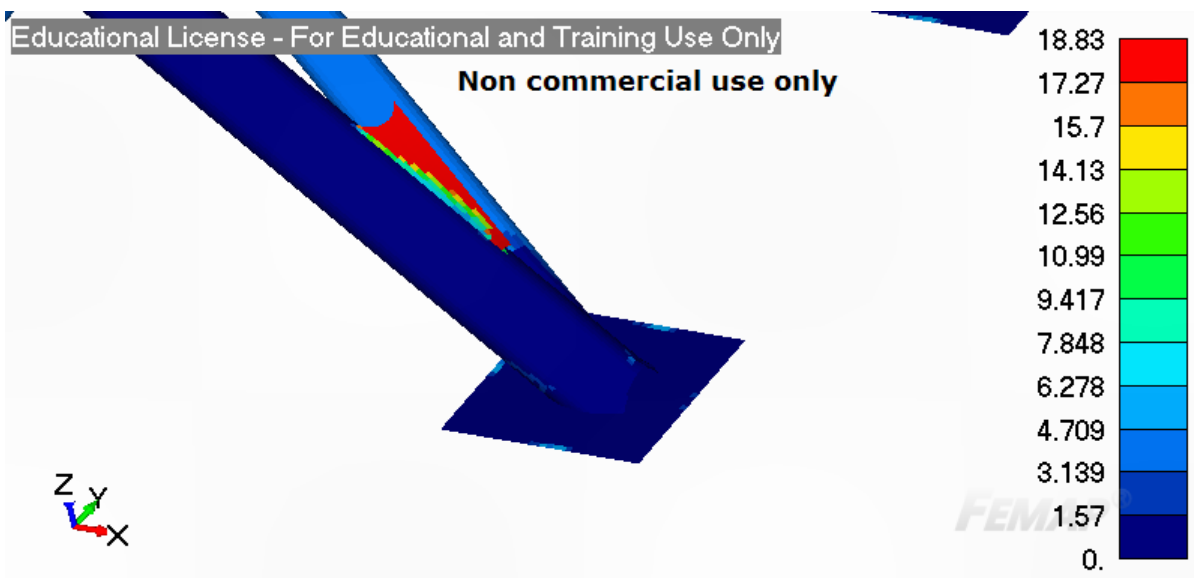


Figure 9-23: This figure displays the critical crack size in metres across the structure.

Figures 9-24 and 9-25 show the remaining fatigue life of the structure according to the crack growth model. The remaining fatigue life is not constant across the structure either, because the loads on each detail are different.

The inspection methods that can be used are displayed as well. Areas that are colored red in Figure 9-26 can be inspected using the visual inspection method because the critical crack sizes are larger than 60 mm. The other areas need to be inspected by the color penetration test.

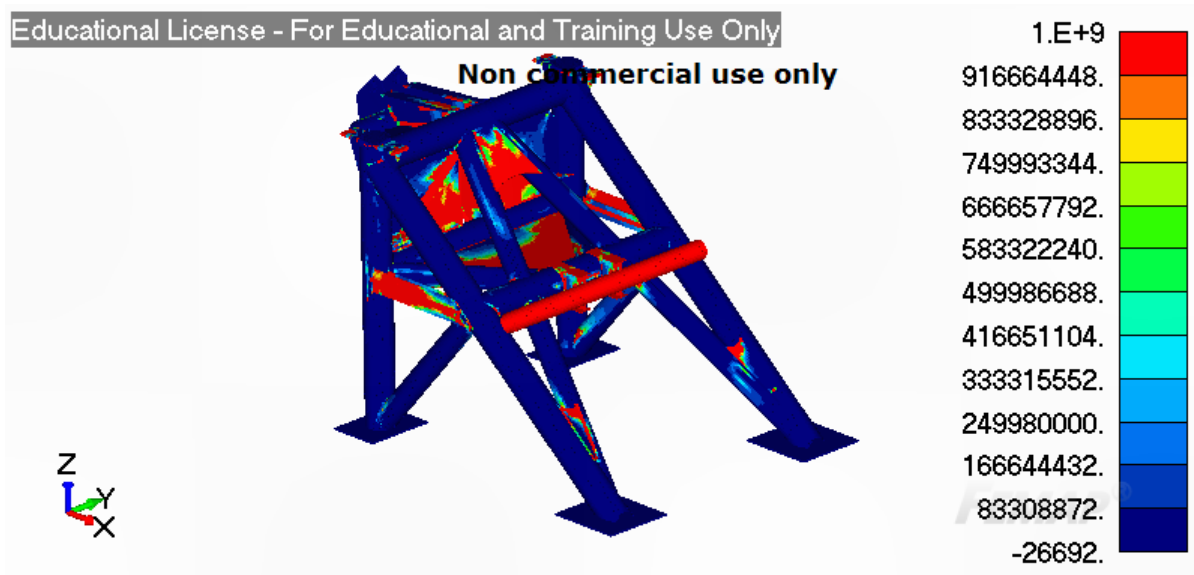


Figure 9-24: This figure displays the remaining fatigue life across the structure.

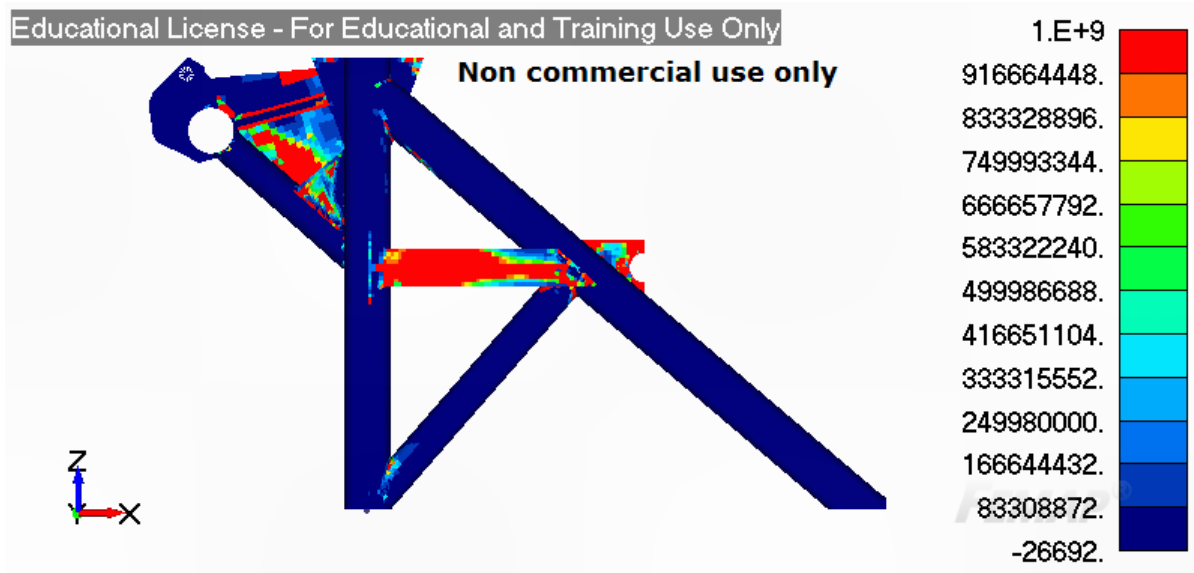


Figure 9-25: This figure displays the remaining fatigue life across the structure.

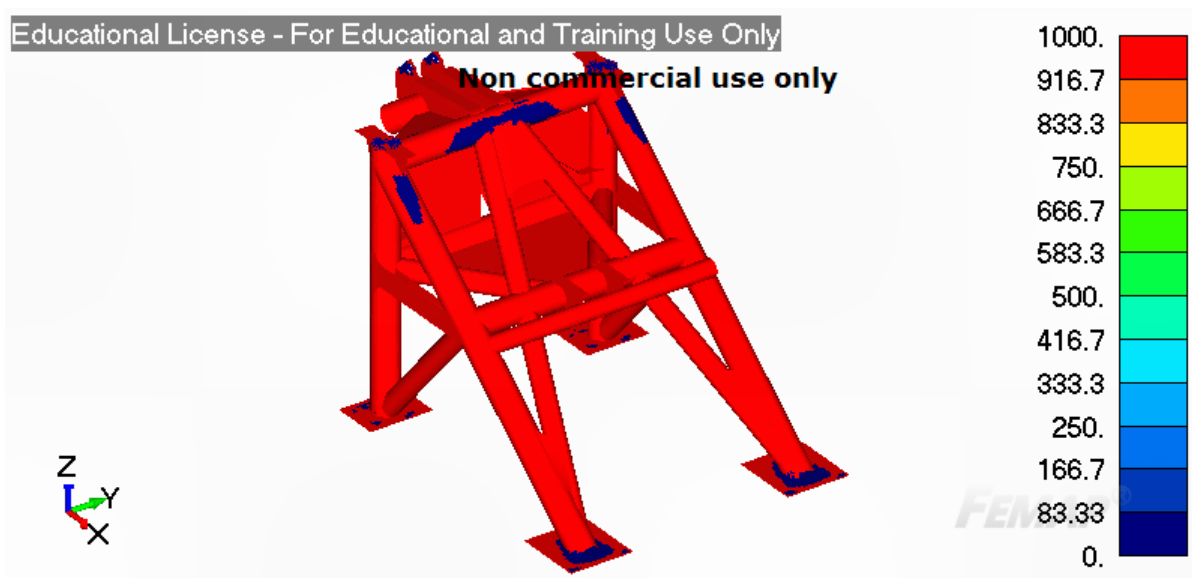


Figure 9-26: This figure displays the remaining fatigue life across the structure.

Chapter 10

Conclusion

This chapter provides the answers to the research questions and recommendations for further research. The first section concerns the answers to the research questions and the recommendations for further research can be found in the second subsection.

10-1 Conclusion

After performing a review of fatigue assessment methods for STS cranes, bridges, aircraft and offshore structures it is determined that a combination of the calculation methods for fatigue used in the design stage and crack growth models are suited to calculate the remaining fatigue life of the steel structure. The design methods to calculate the remaining fatigue life of the crane can be applied with the little effort because the majority of the data that is required is already included in the design documentation. The crack growth model is used to be able to calculate the remaining fatigue life of the crane when operated beyond its design fatigue life.

The steel structure of a general STS crane consists of four main components; bolted connections, pinned connections, welded connections and base material. It is determined that the majority of fatigue failures in steel structures occurs at welds, fatigue cracks in the base material contribute slightly and the amount of fatigue failures of bolted and pinned connections is negligible. The proposed fatigue assessment method therefore only considers cracks in the base material and in welds.

The components located at the connections at the forestay and backstay, the connections between the crane boom and the portal beams as well as the connections at the legs are even more susceptible to fatigue failure because these areas are subjected to relatively large fluctuating loads. These areas need to be assessed more frequently, because a failure in one of these areas may cause the crane to collapse.

In order to determine whether repair procedures are required, the fatigue crack sizes which can be tolerated need to be known. The crack size which can be tolerated can be calculated using a crack growth model. This model is able to calculate the critical crack size, which is the crack size at which a material will fail. Because the critical crack size depends on the geometry, material and applied stress, the maximum crack size which can be tolerated is not a constant for the entire structure.

The crack growth model is also used to calculate the crack growth rate, from which the remaining fatigue life is derived. This model is therefore used to determine the maximum allowable inspection interval as well. The inspection interval depends on the crack size which can be detected with sufficient reliability, which in turn depends on the type of inspection method that is deployed.

The calculated remaining fatigue life might be extended when cracks are repaired. The methods that can be used to repair cracks in steel structures of STS cranes are the gouge-and-weld method, mounting doubler plates, drilling crack arrest holes and modifying the structure. The proposed repair method depends on eventual prior repair works to the crane, location of the crack and the remaining fatigue life.

The information requirement for the proposed fatigue assessment method consists of an estimation of the number of performed cycles, material parameters, geometry parameters and the stresses across the structure. Because this information is available for the majority of cranes, the proposed method can already be deployed to steel structures of existing cranes.

The most appropriate method to assess the remaining fatigue life of the crane therefore consists of an inspection schedule, where the inspection intervals are determined based on the calculated remaining fatigue life. When the crane is operated within its design limits, the inspection intervals are based on the safety factors for fatigue as defined in the EN 13001 design standard for cranes. When the crane is operated after its design fatigue life is expired, the remaining fatigue life is calculated using a crack growth model.

The inspection methods that are used to inspect the crane are determined based on the value for the critical crack size and the inspection interval is based on the crack size which can be reliably determined by the inspection methods. When the remaining fatigue life is insufficient, repair works are scheduled to repair the crack and extend the fatigue life of the crane. The repair methods are selected based on the type of crack (cracks at the surface or internal cracks), its location and the calculated remaining fatigue life. Eventually the crane is taken out of operation when repair works are no longer viable to extend its fatigue life.

10-2 Recommendations for Further Research

This section lists the recommendations for further research. These recommendations concern optimized scheduling of inspections and automatization of the inspection process.

The inspection interval calculated using the proposed method depends on the inspection method that is selected. This research did not take speed of each inspection method into account when selecting the inspection method. The total cost of inspections might be reduced when this is considered. The time it takes to complete an inspection using a certain method can be traded off to the required frequency of inspections to find the lowest cost.

For triple-E class STS cranes which have approximately 52 metres of lifting height, a boom length of 128 metres, a rail span of 31 metres and a width of 27 metres, a minimum of 2272 metres of weld have to be inspected. This figure assumes that each crosssection consists of four welds, stiffeners and details are not taken into account, as is the top structure of the crane. With a velocity of 1.25 m/min for an automated UT device [91], it takes at least 30 manhours to complete the inspection of the crane.

A further reduction in downtime might therefore be realized by automating the inspection process. This can be done using unmanned aerial vehicles equipped with cameras or robots which are able to move across the structure. The first option is only available for automating the visual inspection process, while the second option can also be used for other types of inspection. The advantage is that the crane can be operational during the inspections. When some kind of robot is used, it might even be possible to not only detect cracks, but also to repair them (when the robot is provided with both a gauging tool and a welding tool).

Automating the inspection process is especially beneficial at automated terminals, because (parts of) the terminal need to be shut down in case people are near the automated equipment. Automating the inspection process therefore means that the entire terminal does not need to be down, which increases the productivity potential of the terminal.

Appendix A

Research Paper

Development of a Method for Assessment of the Remaining Fatigue Life of Steel Structures of Existing STS Cranes

J.A. van Jole, ing. W. van Cappellen, ir. W. van der Bos, prof. dr. Ir. G. Lodewijks

Delft University of Technology
 Department of Transportation Engineering and Logistics, Delft, The Netherlands
 Cargotec Netherlands B.V., Rotterdam, The Netherlands
 j.a.vanjole@student.tudelft.nl

Abstract—Because ship-to-shore (STS) cranes are usually operated after their design fatigue life has expired, a method is developed to assess the remaining fatigue life of its steel structure. The proposed method uses a combination of design methods and a crack growth model to determine the remaining fatigue life of the structure. The time between crack initiation and failure of the member is set as the remaining fatigue life. The structure will be inspected for cracks, based on the prediction of the remaining fatigue life. When the remaining fatigue life of the structure is not sufficient, the crack will be repaired in order to increase its fatigue life.

I. INTRODUCTION

STS cranes (Ship-to-Shore cranes) are designed for a finite fatigue life, but it is often preferred by the terminal operators to keep the crane in operation once the fatigue life has expired. When the crane is operated after it reached its expected service life, the risk of fatigue failure increases. Therefore the structural lifetime of the crane needs to be assessed in order to enable operation of the crane after it reaches its fatigue life without compromising safety.

Methods to assess the remaining fatigue life in industries like offshore and aviation are standardized, but for cranes such methods do not exist. Therefore an assessment method for the structure of the crane needs to be put forward. This method should include the structural parts of existing cranes. Parts like cables, drive systems and wheels will not be included.

The goal of this research is to create a method to assess the structural lifetime of existing STS cranes. The assessment method should be able to calculate the remaining lifetime of the crane and determine whether inspection of the crane is necessary (and if so, how long the intervals should be). After inspections are completed, the method should determine whether repair works need to be performed to ensure the structural integrity of the crane.

II. FATIGUE ASSESSMENT METHODS

A literature review into the existing fatigue assessment methods was performed which found that the assessment methods could be categorized as follows:

- Inspecting the structure at fixed intervals
- Fatigue life calculation in the design stage (using the safe-life or damage tolerant calculation methods)
- Fracture mechanics models, where the remaining fatigue life is equal to the timeframe in which a crack grows to a critical size.
- Monitoring the fatigue life by data analysis of the built structure

Two methods are selected to assess the remaining fatigue life of existing STS gantry cranes. The first method uses the result of the fatigue life calculation that is performed in the design process, because the results of these fatigue life calculations are assumed to be available. When the crane is operated after its design fatigue life, the remaining fatigue life will be monitored using a fracture mechanics model.

A model valid for linear elastic material behavior is selected because the design standard for cranes outlaws stresses above the yield strength of the material. The critical crack size is a function of the fracture toughness, yield strength and a geometry factor. The equation is given below:

$$a_{crit} = \frac{K_{Ic}^2}{\pi Y^2 \sigma_{fail}^2}$$

This equation represents an energy balance between the strain energy released during crack growth and the energy required to create new surfaces.

The remaining fatigue life can subsequently be calculated using the crack growth parameters from the Paris-Erdogan crack growth law. The integrated equation is given below:

$$N_f - N_i = \frac{1}{1 - \frac{m}{2}} \frac{1}{C \Delta \sigma^m Y^m \pi^{\frac{m}{2}}} (a_{crit}^{1 - \frac{m}{2}} - a_{eff}^{1 - \frac{m}{2}})$$

The remaining fatigue life (Nf-Ni) is described as a function of the critical crack size and the effective (initial) crack size. This model cannot be used when large deformations are apparent, because this would indicate that the assumption of linear material behavior is violated.

III. CRACK SIZE MEASUREMENT

Fatigue crack sizes are evaluated by inspections. The crack sizes that can be detected differ for each method. Multiple methods are considered in this research [CITE4]. Using a probability of detection of 0.99, crack sizes of 60 mm can be inspected using visual inspection. This means that when the critical crack size exceeds 60 mm, the visual inspection method will be used. For critical crack sizes between 20 and 60 mm the color penetration test will be used and for lower critical crack sizes the eddy current inspection method is applied.

IV. REPAIR METHODS

When the remaining fatigue life of the crane is insufficient, the crack will be repaired. Cracked welds can be repaired using the gauge-and-weld method. For cracks in the base material, doubler plates can be used as well.

When the remaining fatigue life of the crane is very low, operations of the crane will be ceased and the structure of the crane will be modified in order to prevent the structure from collapsing.

V. FATIGUE ASSESSMENT MODEL

The fatigue assessment method consists of five stages. The transition between two subsequent stages is governed by the fatigue specific resistance factor as defined by the EN 13001 design standard. Non-failsafe structures are designed to the safe-life design concept, while fail-safe structures are designed according to the damage-tolerance design concept. Within the structure of a single STS crane, both concepts can be applied. For those elements of the structure where a failure does not have any consequences regarding the structural stability of the crane or the position of the load, the damage-tolerant design principle is used while for other details the safe-life approach is in effect.

For the majority of details used in cranes, the accumulated fatigue damage is proportional to the stress range to the third power (according to the design standard EN 13001). The fatigue specific resistance factor is therefore also put to the third power. Because the fatigue resistance factor is a safety function regarding fatigue failure of STS cranes, the transition

between stages is chosen to be the inverse of the specific resistance factor to the third power. The values for fail-safe operation are not used, because fatigue life monitoring of non-failsafe details is dominant (the inspection intervals are shorter for non-failsafe details, which means that fail-safe details are checked more often than theoretically required). This method is used in the first four stages of this assessment model.

The final stage is an iterative process which starts with an inspection of the entire steel structure. The analysis of the remaining fatigue life is equal to the fatigue life calculation process in stage four. The only addition to this is that for each iteration a decision needs to be made if repair works are viable (in case repair works are required to reach the reference number of cycles). This step is included because even when the fatigue life is monitored well, a STS gantry crane will not have an indefinite service life. At some point in time the crane will have to be decommissioned, because the amount of work required to repair the fatigue damage to the structure becomes too large.

Appendix B

Flowcharts Fatigue Assessment Model

This appendix contains larger images of the flowcharts of the fatigue assessment model (as discussed in Chapter 8). Each flowchart spans two pages, the first flowchart (which concerns the main fatigue life assessment model) is depicted on pages 116 and 117. The second flowchart, which concerns the selection process for inspection procedures is depicted on pages 118 and 119. And the final flowchart which covers the process of repairing fatigue cracks is depicted on pages 120 and 121.

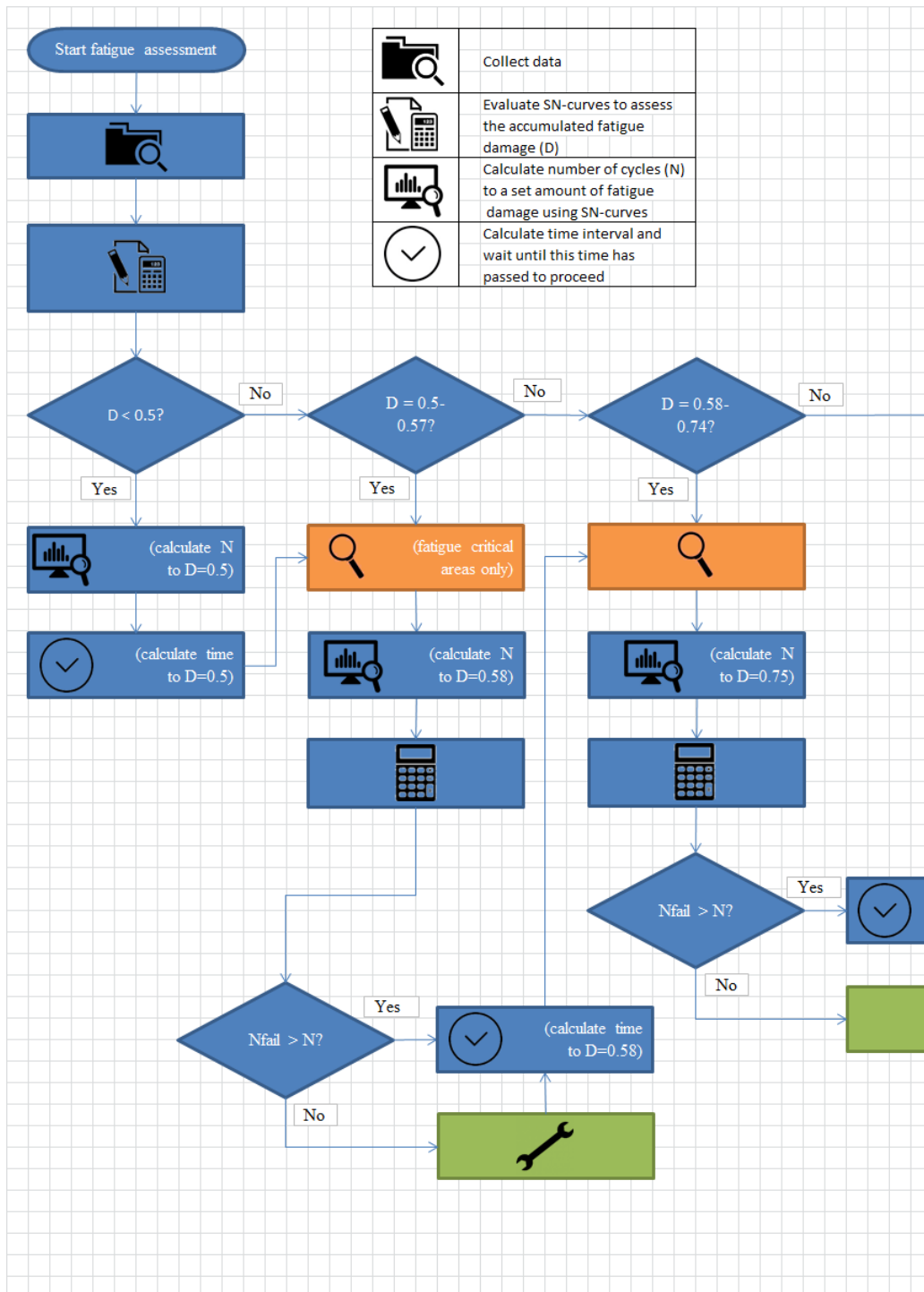


Figure B-1: Flowchart depicting the fatigue assessment method (first part).

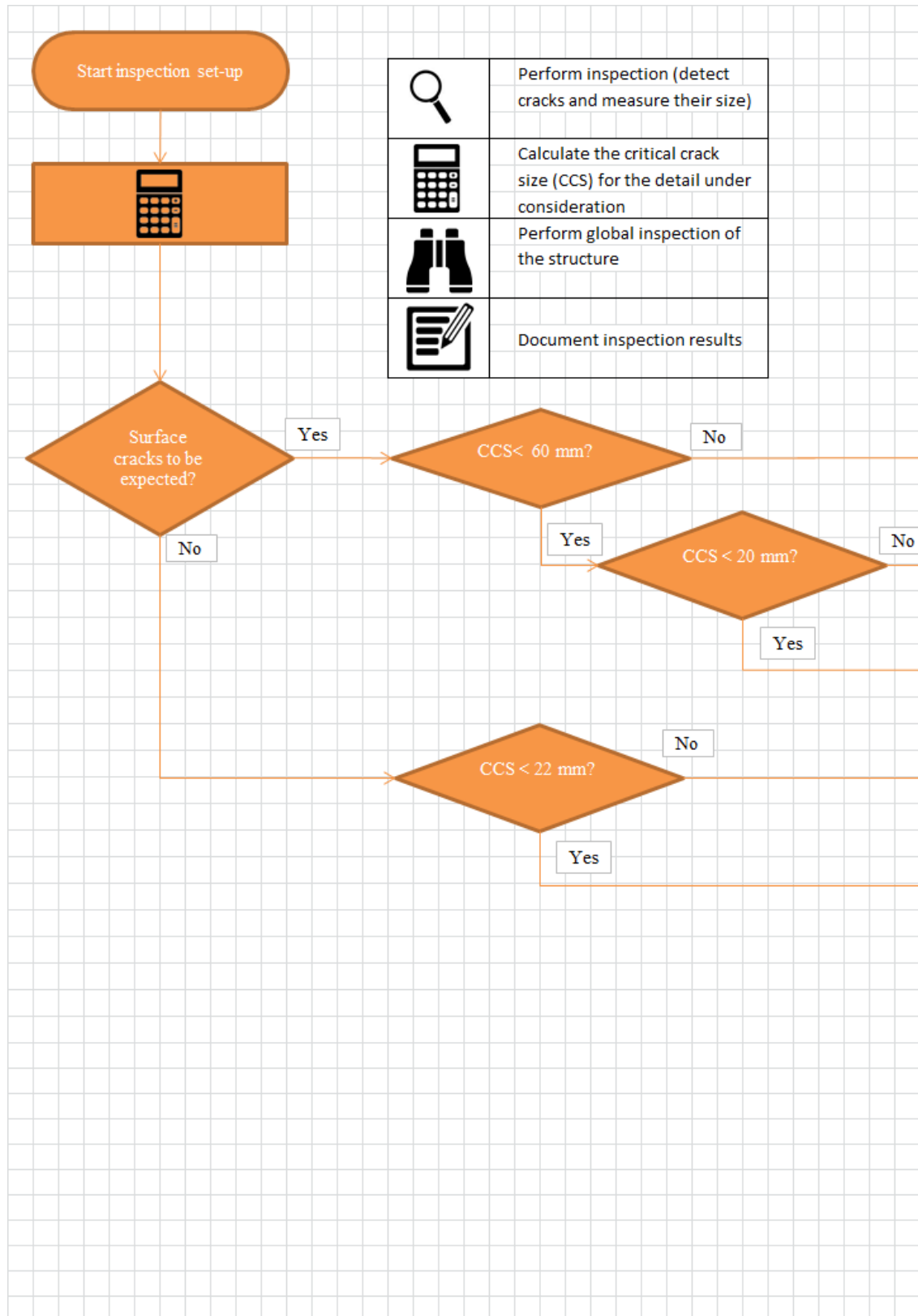


Figure B-3: Flowchart depicting the process of determining the inspection procedure (first part).

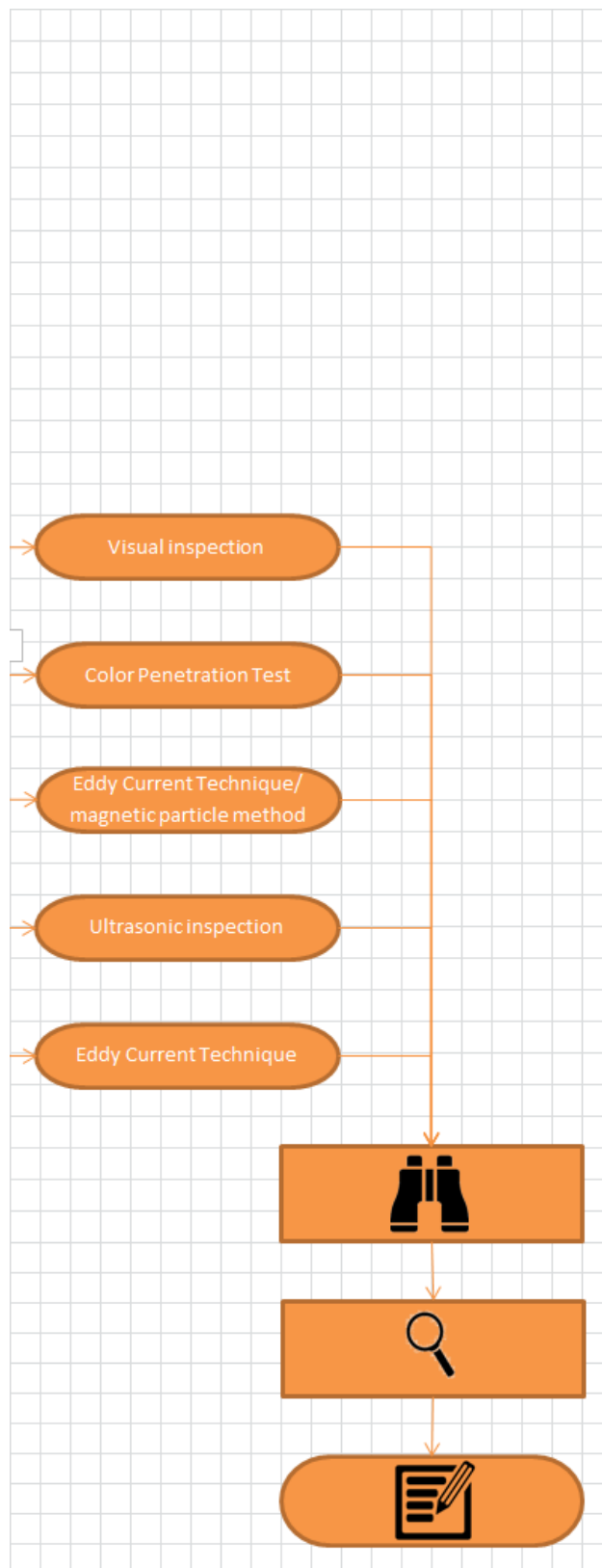


Figure B-4: Flowchart depicting the process of determining the inspection procedure (second part).

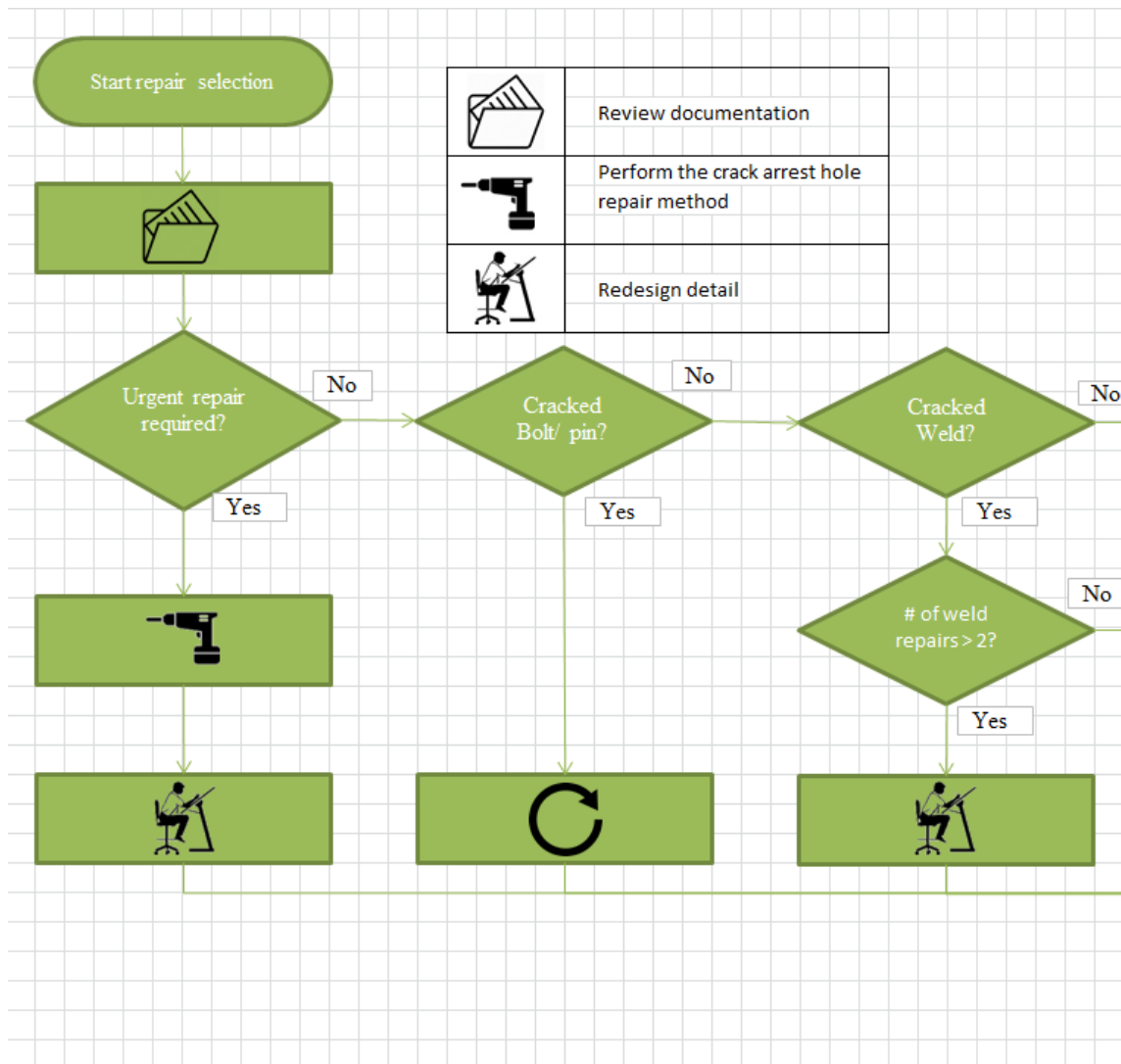


Figure B-5: Flowchart depicting the process of determining the repair procedure (first part).

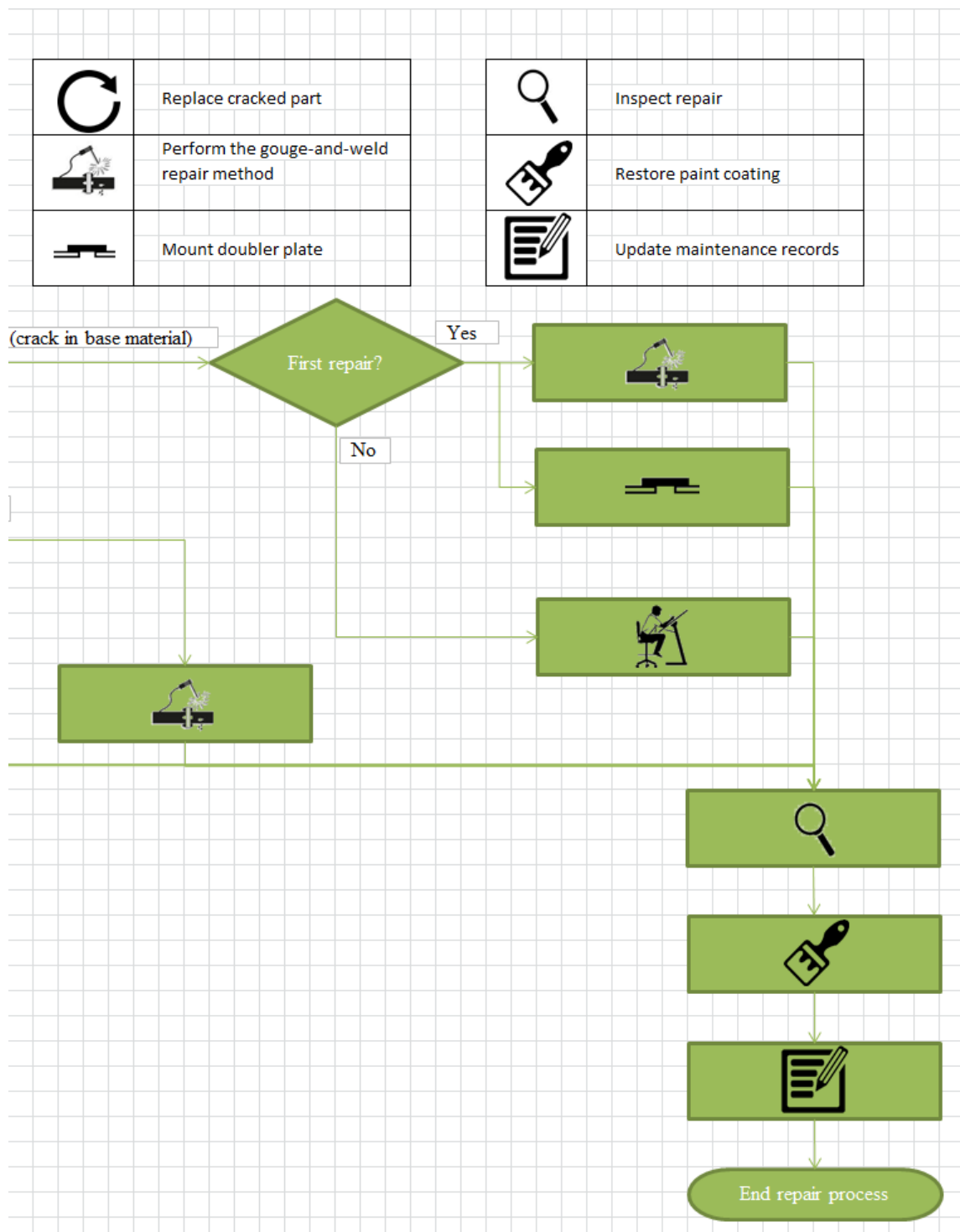


Figure B-6: Flowchart depicting the process of determining the repair procedure (second part).

Appendix C

Fatigue Assessment Calculation Model

This appendix shows the matlab code that is implemented to calculate the remaining fatigue life of a steel structure that is subjected to cracks. The input must be provided for the material properties, the load on the structure and the geometry of the detail under consideration. The output of the model is the remaining fatigue life of the detail.

```
1 % Date: 23-02-2016
2 % Model made by: Johan van Jole
3
4 % This model is used to calculate the remaining fatigue life of steel
5 % structures of STS gantry cranes using fracture mechanics.
6
7 clear all
8 close all
9 clc
10 %% Parameters and Variables
11
12 % general
13 g= 9.81; % Gravitational constant [m/s^2].
14
15 %geometry
16 a0= 20e-3; % Initial crack length [m].
17 Y= 1.12; % Geometry factor [-].
18 t= 100e-3; % Thickness of the detail under consideration [m].
19 %material
20 K1c= 50; % Fracture toughness of material [MPa*(m^0.5)]
21 Syield= 355; % Yield stress of the material [MPa].
22 m= 2.25; % Crack growth exponent used in the Paris equation [-].
23 C= 1.36e-10; % Crack growth constant used in the Paris equation [[m
    ]^((-m/2)+1)*[MPa]^(-m)].
24
25 %load
26 Smax= 250; % Maximum stress [MPa].
27 Smin= 100; % Minimum stress [MPa].
28
29 %% Critical crack length
```

```

30 acrit= (K1c^2)/(pi*Y^2*Smax^2); % Critical crack length [m].
31 rp=(1/(6*pi))*(K1c/Syield)^2; % Plastic zone radius [m].
32 aeff=a0+rp; % Effective initial crack length [m].
33 %% Integral solution to crack growth
34 exp= 1-(m/2); % Exponent in the integral solution [-].
35 DeltaS= Smax-Smin; % Stress range [MPa].
36 Z2= (DeltaS*Y*sqrt(pi))^m; % Term used in the integral equation [-].
37
38 % Integral solution to the Paris-Erdogan crack growth law [-]:
39 DeltaN= ((1/exp)*(1/(C*Z2)))*((acrit^exp)-(aeff^exp));
40
41 % Display the result in a messagebox:
42 msgbox(sprintf('Cycles to failure: %2.3g',DeltaN),'result')
43
44 %% Checks
45 % checks are performed to whether constraints of the model are violated or
46 % not.
47
48 % check on input stresses (check whether max. stress is higher than min.
49 % stress)
50 if Smax<Smin
51     msgbox('Input of stresses is erroneous','Input Violation','error')
52 end
53
54 % check on plane strain assumption:
55 tcheck= 2.5*((K1c/Syield)^2); % Minimum thickness for plane strain [m].
56 if t<tcheck
57     msgbox(sprintf('Use of plane strain model invalid (thickness is too small). \
nThe thickness must be %2.3g mm larger for this model to be valid.',(tcheck
-t)*1000),'Validity Violation','error')
58 end
59
60 % check on initial crack length (which should be smaller than critical
61 % crack length):
62 if acrit<a0
63     msgbox('Initial crack length exceeds the critical crack length!','Error','
error')
64 end

```

Appendix D

Calculation of Geometry Factors

This Appendix concerns the model that is developed in order to calculate the geometry factors. These factors are used to calculate the critical crack size and the remaining fatigue life (the calculation model for the remaining fatigue life is included in Appendix C). The first section concerns the formulations of the geometry factors for cracks in plates. Geometry factors for cracks in cylinders are covered in section two and cracks at holes are discussed in the third section. The final section concerns geometry factors for cracked welds.

The cells which have been marked blue must be filled in by the engineer performing the fatigue analysis. The geometry factor is subsequently displayed in the orange marked cell. The unmarked cells are the variables used in the equations for the geometry factor, some of which are used to check the validity of the equations.

The defect size that is used to calculate the geometry factor is initially selected to span a large part of the cross section. When there is a large deviation with respect to the calculated critical crack size, the defect size will be updated and the geometry factor is recalculated. When deemed necessary, this process is repeated until the results converge sufficiently. The other parameters that are required to calculate the geometry factor can be derived from design drawings or measurements of the built structure.

D-1 Geometry Factors For Cracks in Plates

This section concerns the geometry factors for cracked plates. Figure D-1 displays expressions for a center cracked plate which is subjected to tensile or bending stresses. Expressions for the geometry factor for a double-edge cracked plate are covered in Figure D-2 and expressions for single edge cracked plates are covered in Figure D-3.

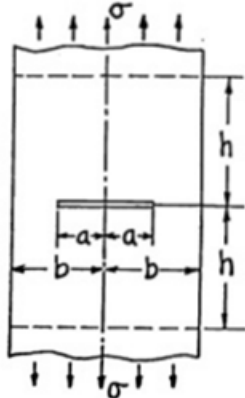
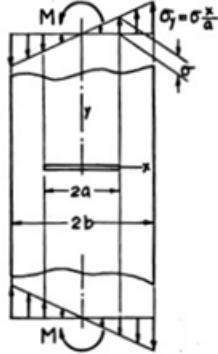
Center crack in finite width plate			Tensile stress
a	0,75	Half crack length [m]	
b	2	Half plate width [m]	
a/b	0,375	Crack size ratio [-]	
Y	1,09412	Geometry factor [-]	
$F(a/b) = \left\{ 1 - 0.025(a/b)^2 + 0.06(a/b)^4 \right\} \sqrt{\sec \frac{\pi a}{2b}}$ <p>a. 0.1% for any a/b b. Modification of Feddersen's formula, Tada 1973</p>			
Center crack in finite width plate			Bending stress
a	1,95	Half crack length [m]	
B	2	Half plate width [m]	
a/B	0,975	Crack size ratio [-]	
1-(a/B)	0,025	Residual area ratio [-]	
G	0,81304	Shape function [-]	
Y	1,75761	Geometry factor [-]	

Figure D-1: Calculation of the geometry factor for a center crack in a plate subjected to bending or tensile loads.

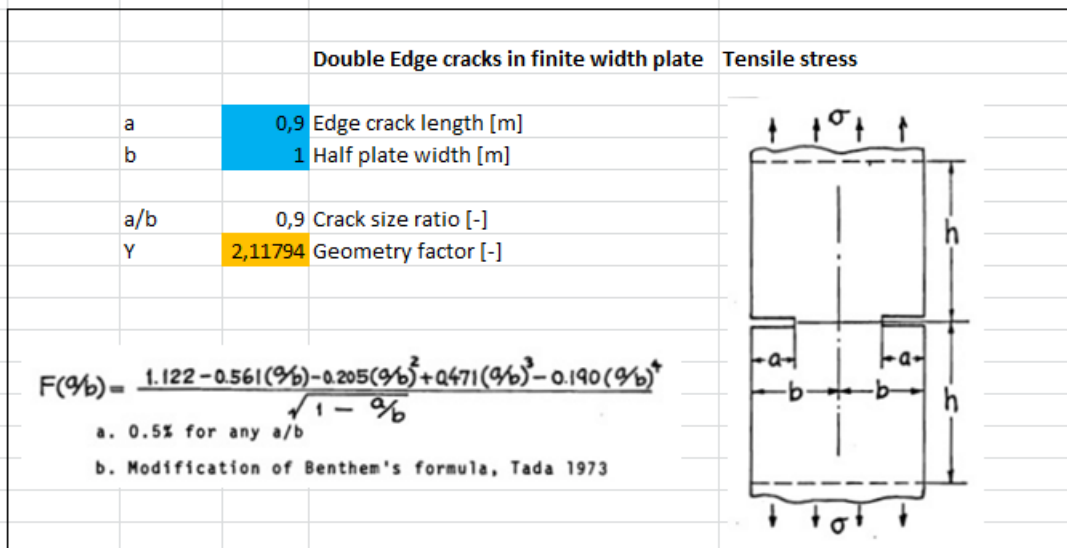
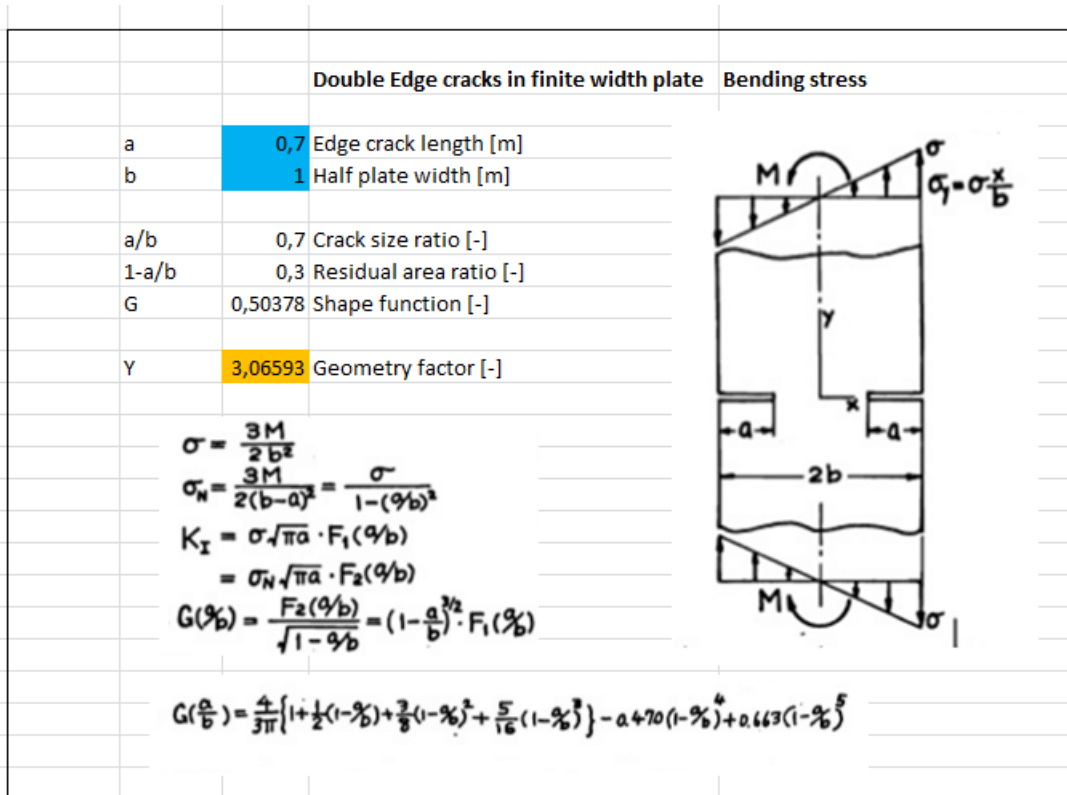


Figure D-2: Calculation of the geometry factor for a double-edge cracked plate subjected to bending or tensile loads.

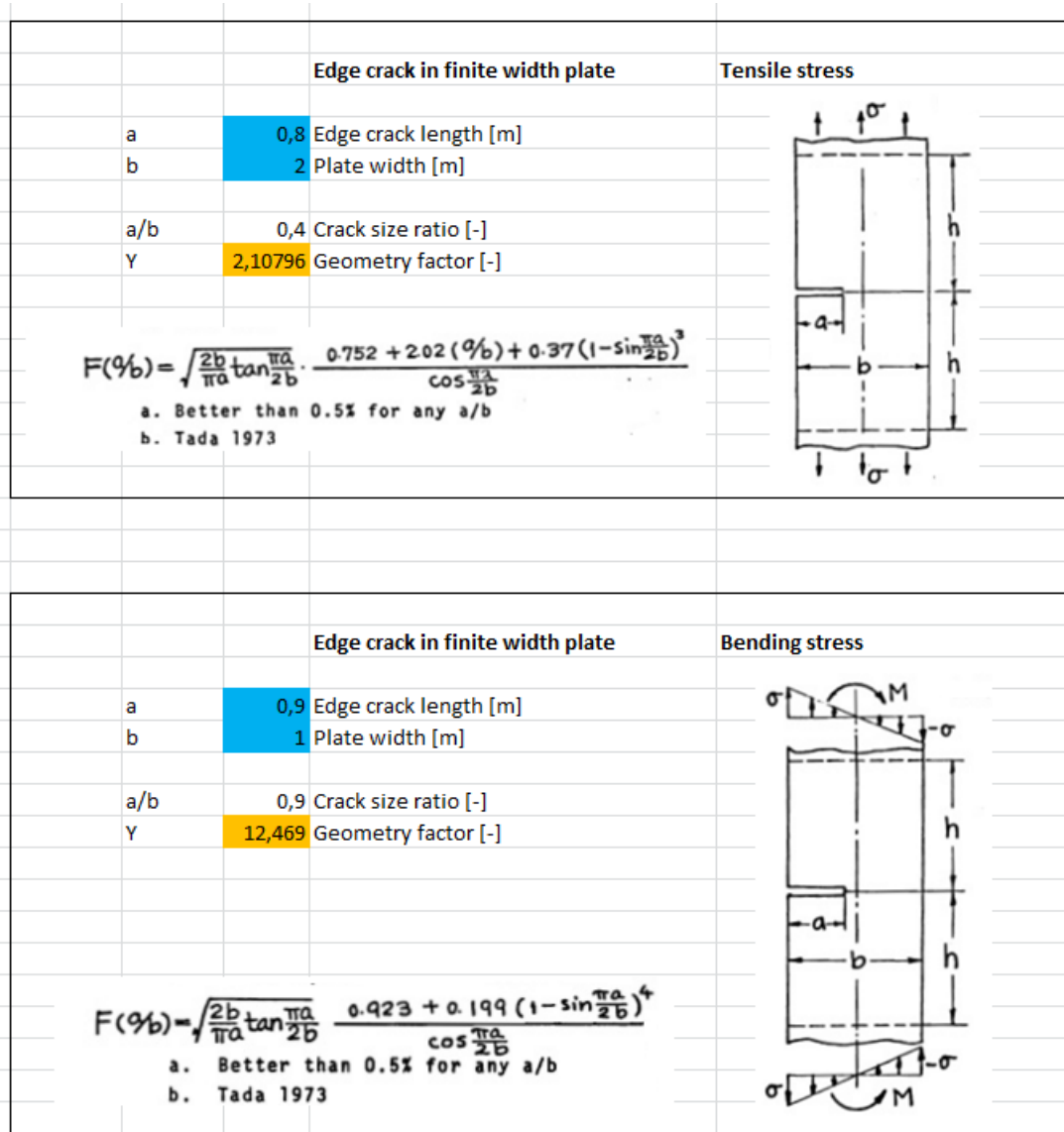


Figure D-3: Calculation of the geometry factor for a single edge cracked plate subjected to bending or tensile loads.

D-2 Geometry Factors For Cracks in Cylinders

Axial cracks only grow when there is a pressure difference between the inside and the outside of the cylinder. This is not the case for cylindrical sections of STS cranes, therefore only circumferential cracks in cylinders are considered. The geometry factors for bending and tensile stresses are displayed in Figure D-4

	circumferentially cracked cylinder	Tensile or bending stress
R	1 m	<p> $c = \alpha R$ $R = \text{mean radius} = (D - t) / 2$ </p>
t	0,033 m	
a	1,134 m	
nu	0,3 -	
alpha	1,134 rad	
eta	0,1 -	
g function	5,24 -	
lambda	5,646 -	
C function	2,302 Mpa*sqrt(m)	
I ₀	68,64 -	
mu	1,398 -	
I _b	46,72 -	
Y _t	3,104	
Y _b	2,56	

Figure D-4: Calculation of the geometry factor for a circumferentially cracked cylinder subjected to bending or tensile loads.

D-3 Geometry Factors For Cracks at Holes

The geometry factors for cracks at holes are considered as well, which are displayed in Figure D-5. Geometry factors for single cracked holes and double cracked holes are considered in this research.

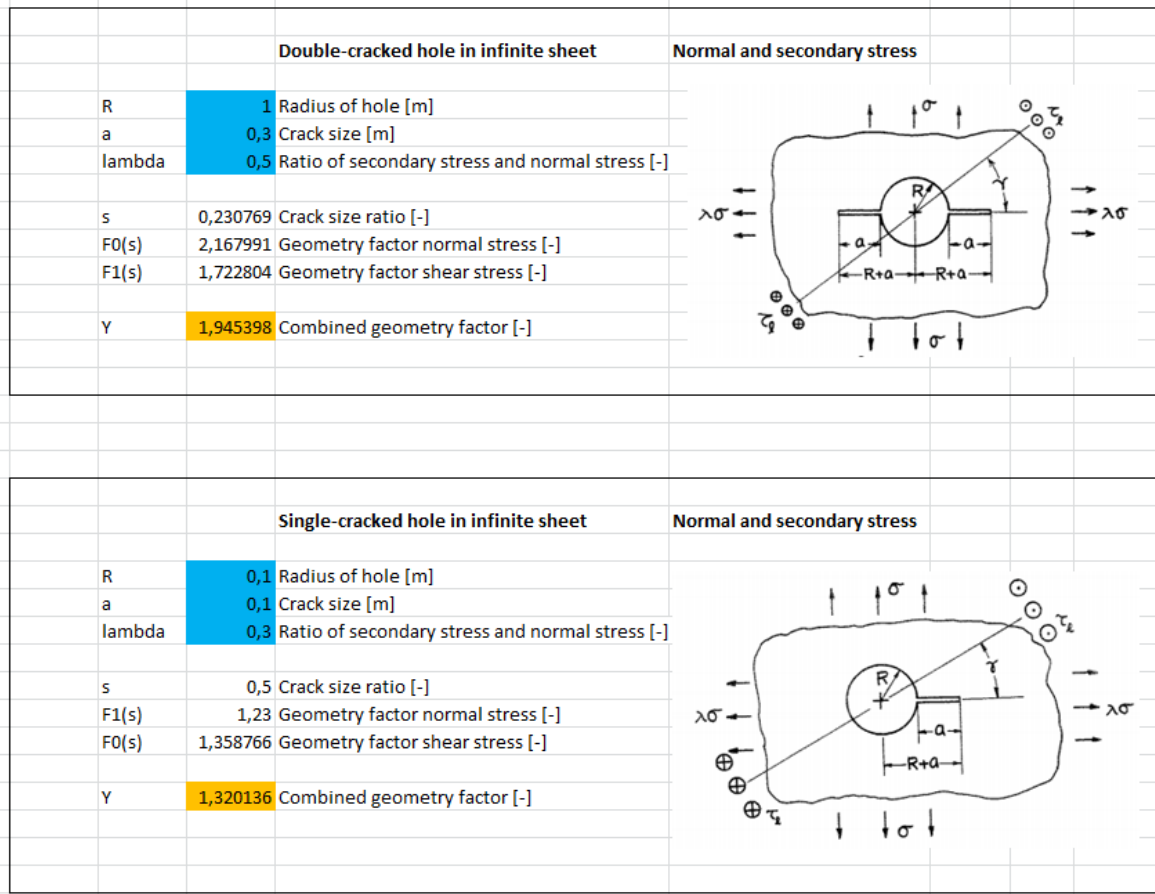


Figure D-5: Calculation of the geometry factor for a cracked hole subjected to normal and secondary stresses.

D-4 Geometry Factors For Cracks at Welds

This section concerns the geometry factors for cracked welds, which are required because welded connections are an important part of the structure of a general STS crane. Geometry factors for butt welds subjected to tensile or bending loads can be found in Figure D-6. Figure D-7 shows the calculation procedure for geometry factors for fillet welds with weld toe cracks. The geometry factor for a lap joint with a weld toe crack subjected to a tensile load is displayed in Figure D-8 and geometry factors for cruciform joints can be found in Figures D-9 (for a weld root crack) and D-10 (for a weld toe crack).

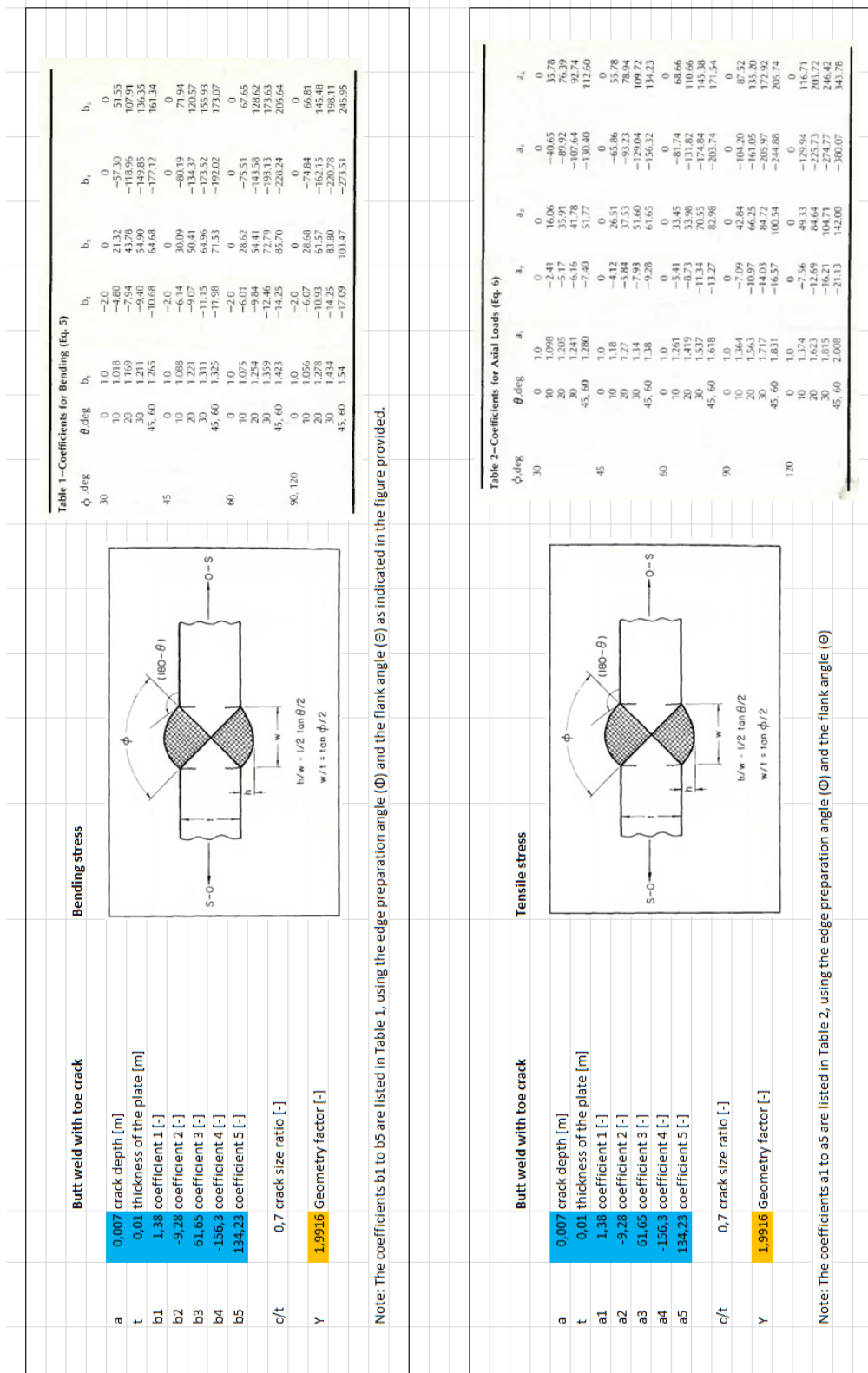


Figure D-6: Calculation of the geometry factor for a cracked butt weld subjected to bending or tensile loads.

Fillet weld with toe crack		Tensile stress
a	0,1 Crack depth [m]	
c	1 Half crack length [m]	
T	0,1 Thickness of main plate [m]	
rho	3 Weld toe radius [m]	
alpha	4 Weld angle [rad]	
L	0,3 Cross section of weld [m]	
a/T	1 Crack size ratio [-]	
a/c	0,1 Crack shape parameter [-]	
T/rho	0,0333 Ratio thickness to weld toe radius [-]	
L/T	3 Ratio cross section of weld to thickness [-]	
s4	0,006 Parameter in equation of fourth coefficient [-]	
Mp	-0,448 Shape factor for exponent [-]	
M0	-0,428 Shape factor for base coefficient [-]	
M1	-0,271 Shape factor for first coefficient [-]	
M2	0,8283 Shape factor for second coefficient [-]	
P	-0,762 Exponent [-]	
C0	-1,186 Base Coefficient [-]	
C1	1,6469 Coefficient 1 [-]	
C2.1	0,1775 Help variable for coefficient 2 [-]	
C2	1,7423 Coefficient 2 [-]	
C3	0 Coefficient 3 [-]	
C4	0 Coefficient 4 [-]	
Y	9,3285 Geometry factor [-]	

Fillet weld with toe crack		Bending stress
a	0,03 Crack depth [m]	
c	1 Half crack length [m]	
T	0,2 Thickness of main plate [m]	
rho	3 Weld toe radius [m]	
alpha	1,5708 Weld angle [rad]	
L	2 Cross section of weld [m]	
a/T	0,15 Crack size ratio [-]	
a/c	0,03 Crack shape parameter [-]	
T/rho	0,0667 Ratio thickness to weld toe radius [-]	
L/T	10 Ratio cross section of weld to thickness [-]	
s4	0,05 Parameter in equation of fourth coefficient [-]	
MA	-0,423 Shape factor for exponent [-]	
M0	-0,8 Shape factor for base coefficient [-]	
M1	1,1626 Shape factor for first coefficient [-]	
M2	-0,187 Shape factor for second coefficient [-]	
A	-0,943 Exponent [-]	
C0	-0,85 Base Coefficient [-]	
C1	1,7119 Coefficient 1 [-]	
C2	2,3355 Coefficient 2 [-]	
C3	-0,02 Coefficient 3 [-]	
C4	0 Coefficient 4 [-]	
C5	0 Coefficient 5 [-]	
YB	1,1579 Geometry factor [-]	

Figure D-7: Calculation of the geometry factor for a fillet weld with weld toe crack subjected to bending or tensile loads.

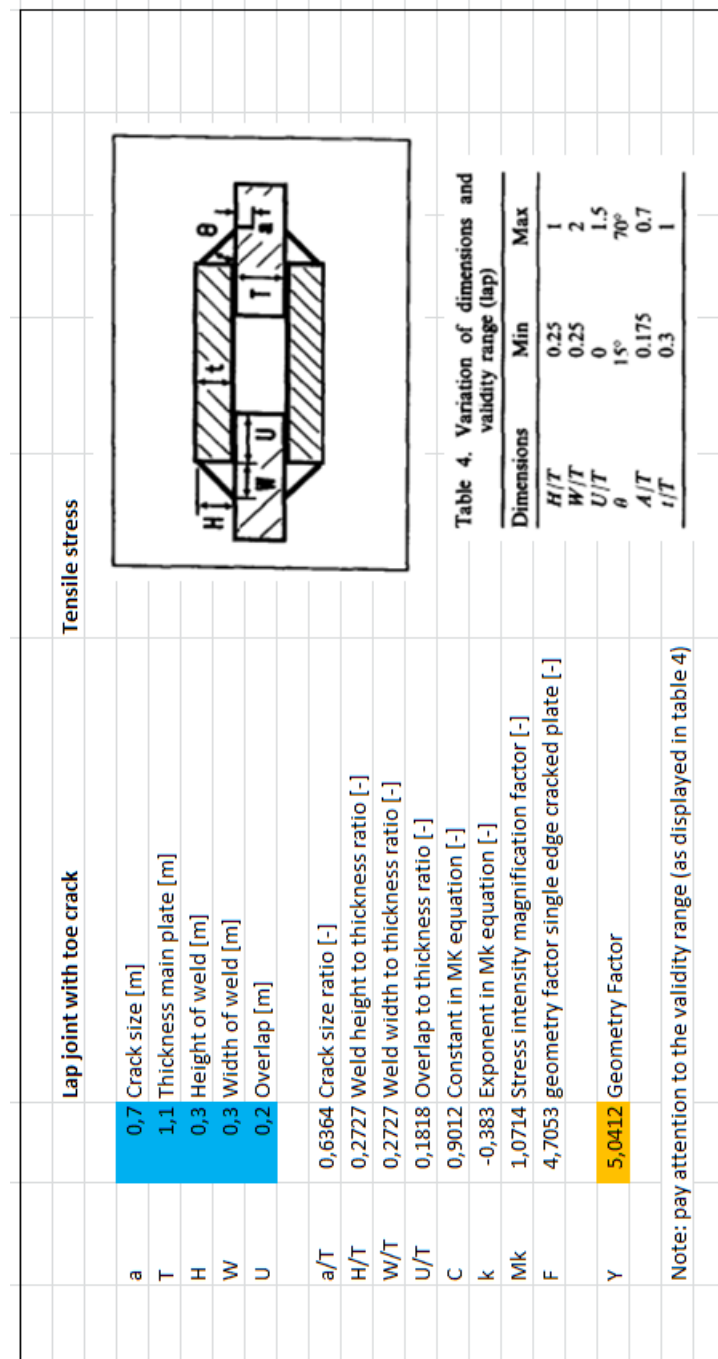


Figure D-8: Calculation of the geometry factor for a lap joint with a weld toe crack subjected to a tensile load.

		Cruciform joint weld root crack	Tensile stress
a	0,99	half crack length [m]	
B	1	thickness of main plate [m]	
h	0,5	width of weld [m]	
w	2	width of cross section [m]	
A0	0,7845	first term in Mk equation [-]	
A1	-0,12731	second term in Mk equation [-]	
A2	0,274188	third term in Mk equation [-]	
Mk	0,927192	weld shape factor [-]	
Y	7,398072	geometry factor [-]	

		Transverse attachment weld toe crack	Tensile stress
a	0,5	Crack size [m]	
T	1,1	Thickness main plate [m]	
H	0,3	Height of weld [m]	
W	0,3	Width of weld [m]	
a/T	0,454545	Crack size ratio [-]	
H/T	0,272727	Weld height to thickness ratio [-]	
W/T	0,272727	Weld width to thickness ratio [-]	
C	0,789264	Constant in MK equation [-]	
k	-0,22355	Exponent in Mk equation [-]	
Mk	1	Stress intensity magnification factor [-]	
F	2,456747	geometry factor single edge cracked plate [-]	
Y	2,456747	Geometry Factor	

Dimension	Min	Max
H/T	0.2	1
W/T	0.2	1
theta	15°	60°
A/T	0.175	0.72
t/T	0.125	2(4)

Note: pay attention to the validity range (as displayed in table 1)

Figure D-9: Calculation of the geometry factor for a cruciform joint with a weld root crack and a transverse attachment with a weld toe crack subjected to a tensile load.

		Cruciform joint K-butt weld toe crack	Tensile stress																		
a	0,7	Crack size [m]																			
T	1,1	Thickness main plate [m]																			
H	0,3	Height of weld [m]																			
W	0,3	Width of weld [m]																			
a/T	0,636364	Crack size ratio [-]																			
H/T	0,272727	Weld height to thickness ratio [-]	<p>Table 2. Variation of dimensions and validity range (cruc. K-butt)</p> <table border="1"> <thead> <tr> <th>Dimension</th> <th>Min</th> <th>Max</th> </tr> </thead> <tbody> <tr> <td>H/T</td> <td>0.2</td> <td>1</td> </tr> <tr> <td>W/T</td> <td>0.2</td> <td>1</td> </tr> <tr> <td>θ</td> <td>15°</td> <td>60°</td> </tr> <tr> <td>A/T</td> <td>0.175</td> <td>1.3</td> </tr> <tr> <td>t/T</td> <td>0.5</td> <td>20</td> </tr> </tbody> </table>	Dimension	Min	Max	H/T	0.2	1	W/T	0.2	1	θ	15°	60°	A/T	0.175	1.3	t/T	0.5	20
Dimension	Min	Max																			
H/T	0.2	1																			
W/T	0.2	1																			
θ	15°	60°																			
A/T	0.175	1.3																			
t/T	0.5	20																			
W/T	0,272727	Weld width to thickness ratio [-]																			
C	0,698486	Constant in MK equation [-]																			
k	-0,26488	Exponent in Mk equation [-]																			
Mk	1	Stress intensity magnification factor [-]																			
F	4,705339	geometry factor single edge cracked plate [-]																			
Y	4,705339	Geometry Factor																			
Note: pay attention to the validity range (as displayed in table 2)																					

		Cruciform joint fillet weld toe crack	Tensile stress																		
a	0,7	Crack size [m]																			
T	1,1	Thickness main plate [m]																			
H	0,3	Height of weld [m]																			
W	0,3	Width of weld [m]																			
a/T	0,636364	Crack size ratio [-]																			
H/T	0,272727	Weld height to thickness ratio [-]	<p>Table 3. Variation of dimensions and validity range (cruc. fillet)</p> <table border="1"> <thead> <tr> <th>Dimensions</th> <th>Min</th> <th>Max</th> </tr> </thead> <tbody> <tr> <td>H/T</td> <td>0.2</td> <td>1</td> </tr> <tr> <td>W/T</td> <td>0.2</td> <td>1</td> </tr> <tr> <td>θ</td> <td>15°</td> <td>60°</td> </tr> <tr> <td>A/T</td> <td>0.175</td> <td>0.8</td> </tr> <tr> <td>t/T</td> <td>0.5</td> <td>10</td> </tr> </tbody> </table>	Dimensions	Min	Max	H/T	0.2	1	W/T	0.2	1	θ	15°	60°	A/T	0.175	0.8	t/T	0.5	10
Dimensions	Min	Max																			
H/T	0.2	1																			
W/T	0.2	1																			
θ	15°	60°																			
A/T	0.175	0.8																			
t/T	0.5	10																			
W/T	0,272727	Weld width to thickness ratio [-]																			
C	0,464021																				
k	-0,78223																				
Mk	1	Stress intensity magnification factor [-]																			
F	4,705339	geometry factor single edge cracked plate [-]																			
Y	4,705339	Geometry Factor																			
Note: pay attention to the validity range (as displayed in table 3)																					

Figure D-10: Calculation of the geometry factor for a cruciform joint (K-butt and fillet welded) with a weld toe crack subjected to a tensile load.

Bibliography

- [1] DNV GL, “Probabilistic methods for planning of inspection for fatigue cracks in offshore structures,” *Recommended Practice*, 2015.
- [2] Gottwald, “Crane service life, classification of cranes,” *Gottwald Port Technology*, 2003.
- [3] U. D. of Transportation, “Manual for repair and retrofit of fatigue cracks in steel bridges,” *FHWA*, 2013.
- [4] L. Meurling and B. Zwygart, “Weighing containers in ports and terminals,” *PEMA Information Papers*, 2013.
- [5] A. Mello and D. Ferreira, “Reliability prediction for structures under cyclic loads and recurring inspections,” *Journal of Aerospace Technology and Management*, vol. 1, no. 2, pp. 201–209, 2009.
- [6] CEN, “Cranes- general design part 3-1: Limit states and proof of competence of the steel structure,” *European Committee for Standardization*, vol. EN 13001-3-1:2012, 2012.
- [7] Nederlands Normalisatie Instituut, *NEN-EN 15011:2011+ A1:2014*, 2014.
- [8] BAE Systems (Land and Sea Systems) Ltd, *Beyond Lifetime Criteria for Offshore Cranes*. HSE Books, 2002.
- [9] S. Tok and L. Lam, “Premature crane structure failure & finite element method analysis and rectification,” 2011.
- [10] A. van Beek, *Advanced Engineering Design; Lifetime Performance and Reliability*. TU Delft, 2009.
- [11] M. Ashby, H. Shercliff, and D. Cebon, *Materials: Engineering, Science, Processing and Design*. Butterworth/Heinemann, 2010.
- [12] PEMA, TT club and ICHCA, “Recommended minimum safety specifications for quay container cranes,” 2011.

- [13] World Maritime News, “Bremerhaven crane operator dies in boom collapse.” <http://worldmaritimeneeds.com/archives/160989/bremerhaven-crane-operator-dies-in-boom-collapse/> (accessed 17-09-2015), 2015.
- [14] J. Verschoof, *Cranes; Design, Practice and Maintenance*. Professional Engineering Publishing, 2000.
- [15] ISO, *ISO 9927:1-2013 (Cranes: Inspection)*, 2013.
- [16] Oregon Department of Transportation, *Fatigue Prone Detail Bridge Inspection Program Policy*, 1996.
- [17] A. Athanasopoulou *et al.*, “Bridge design to eurocodes; worked examples,” *JRC Scientific and Technical Reports*, 2012.
- [18] J. Maljaars and C. Giezen, “Inspectie-interval is geen toeval,” *Bouwen met Staal*, no. 242, pp. 52–59, 2014.
- [19] S. Lovejoy, “Determining appropriate fatigue inspection intervals for steel bridge members,” *Journal of Bridge Engineering*, 2003.
- [20] Government of India; Ministry of Railways, “Study of probable cause of cracks in different members and assessment of residual fatigue life of bridge no.46 up/mid line near bilaspur, secr.,” *REPORT NO. BS 90*, 2008.
- [21] G. Sedlacek *et al.*, “Condition assessment and inspection of steel railway bridges, including stress measurements in riveted, bolted and welded structures,” *Sustainable Bridges*, 2007.
- [22] DNV, “Fatigue assessment of ship structures,” *Classification Notes*, 2014.
- [23] DNV, “Design of offshore steel structures, general (lrfd method),” *Offshore Standard Det Norske Veritas DNV-OS-C101*, 2008.
- [24] DNV, “Fatigue design of offshore steel structures,” *Offshore Standard Det Norske Veritas DNV-RP-C203*, 2010.
- [25] DNV, “Fatigue methodology of offshore ships,” *Recommended Practice DNV-RP-C206*, 2006.
- [26] T. Moan, “Reliability-based management of inspection, maintenance and repair of offshore structures,” *Structure and Infrastructure Engineering*, vol. 1, no. 1, pp. 33–62, 2005.
- [27] W. Dong, T. Moan, and Z. Gao., “Fatigue reliability analysis of the jacket support structure for offshore wind turbine considering the effect of corrosion and inspection,” *Reliability Engineering and System Safety*, no. 106, pp. 11–27, 2012.
- [28] FAA, “Maintenance, preventive maintenance and alterations: Approved inspection program.” www.ecfr.gov/cgi-bin/text-idx?SID=cb95f670000e54381610f9458a553ec3&mc=true&node=se14.3.1351419&rgn=div8 (accessed 08-09-2015), 2006.

-
- [29] A. Hoggard and S. Johnson, “Fatigue in aerostructures; where structural health monitoring can contribute to a complex subject,” *Boeing Aeromagazine*, 2012.
- [30] L. Lazzeri and U. Mariani, “Application of damage tolerant principles to the design of helicopters,” *International Journal of Fatigue*, vol. 31, 2009.
- [31] U. Goranson, “Fatigue issues in aircraft maintenance and repairs,” *International Journal of Fatigue*, vol. 20, no. 6, pp. 413–431, 1997.
- [32] C. Boller and M. Buderath, “Fatigue in aerostructures; where structural health monitoring can contribute to a complex subject,” *Structural Health Monitoring*, 2007.
- [33] J. Schijve, “Fatigue damage in aircraft structures, not wanted, but tolerated?,” *International Journal of Fatigue*, vol. 31, 2008.
- [34] K. Nechval, “Planning inspection in service of fatigue-sensitive aircraft structure components under crack propagation,” *Eksploatacja I Niezawodnosc*, vol. 4, 2007.
- [35] NTSB, “Aloha airlines, flight 243, boeing 737-200, n73711.” <http://www.nts.gov/investigations/accidentreports/pages/aar8903.aspx> (accessed 23-09-2015), 2015.
- [36] Y. Chuliang and L. Kege, “Theory of economic life prediction and reliability assessment of aircraft structures,” *Chinese Journal of Aeronautics*, 2011.
- [37] D. Nowlan, “Racing by the numbers,” *Racecar Engineering*, vol. 25, no. 9, pp. 74–78, 2015.
- [38] K. Rintanen, “Tos-equipment control interface standard,” *PEMA Information Papers*, 2014.
- [39] FÉDÉRATION EUROPÉENNE DE LA MANUTENTION, *RULES FOR THE DESIGN OF HOISTING APPLIANCES*. FÉDÉRATION EUROPÉENNE DE LA MANUTENTION, 1998.
- [40] W. Fricke, “Guideline for the assessment of weld root fatigue,” *International Institute of Welding*, 2011.
- [41] P. Schreurs, “Fracture mechanics; lecture notes,” *Eindhoven University of Technology*, 2012.
- [42] B. McGinty, “Griffith’s energy release rate.” <http://www.fracturemechanics.org/fm/griffith.html> (accessed 15-10-2015), 2015.
- [43] P. Lagace, “Plane stress and plane strain.” <http://ocw.mit.edu/courses/aeronautics-and-astronautics/16-20-structural-mechanics-fall-2002/lecture-notes/unit6.pdf> (accessed 19-10-2015), 2001.
- [44] H. Tawancy, A. Ul-Hamid, and N. Abbas, *Practical Engineering Failure Analysis*. Taylor and Francis, 2004.
- [45] Clarkson University, “Chapter 9; fracture mechanics.” <http://people.clarkson.edu/isuni/Chap-9.pdf> (accessed 26-10-2015), 2015.

- [46] AFGROW, “Handbook for damage tolerant design.” <http://www.afgrow.net/applications/DTDDHandbook/> (accessed 10-11-2015), 2011.
- [47] S. Laham, “Stress intensity factor and limit load handbook,” *British Energy Generation*, vol. 2, 1998.
- [48] Y. Murakami, *Stress Intensity Factors Handbook*. Pergamon, 1987.
- [49] G. Sih, *Handbook of Stress-intensity Factors*. Lehigh University, 1973.
- [50] T. Fett, “Stress intensity factors, t-stresses and weight functions,” *Institute of Ceramics in Mechanical Engineering*, 2008.
- [51] T. Fett, “Stress intensity factors and weight function for special crack problems,” *Institut für Materialforschung*, 1998.
- [52] B. Boyce and R. Ritchie, “Effect of load ratio and maximum stress intensity on the fatigue threshold in ti-6al-4v,” *Engineering Fracture Mechanics*, vol. 68, pp. 129–147, 2001.
- [53] F. Cai, X. Wang, J. Liu, and F. Zhao, “Fatigue life analysis of crane k-type welded joints based on non-linear cumulative damage theory,” *Journal of Mechanical Engineering*, vol. 60, no. 2, pp. 135–144, 2014.
- [54] D. Radonovich, “Methods of extrapolating low cycle fatigue data to high stress amplitudes,” *University of Central Florida*, 2007.
- [55] A. Chattopadhyay *et al.*, “Stress analysis and fatigue of welded structures,” *welding in the world*, vol. 55, no. 7, 2011.
- [56] CEN, “Crane safety- general design part 3: Load actions,” *European Committee for Standardization*, vol. EN 13001-2:2010, 2010.
- [57] A. Blog, “Which fatigue methodology is appropriate stress-life or strain-life?.” <http://www.ansys-blog.com/which-fatigue-methodology-is-appropriate-stress-life-or-strain-life/> (accessed 16-02-2016), 2016.
- [58] C. Richardson *et al.*, “An xfem method for modelling geometrically elaborate crack propagation in brittle materials,” *INTERNATIONAL JOURNAL FOR NUMERICAL METHODS IN ENGINEERING*, vol. 1, no. 1, 2009.
- [59] P. University, “Fatigue crack growth; problem 1 (with solution).” <http://www.tech.plym.ac.uk/sme/tutorials/FMTut/Fatigue/Solutions/Solution1.htm> (accessed 09-12-2015), 2015.
- [60] P. University, “Fatigue crack growth; problem 3 (with solution).” <http://www.tech.plymouth.ac.uk/sme/Tutorials/FMtut/Fatigue/Solutions/Solution3.htm> (accessed 10-12-2015), 2015.
- [61] F. FFS, “Stress intensity factor (sif) solutions.” http://fracture.tu.kielce.pl/procedury_2/AnnexA.pdf (accessed 10-03-2016), 2006.

-
- [62] J. Harter, “Life analysis development and verification,” *Air Force Research Laboratory*, 2004.
- [63] F. Lawrence, “Estimation of fatigue-crack propagation life in butt welds,” *Welding Research Supplement*, vol. 5, pp. 212–220, 1973.
- [64] H. Tada, *The stress analysis of cracks handbook*. Professional Engineering Publishing., 1985.
- [65] R. Forman, “Stress intensity factors for circumferential trough cracks in hollow cylinders subjected to combined tension and bending loads,” *Engineering Fracture Mechanics*, vol. 21, no. 3, pp. 563–571, 1985.
- [66] J. Burk and F. Lawrence, “Influence of bending stresses on fatigue crack propagation life in butt joint welds,” *Welding Research Supplement*, vol. 2, pp. 61–66, 1977.
- [67] F. Brennan, W. Dover, R. Kare, and A. Hellier, “Parametric equations for t-butt weld toe stress intensity factors,” *International Journal of Fatigue*, vol. 21, pp. 1051–1062, 1991.
- [68] A. Hobbacher, “Stress intensity factors of welded joints,” *Engineering Fracture Mechanics*, vol. 46, no. 2, pp. 173–182, 1993.
- [69] H. Chung, S. Liu, R. Lin, and S. Ju, “Assessment of stress intensity factors for load-carrying fillet welded cruciform joints using a digital camera,” *International Journal of Fatigue*, vol. 30, pp. 1861–1872, 2008.
- [70] S. Kainuma and T. Mori, “A study on fatigue crack initiation point of load-carrying fillet welded cruciform joints,” *International Journal of Fatigue*, vol. 30, pp. 1669–1677, 2008.
- [71] S. C. info, “Steel material properties.” http://www.steelconstruction.info/Steel_material_properties (accessed 14-03-2016), 2016.
- [72] D. Roylance, “Introduction to fracture mechanics,” *Michigan Institute of Technology*, 2001.
- [73] A. Almar-Naess, *Fatigue handbook of offshore structures*. Tapir, 1985.
- [74] F. Spencer, “Visual inspection research project report on benchmark inspections,” *FAA Aging Aircraft NDI Validation Center*, 1996.
- [75] B. Kühn *et al.*, “Assessment of existing steel structures: Recommendations for estimation of remaining fatigue life,” *JRC Scientific and Technical Reports*, 2008.
- [76] TWI, “Eddy current testing.” <http://www.twi-global.com/capabilities/integrity-management/non-destructive-testing/ndt-techniques/eddy-current-testing/> (accessed 04-12-2015), 2015.
- [77] J. C. Ltd., “Probability of detection (pod) curves (derivation, applications and limitations),” *HSE, RESEARCH REPORT 454*, 2006.

- [78] T. W. Institute, “What is the recommended method of repairing fatigue cracking and how long will the repairs last?.” www.twi-global.com/technical-knowledge/faqs/structural-integrity-faqs/faq-what-is-the-recommended-method-of-repairing-fatigue-cracking-and-how-long-will-the-repairs-last (accessed 08-09-2015), 2015.
- [79] ESDEP, “Lecture 12.5; improvement techniques in welded joints,” 2015.
- [80] T. W. Institute, “What is meant by postweld heat treatment/stress relief heat treatment?.” <http://www.twi-global.com/technical-knowledge/faqs/material-faqs/faq-what-is-meant-by-postweld-heat-treatment-stress-relief-heat-treatment/> (accessed 02-12-2015), 2015.
- [81] ABS, “No.47 shipbuilding and repair quality standard,” *American Bureau of Shipping*, 2010.
- [82] T. Richardson, “Analytical investigation of repair methods for fatigue cracks in steel bridges,” *University of Kansas*, 2012.
- [83] FHWA, “Manual for repair and retrofit of fatigue cracks in steel bridges,” *FHWA Publications*, 2013.
- [84] F. Technology, “Stopcrack ex; overview and technical data.” <http://www.fatiguetech.com/products-stopcrackex.asp> (accessed 27-11-2015), 2015.
- [85] N. Fanni, N. Fouda, M. Shabara, and M. Awad, “New crack stop hole shape using structural optimizing technique,” *Ain Shams Engineering International*, 2015.
- [86] T. W. Institute, “Alexander I kielland accommodation platform; a case study.” <http://www.twi-global.com/news-events/case-studies/alexander-i-kielland-accommodation-platform-145/> (accessed 28-12-2015), 2015.
- [87] G. Nieuwenhuis, “De lemniscaatkraan,” *NAW*, no. 3, pp. 162–166, 2006.
- [88] M. Patricio and R. Mattheij, “Crack propagation analysis,” pp. 1–22, 2006.
- [89] A. D. Jesus, B. Fontoura, L. da Silva, and M. Veljkovic, “A comparison of the fatigue behaviour between s355 and s690 steel grades,” *Journal of constructional steel research*.
- [90] M. Szata and G. Lesiuk, “Algorithms for estimating fatigue crack growth using energy method,” *Archives of civil and mechanical engineering*.
- [91] O. Olsdal, S. Nielsen, and L. Jeppessen, “Automated ultrasonic inspection improves quality and benefits economy in welding workshops,” *Sensor and NDE Innovation*.